UNIVERSITY OF LONDON THESIS

Degree PhD Year 2007 Name of Author VEHLOW, Anne

Signalling Mechanisms Contributing to Integrin Activation and Immunological Synapse Formation in B cells

Anne Vehlow

University College London

ProQuest LLC
789 East Eisenhower Parkway
P.O. Box 1346
Ann Arbor, MI 48106-1346

Declaration

I confirm that the work presented in this Thesis is my own. The contribution of others has been specifically stated in the body of the text and the figure legends where appropriate.

Abstract

When a B cell encounters specific membrane-bound antigen, a series of signalling events trigger cytoskeletal rearrangements, integrin activation and cell polarisation. This, in turn, allows for B cell spreading and the formation of the immunological synapse (IS) by segregation of the B cell receptor (BCR) and integrins into domains known as central and peripheral supramolecular activation cluster (cSMAC and pSMAC, respectively). While much is known about the signalling pathways triggered by antigen recognition, evidence linking these pathways to integrin activation and IS formation is lacking.

Here, confocal microscopy and biochemical approaches were used to dissect the signalling pathways regulating integrin activation and formation of the B cell IS. The obtained data reveals that membrane-bound antigen recognition by the BCR triggers activation of the integrin leukocyte function-associated antigen 1 (LFA-1) by a signalling mechanism involving tyrosine kinases, the GTP/GDP exchange factors Vav1 and Vav2, the small GTPase Rac2 and phosphoinositide-3 kinase (PI3K). By supporting LFA-1 activation, this pathway regulates B cell adhesion and formation of the pSMAC at the IS. Furthermore, Vav1 is revealed as the master regulator of B cell spreading.

B cell adhesion mediated by the integrin very late antigen 4 (VLA-4) and its recruitment to the IS also rely on tyrosine kinase and PI3K activity. However, in contrast to LFA-1, Vav and Rac proteins seem to have redundant functions.

Finally, engagement of LFA-1 and VLA-4 during the initial stage of membrane-antigen recognition leads to tight B cell adhesion and therefore supports B cell spreading when the amount of antigen is low. This may represent a critical mechanism supporting efficient B cell activation in situations of limited antigen availability.

Acknowledgements

I would like to thank my supervisor, Dr. Facundo Batista, for giving me the opportunity to be a part of your team, for your advice and criticism throughout my PhD.

Thank you to past and present members of the Lymphocyte Interaction Laboratory, for your support, advice and friendship. Especially Yolanda, Sebastian, Kathy, Eloisa, Michele, Julia, Bebhinn and David – it was great fun working with you!

Thank you to Dr. Michael Way and Dr. Banafshe Larijani for being my Thesis committee. And to my collaborators, Robert Henderson, Victor Tybulewicz and Martin Turner for providing reagents and for our useful discussions.

Outside the lab I would like to thank Andreas, Anett, Ina and Jon – for all those fruitful discussions over a glass of wine or a pint of beer and for reading my Thesis!

Ein besonderes Dankeschön geht an meine Eltern, meinen Bruder und meine Großeltern, für Eure unermüdliche Unterstützung während meiner gesamten Ausbildung, für stundenlange Telefongespräche und für die vielen kleinen Pakete, die in den letzten Jahren bei mir eingetroffen sind. Ich hab Euch lieb!

And a special thank you to a very important person, Luis. You have lifted me up after each failed experiment and have shared all my frustrations! Thank you for your support during the last years!

Table of Contents

Table of Figures

Abbreviations

ADAP	adhesion and degranulation promoting adaptor protein
APC	antigen-presenting cell
APS	ammonium persulfate
BCAP	B cell adaptor for PI3K
BCR	B cell receptor
BLNK	B cell linker protein
BSA	bovine serum albumine
CDR	complementarity-determining region
CLP	common lymphoid progenitor
CRIB	Cdc42/Rac interactive binding domain
cSMAC	central supramolecular activation cluster
DAG	diacylglycerol
DC	dendritic cell
DIC	differential interference contrast
DMSO	dimethyl sulfoxide
DOPC	1,2-dioleoyl-sn-glycero-3-phosphocholine
dSMAC	distal supramolecular activation cluster
DTT	1,4-dithiothreitol
ELISA	enzyme linked immunosorbent assay
FACS	fluorescence activated cell sorting
FCS	fetal calf serum
FDC	follicular dendritic cell
GC	germinal centre
GDP	guanosine diphosphate
GEF	guanine nucleotide exchange factor
GM1	Ganglioside 1
GST	glutathione-S-transferase
GTP	guanosine triphosphate
HCl	hydrochloric acid
HEL	hen egg lysozyme
HRP	horse radish peroxidase
HSC	haematopoietic stem cell
ICAM-1	intracellular adhesion molecule 1
IF	immunofluorescence
Ig	immunoglobulin
IP_3	inositol-(1,4,5)-triphosphate
IPTG	isopropyl-β-D-thiogalactopyranosid
IRM	interference reflection microscopy
IS	immunological synapse
ITAM	immunoreceptor tyrosine-based activation motif
ITIM	immunoreceptor tyrosine-based inhibitory motif
KCl	potassium chloride
LB medium	Luria Bertani medium
LFA-1	leukocyte function-associated antigen 1
LPS	lipopolysaccharide
LY	LY294002
mAb	monoclonal antibody

$MgCl_2$	magnesium chloride
MHC	major histocompatibility complex
MIDAS	metal-ion-dependent adhesion site
mIg	membrane-bound immunoglobulin
n/a	not applicable
NaCl	sodium chloride
NaN_3	sodium azide
N-biotinyl Cap-PE	1,2-dioleoyl-sn-glycero-3-phosphoethanolamine-N-(Cap-Biotinyl)
NF-AT	nuclear factor of activated T cells
NF-κB	nuclear factor-κB
NT	not treated
PBS	phosphate buffered saline
PCR	polymerase chain reaction
PFA	paraformaldehyde
PH	pleckstrin homology
PI	propidium iodide
PI3K	phosphoinositide-3 kinase
PIP_2	phosphatidylinositol-(4,5)-bisphosphate
PIP_3	phosphatidylinositol-(3,4,5)-triphosphate
PKC	protein kinase C
PLCγ	phospholipase Cγ
pSMAC	peripheral supramolecular activation cluster
PTK	protein tyrosine kinase
pTyr	phosphotyrosine
RalGDS-RBD	Rap1-binding domain of RalGDS
RAPL	regulator of cell adhesion and polarisation enriched in lymphoid tissues
rpm	rounds per minute
RT	room temperature
SDS	sodium dodecyl sulfate
SDS-PAGE	SDS polyacrylamid gel electrophoresis
SFK	Src-family tyrosine kinase
SH2	Src-homology 2
SKAP55	Src-kinase-associated phosphoprotein of 55kDa
SKAP-HOM	SKAP55 homologue
TCR	T cell receptor
TLR	Toll-like receptor
TEMED	N,N,N',N'-tetramethylethylenediamine
VCAM-1	vascular cell adhesion molecule 1
VLA-4	very late antigen 1
WB	Western Blot
WM	Wortmannin
WT	wild type
Xid	X-linked immunodeficiency
XLA	X-linked agammaglobulinemia
α-κ	rat anti-mouse kappa antibody

1 Introduction

1.1 The Immune System

The immune system is the body's own defence mechanism. It is composed of a network of specialized tissues, cells and molecules that work together to develop immunity, the ability to defend against invading pathogens and to resist infections.

1.1.1 The Innate Immune System

Innate, or natural immunity is the first line of defence against invading pathogens. It is present in each individual, at any given time. Innate immunity mediates the early phases of the immune response against pathogens through a complex cooperation of physical and chemical barriers, phagocytotic cells and natural killer cells, blood proteins and cytokines. These innate components respond to molecular patterns that are conserved in a large group of pathogens (Medzhitov and Janeway, 1997).

1.1.2 The Adaptive Immune System

In contrast to innate immunity, adaptive immunity develops through the recognition of specific structures on pathogens. The adaptive immune system constantly evolves its capacity to respond to infection and acquires long-lasting memory to rapidly protect the organism from reoccurring infections (Janeway et al., 2005).

There are two subtypes of the adaptive immune system, called humoral and cellular immunity: Humoral immunity is mediated by antibodies, which are produced by B lymphocytes (B cells) and neutralise extracellular pathogens. Cellular immunity is mediated by T lymphocytes (T cells), which eliminate intracellular pathogens by killing infected cells. Furthermore, T cells play a central

role in supporting humoral immunity by promoting the activation of B cells (Janeway et al., 2005).

1.2 B Cells in the Adaptive Immune System

B lymphocytes take their name from the *B*ursa of Fabricius, which is the main production site of B cells in birds and has been widely used as a model system (Glick, 1991). B cells are 6-10 μm small, with a dense nucleus and little cytoplasm. They are able to respond to a large variety of antigens due to the expression of a unique antigen receptor – called the B Cell Receptor (BCR).

1.2.1 The B Cell Receptor (BCR)

Each B cell carries a unique BCR complex consisting of a variant and invariant component, which is depicted in detail in Figure 1.1.
The variant part is a membrane-bound immunoglobulin (mIg) that determines the antigen specificity of a given B cell. Each mIg consists of two heavy and two light chains, both of which are composed of variable (V) and constant (C) portions (Hombach et al., 1990). The variable portions of both heavy and light chains form the antigen-binding site (see section 1.2.2 below).
The invariant part is the signalling component and consists of one Igα and one Igβ transmembrane protein, which form a disulfide-linked heterodimer that associates noncovalently with the mIg (Hombach et al., 1990), (Schamel and Reth, 2000).

1.2.2 BCR specificity: V(D)J Recombination

The need for a large repertoire of antigen-specific B cells carrying distinct receptors is served by the mechanism of gene rearrangement. During B cell development this process brings together gene segments coding for the variable and constant parts of the mIg (Figure 1.2).

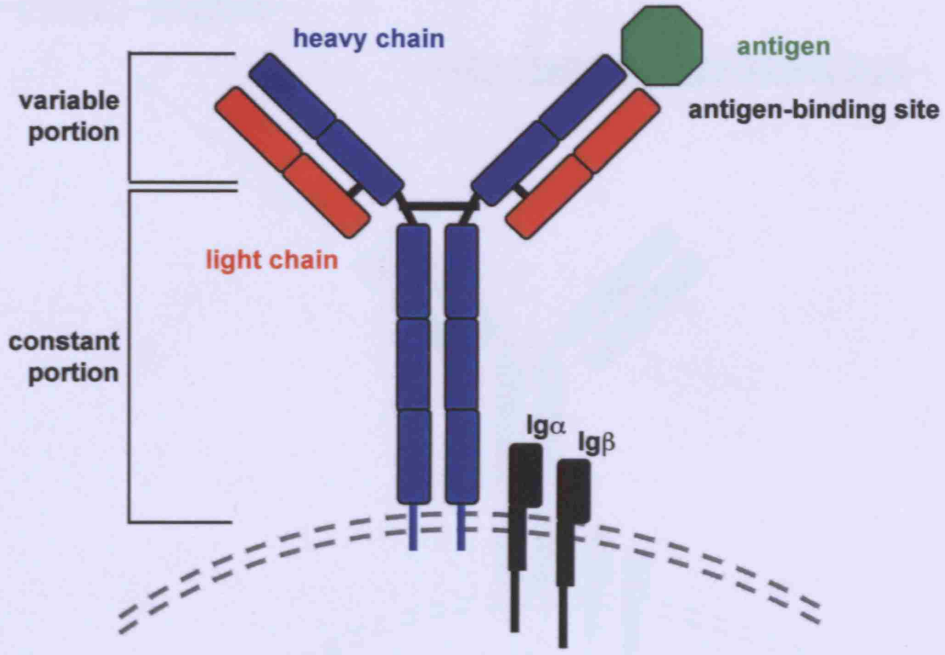

Figure 1.1 The B cell receptor (BCR)
This figure shows the composition of B cell receptor complex. It is composed of a variant antigen-binding membrane-bound immunoglobulin (mIg) and the invariant signal-initiating transmembrane proteins Igα and one Igβ. The mIg consists of two heavy chains (blue) and two light chains (red), which are composed of variable and constant portions. The variable portions of both heavy and light chains form the antigen-binding site. Adapted from Janeway et al., 2005.

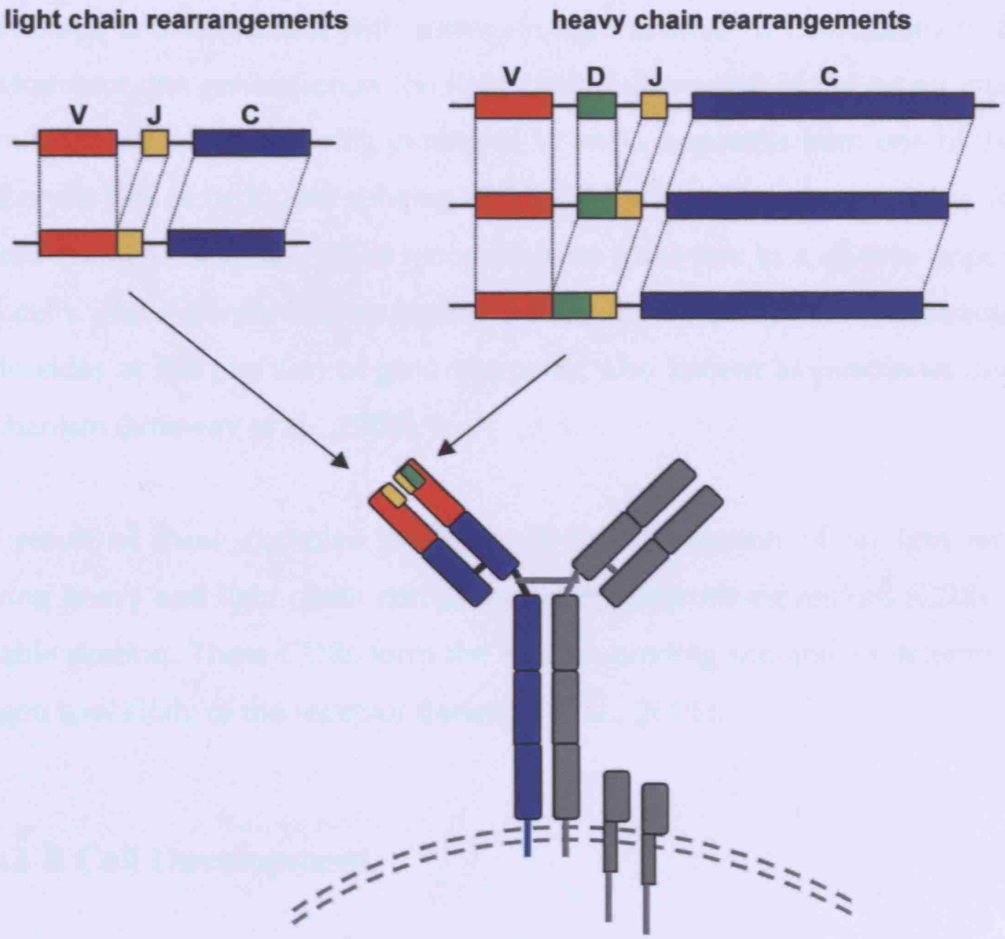

Figure 1.2 V(D)J recombination
This figure shows a simplified schema of V(D)J recombination of the light and heavy chain genes. For light chain rearrangements: a variable (V) and joining (J) gene segment are joined form a complete light chain variable region exon. The light chain constant region is encoded in a separate exon and joined to the variable exon by splicing. For heavy chain rearrangements: First, a diversity (D) and J gene segment are joined, then the V gene sement joins the DJ segment, forming a heavy chain variable region exon. The heavy chain constant region is encoded in several exons (depiced as one square) and joined to the variable exon by splicing. Adapted from Janeway et al., 2005.

The first step is the random recombination of a given D_H (diversity gene of the heavy chain locus) segment with one J_H (joining) segment. At the next step a V_H (variable) segment is chosen to join a DJ_H pair. Finally, the μ chain (C_μ) is spliced to a VDJ_H segment. If the assembly happens correctly, the heavy chain protein is synthesised and associated with surrogate light chains. At later stages of B cell development, the generation of the light chain follows that of the heavy chain by a similar mechanism involving joining of V_L and J_L segments from one of the two light chain loci (κ or λ) and splicing of the light chain (C_L) segment. Thus, from a limited quantity of genes, V(D)J recombination gives rise to a diverse population of B cells. This diversity is even further increased by the addition or subtraction of nucleotides at the junction of gene segments, also known as junctional diversity mechanism (Janeway et al., 2005).

The result of these complex processes is the production of an IgM receptor bearing heavy and light chain complementarity-determining regions (CDRs) in its variable portion. These CDRs form the antigen-binding site and so determine the antigen specificity of the receptor (Janeway et al., 2005).

1.2.3 B Cell Development

B cells are continuously generated throughout lifetime in the bone marrow from haematopoietic stem cells (HSC), which differentiate into common lymphoid progenitors (CLP) and progress to the B cell lineage (Hardy and Hayakawa, 2001).

The early stages of B cell development can be subdivided into several stages based on the rearrangement status of their immunoglobulin (Ig) genes (Osmond et al., 1998). Firstly pro-B cells undergo D_H-J_H joining. This is followed by progress to the pre-B cell stage and V_H-DJ_H rearrangements.

Additionally to the rearranged μ heavy chain (C_μ) pre-B cells express the surrogate light chains VpreB and λ5, which associate and form the pre-BCR. Together with Igα and Igβ the pre-BCR complex is transported to the cell surface and expressed at low levels in a transient manner. This step constitutes a crucial checkpoint

during B cell development as the pre-BCR contributes to the positive selection of pre-B cells. Firstly, it signals to stop heavy chain gene rearrangements, which ensures production of only one functional heavy chain (allelic exclusion). Furthermore, it induces expansion of pre-B cells and rearrangements of the light chain genes. The κ light chain locus tends to rearrange first and blocks recombination of the λ locus (isotype exclusion) (Corcoran, 2005). If successive rounds of rearrangement of the κ locus are not productive, the λ locus is rearranged. Unproductive rearrangement of both loci results in apoptosis, productive rearrangement leads to expression of the surface-bound IgM. To date it is unclear, how the pre-BCR regulates this progress from the pre-B cell into the immature B cell stage. It may interact with an external ligand or it may simply be its intracellular assembly that generate signals, which are required for B cell development (Janeway et al., 2005).

To avoid autoimmune reactions, immature B cells are negatively selected by testing of their IgM for reactivity against self-antigen. Autoreactive B cells are either deleted, undergo receptor editing or become anergised, processes that contribute to self-tolerance.

Immature B cells bearing self-reactive IgM are efficiently eliminated in large numbers (Nemazee and Burki, 1989). It is suggested that deletion depends on the strength of receptor binding to the antigen: Whereas high-affinity interactions with membrane-bound antigen lead to apoptosis, lower-affinity interactions and soluble antigens allow receptor editing or result in anergy (Hartley et al., 1991), (Lang et al., 1996).

During receptor editing, continuous rearrangement of the light chain locus takes place. This leads to the generation of a receptor with altered specificity, which is again tested for reactivity against self-antigens (Gay et al., 1993).

Anergy is the third mechanism by which self-reactive B cells might be rendered inactive. Anergic B cells persist in the periphery in an antigen-unresponsive state (Goodnow et al., 1988) (Nossal and Pike, 1980). These B cells show high basal intracellular calcium, reduced IgM surface expression and do not proliferate or mount an immune response upon antigen encounter (Goodnow et al., 1988), (Benschop et al., 2001), (Merrell et al., 2006), (Gauld et al., 2006).

Once overcome negative selection, immature B cells exit the bone marrow, enter the peripheral circulation and migrate to the spleen. In the spleen, immature B cells mature further through two distinct developmental stages; known as transitional 1 (T1) and transitional 2 (T2) B cells (Loder et al., 1999). T1 B cells are recent immigrants from the bone marrow and retain phenotypic characteristics of immature B cells, such as a high expression level of IgM and susceptibility to negative selection. Development into T2 B cells is characterised by the additional expression of IgD (C_δ), CD21 and CD23. Furthermore, a loss of sensitivity to negative selection events and an accompanying increase in responsiveness to T cell help upon recognition of specific antigen may cause the progress of T2 B cells into the mature B cell compartment (Chung et al., 2003).

These "naïve" mature B cells recirculate through secondary lymphoid organs, where they eventually encounter their specific antigen. Specific antigen recognition leads to B cell activation and differentiation into antibody-secreting plasma B cells and memory B cells. A summary of the B cell developmental stages is shown in Figure 1.3.

1.2.4 BCR Affinity Maturation: the Germinal Centre

While recirculating through the periphery, mature B cells eventually encounter their specific antigen in secondary lymphoid organs.

Antigen recognition by the BCR triggers two events that support B cell activation: Firstly, it triggers intracellular signalling cascades that regulate B cell fate decisions. Secondly, it mediates antigen uptake, processing and presentation of antigenic peptides in the context of the major histocompatibility complex (MHC) molecules to T cells, which supports B cell activation (Niiro and Clark, 2002), (Benschop and Cambier, 1999) (Figure 1.4).

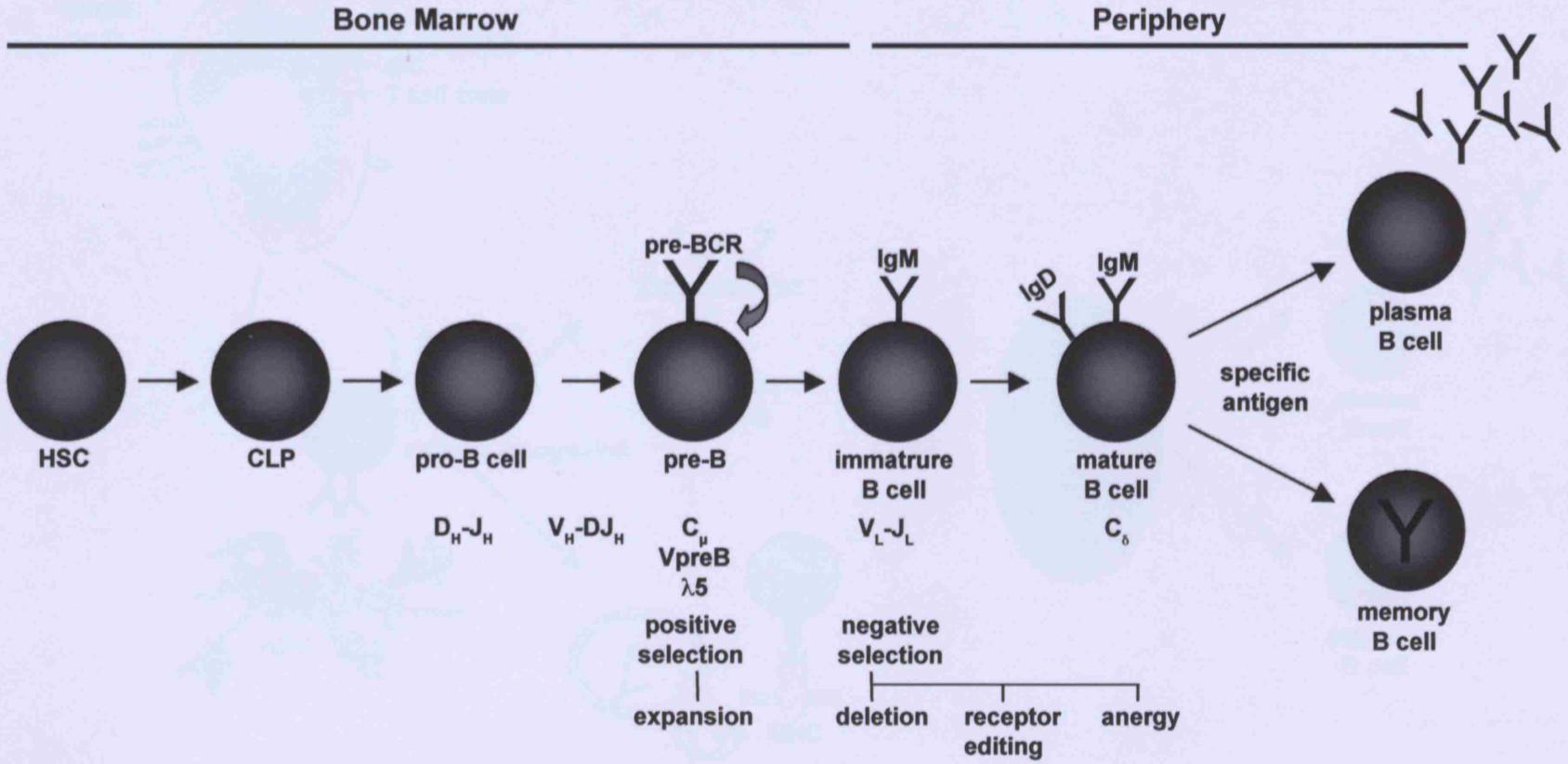

Figure 1.3 B cell development

This figure shows a simplified schema of B cell development. Haematopoietic stem cells (HSC) in the bone marrow differentiate into common lymphoid progenitors (CLP) and progess to the B lineage. Pro-B cells develop into pre-B cells, which undergo positive selection and expansion. After negative selection, remaining immature B cells exit the bone marrow, enter the peripheral circulation and mature. Specific antigen encounter induces differentiation into plasma and memory B cells. Transitional B cells are not shown in this Figure. Rearrangements of the heavy and light chain genes are shown at each develomental stage.

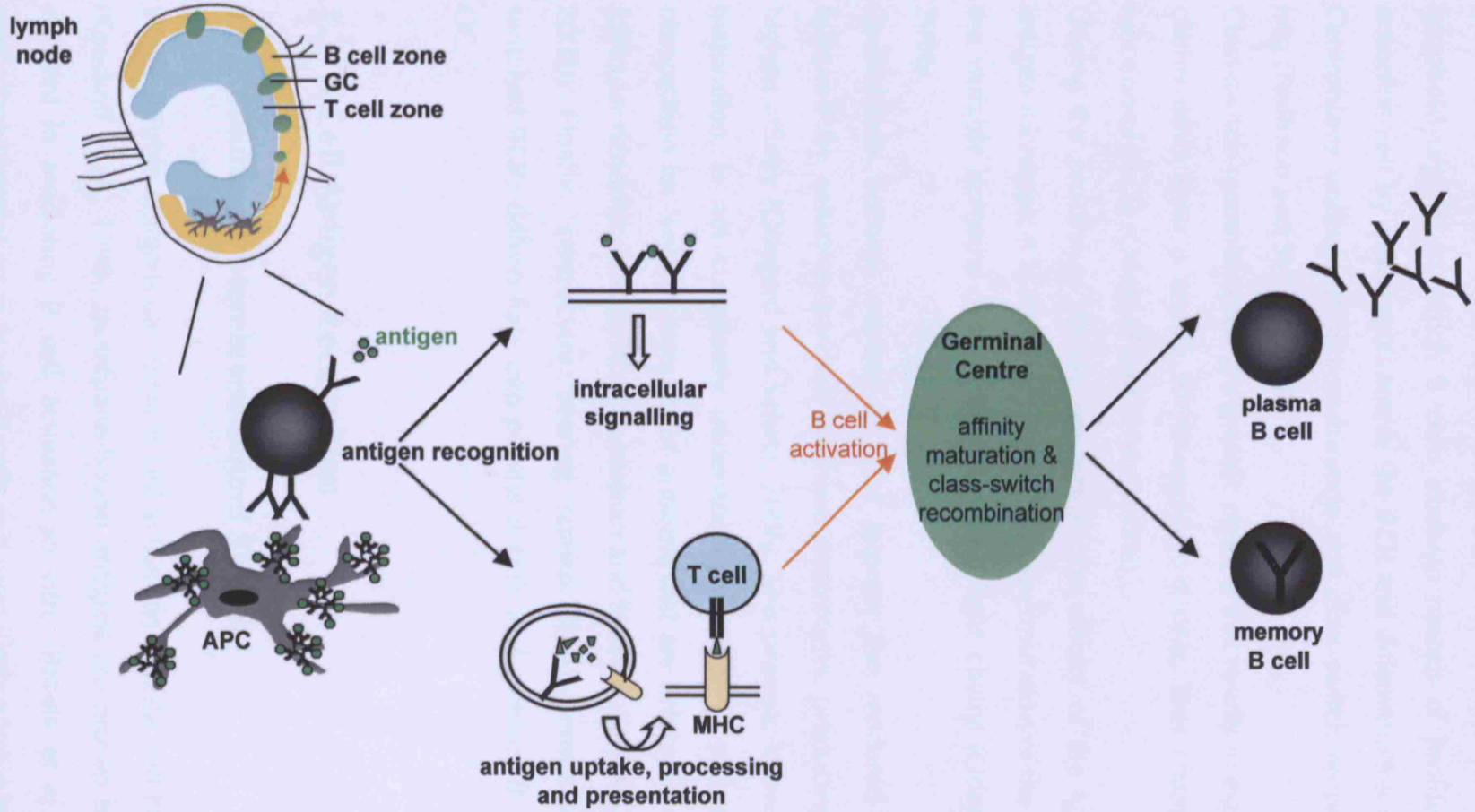

Figure 1.4 B cell antigen recognition
B cells are able to recognize solube and membrane-bound antigens. B cells encounter antigen in secondary lymphoid organs, such as lymph nodes, most likely in form of immune complexes tethered to the surface of antigen-presentign cells (APC). Antigen recognition by the BCR triggers intracellular signalling events and mediates antigen uptake, processing and presentation in the context of MHC molecules to T cells, which supports B cell activation. Activated B cells form germinal centres (GC) and undergo affinity maturation and class-switch recombination. Plasma and memory B cells finally exit the GC.

Upon specific antigen encounter and T cell help, B cells are recruited to form germinal centres (GCs). GCs are specialised areas in the follicles of secondary lymphoid organs, in which B cells undergo rounds of proliferation, which is accompanied by downregulation of the BCR and differentiation into centroblasts. Centroblasts undergo affinity maturation and class-switch recombination of the mIg (Tarlinton and Smith, 2000).

Class-switch recombination is a genetic process that results in expression of heavy chains other than μ and δ, for example γ, α or ε, thus changing the effector function of the Ig (Odegard and Schatz, 2006).

During the process of affinity maturation the affinity of the Ig for the specific antigen increases. It is the result of somatic hypermutation of the genes coding for the variable domains of the mIg heavy and light chains (Odegard and Schatz, 2006).

Centroblasts become centrocytes that express the rendered mIgs, which is followed by selective survival of those centrocytes producing mIgs with the highest affinity (Odegard and Schatz, 2006). This process, known as BCR affinity maturation, is not completely understood. However, it seems to rely on the competition for limiting amounts of antigens that are displayed on the surface of follicular dendritic cells (FDCs) (Haberman and Shlomchik, 2003), (Kosco-Vilbois, 2003). Finally, centrocytes bearing somatically hypermutated and isotype switched BCRs differentiate into plasma B cells and memory B cells and exit the GC.

1.3 B Cell Antigen Recognition

1.3.1 Soluble vs. Membrane-Bound Antigen

While soluble antigens can drive B cell activation (Batista and Neuberger, 1998), (Kouskoff et al., 1998), membrane-bound antigens are proven to be much more efficient in mediating B cell activation *in vitro* (Batista et al., 2001). This is particularly interesting as *in vivo* B cells will most likely encounter antigen in form of immune complexes tethered to the surface of cells such as FDCs or dendritic

cells (DCs) by Fc or complement receptors (Haberman and Shlomchik, 2003), (Kosco-Vilbois, 2003) (Figure 1.4).

Indeed, DCs are able to retain and present specific antigen *in vivo* and *in vitro* and DC-B cell interactions are necessary for B cell activation (Wykes et al., 1998). Furthermore, pulsing DCs with specific antigen led to B cell stimulation, when transferred into non-immunised recipients (Balazs et al., 2002), (Berney et al., 1999), (Colino et al., 2002), (Wykes et al., 1998). The mechanism of antigen presentation by DCs is not completely understood, but might involve internalization of the antigen and recycling back to the cell surface (Bergtold et al., 2005).

FDCs are able to retain immune complexed antigen on their surface tethered to Fc receptors (Haberman and Shlomchik, 2003), (Kosco-Vilbois, 2003). Importantly, FDC-B cell interactions stimulated B cell activation and differentiation into plasma and memory B cells (Szakal et al., 1988), (Wu et al., 1996), (Aydar et al., 2005).

Moreover, also other surface proteins are expressed on the membrane of antigen-presenting DCs or FDCs, which can support the interaction with B cells and assist B cell activation. Two examples are intracellular adhesion molecule 1 (ICAM-1) and vascular cell adhesion molecule 1 (VCAM-1), which have been shown to mediate FDC or DC/B cell contacts by interaction with the integrins leukocyte function-associated antigen 1 (LFA-1) and very late antigen 4 (VLA-4), respectively, which are expressed on the B cell membrane (Koopman et al., 1991), (Kushnir et al., 1998), (Freedman et al., 1990). Furhtermore, they are reported to promote B cell survival in the GC (Koopman et al., 1994).

1.3.2 BCR Signalling upon Antigen Recognition

Upon specific antigen recognition by the BCR, the invariant subunits Igα and Igβ are responsible for initiating B cell responses. The signalling capacity of Igα and Igβ lies within a specific motif in each cytoplasmatic tail, known as

immunoreceptor-based activation motif (ITAM). The ITAM motif is composed of two tyrosine residues separated by 9-12 amino acids. The core of the ITAM sequence is comprised of YXX[L/I]X_{6-9}YXX[L/I], whereby Y represents the tyrosine, L is leucine, I is isoleucine and X could be any amino acid (Reth, 1989), (Cambier, 1995).

BCR clustering triggers activation of Src-family tyrosine kinases (SFKs) such as Lyn, Fyn or Blk (Burkhardt et al., 1991). This is regulated by dephosphorylation of their negative regulatory tyrosine by the phosphatase CD45 (Hermiston et al., 2003), however the exact mechanism underlying this activation is not fully understood. SFKs then phosphorylate the tyrosine residues in the ITAM motifs of Igα and Igβ, which in turn facilitate recruitment and activation of the Syk/Zap70-family tyrosine kinase Syk. Activation of SFKs and Syk leads to the phosphorylation of several other signalling molecules, which in turn activate signalling networks leading to gene transcription, differentiation and proliferation (Niiro and Clark, 2002) (Figure 1.5).

1.3.2.1 Protein Tyrosine Kinases (PTKs)

Three families of PTKs are implicated in the earliest steps of BCR signalling: tyrosine kinases from the Src-family, the Syk/Zap-70 family and the Tec-family.

B cells express several SFKs including Lyn, Fyn, Blk, Hck, Fgr, Lck (Law et al., 1992). Mutations in individual SFKs have little effect on B cell function, indicating a redundancy between the different SFKs for BCR signalling (Lowell and Soriano, 1996), (Texido et al., 2000).

Lyn is thought to be the main SFK responsible for phosphorylating the Igα and Igβ ITAMs; nevertheless B cell development in Lyn-deficient mice is normal, confirming the redundancy with other SFKs in positively regulating BCR signalling (Chan et al., 1997). In fact, the main role of Lyn appears to be negative, as Lyn deficient B cells exhibit enhanced intracellular calcium flux, proliferative responses in *vitro* and increased autoantibody levels *in vivo* (Hibbs et al., 1995), (Nishizumi et al., 1995). This negative function results from the ability of Lyn to

phosphorylate immunoreceptor tyrosine-based inhibitory motifs (ITIMs) in the BCR co-receptor CD22 and the Ig receptor FcγRIIB1, which are suggested to dampen the BCR response (Smith et al., 1998), (Chan et al., 1998), (Nishizumi et al., 1998).

The recruitment of the Syk/Zap-70-family tyrosine kinase Syk to the ITAM motifs is dependent on phosphorylation of both tyrosine residues, which function as docking sites for Syk's Src-homology 2 (SH2) domain (Rowley et al., 1995). Syk is the key molecule linking antigen recognition by the BCR with downstream signalling cascades, as deletion of Syk results in a substantial defect in BCR-mediated activation of downstream signalling pathways (Takata et al., 1994) and a block in B cell development at the pre-B cell stage (Turner et al., 1995).

The Tec-family tyrosine kinase Btk is crucial for BCR signalling and B cell development. Loss or mutation of Btk results in the immunodeficiency X-linked agammaglobulinemia (XLA) in humans and X-linked immunodeficiency (Xid) in mice, which is characterised by a block in B cell development and the absence of antibodies (Tsukada et al., 1993), (Vorechovsky et al., 1995), (Rawlings et al., 1993). Downstream of the BCR activation of Btk requires its phosphorylation by SFKs and recruitment to the plasma membrane through binding of its pleckstrin homology (PH) domain to second messenger lipids (Scharenberg et al., 1998).

1.3.2.2 The Family of Vav Proteins

Vav proteins are rapidly phosphorylated by tyrosine kinases downstream of lymphocyte receptors, which results in their activation (Deckert et al., 1996), (Schuebel et al., 1998), (Movilla and Bustelo, 1999). The main function of Vav proteins is the activation of Rho GTPases by catalysing the exchange of guanosine diphosphate (GDP) for guanosine triphosphate (GTP). Therefore, Vav proteins are also known as guanine nucleotide exchange factors (GEFs).

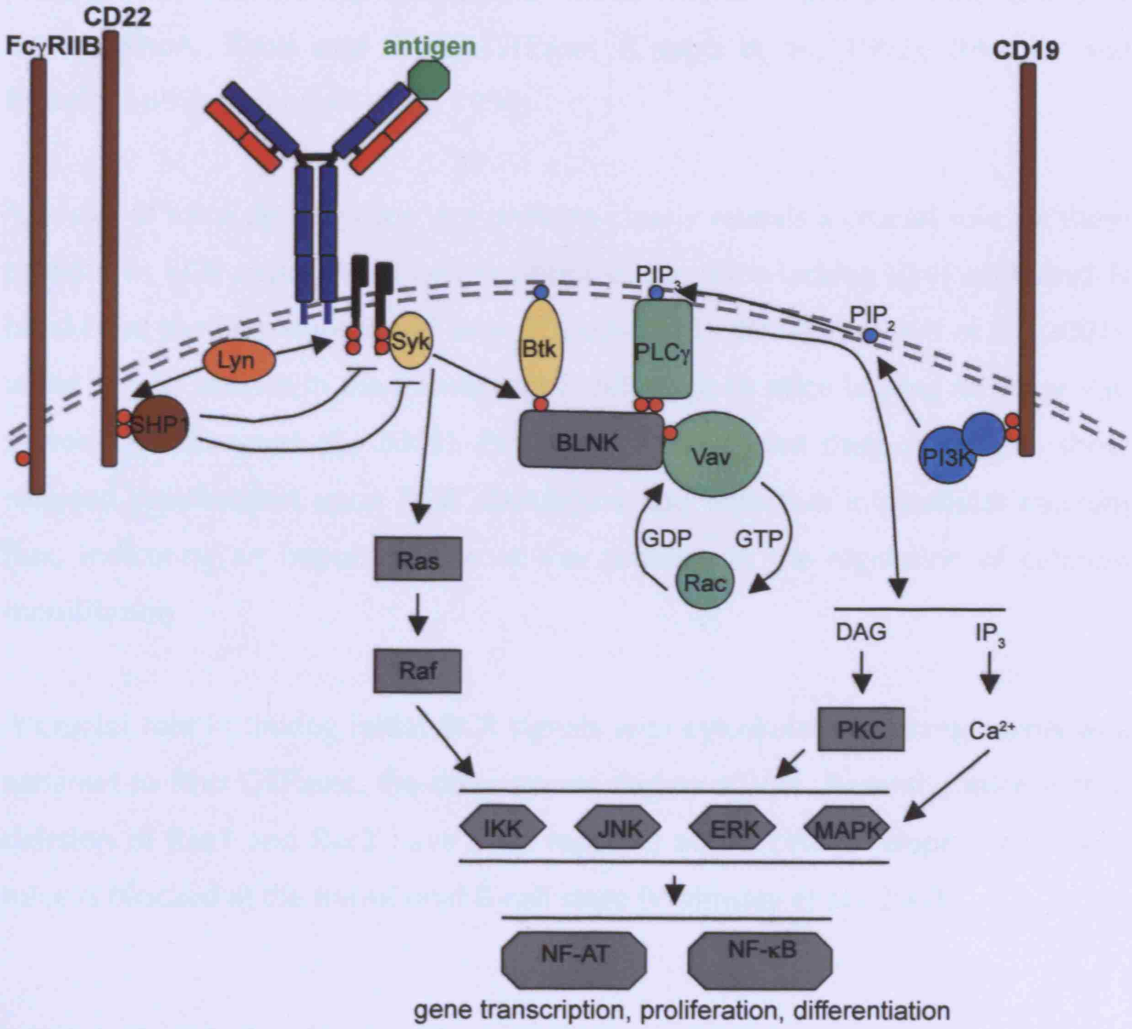

Figure 1.5 BCR signalling
This figure shows a simplified model of BCR-induced signalling pathways as described in chapter 1.3.2 of this Thesis. Adapted from Niiro and Clark, 2002.

The family of Vav proteins consists of three known members; Vav1, Vav2 and Vav3. The expression of Vav1 seems to be limited to cells of the haematopoietic system, whereas Vav2 and Vav3 are expressed more ubiquitously (Katzav et al., 1989), (Schuebel et al., 1996), (Movilla and Bustelo, 1999). Vav1 is suggested to preferentially activate Rac1, Rac2 and RhoG, whereas Vav2 and Vav3 primarily act on RhoA, RhoB and RhoG GTPases (Crespo et al., 1997), (Movilla and Bustelo, 1999), (Schuebel et al., 1998).

Analysis of mice deficient for Vav proteins clearly reveals a crucial role for these proteins in BCR signalling. B cell development in mice lacking Vav1 and Vav2 is blocked at the immature B cell stage (Doody et al., 2001), (Tedford et al., 2001), while B cells remain in the transitional B cell stage in mice lacking all three Vav proteins (Fujikawa et al., 2003). Peripheral B cells from these mice also show reduced proliferation upon BCR stimulation and defective intracellular calcium flux, indicating an important role of Vav proteins in the regulation of calcium mobilisation.

A crucial role in linking initial BCR signals with cytoskeletal rearrangements was assigned to Rho GTPases, the downstream targets of Vav. Recently, mice with a deletion of Rac1 and Rac2 have been reported and B cell development in these mice is blocked at the transitional B cell stage (Walmsley et al., 2003).

1.3.2.3 Phosphoinositide-3 Kinases (PI3Ks)

PI3Ks are a family of proteins that regulate a variety of biological functions by generating second messenger lipids. The family of PI3Ks can be subdivided into three classes: class I, class II and class III. Little is known about the role of class II and class III PI3K in B cells. Class I PI3K however are well characterised and can be further subdivided into class IA and class IB, which are activated downstream of the BCR and G-protein coupled receptors, respectively (Okkenhaug and Vanhaesebroeck, 2003).

Class IA PI3K are heterodimeric proteins, consisting of a regulatory subunit (p85α, p85β or p55γ) and a catalytic subunit (p110 α, p110 β or p110δ). Upon antigen recognition by the BCR, SFKs phosphorylate CD19 and B cell adaptor for PI3K (BCAP), which provide docking sites for the SH2 domain of the PI3K regulatory subunit (Wang et al., 2002), (Tuveson et al., 1993). By this mechanism, the regulatory subunit mediates the recruitment of the catalytic subunit to the plasma membrane, where it converts phosphatidylinositol-(4,5)-bisphosphate (PIP_2) to phosphatidylinositol-(3,4,5)-triphosphate (PIP_3). PIP_3 in turn acts as a binding site for numerous intracellular proteins that contain PH domains with selectivity for this lipid and so contributes to their recruitment and activation of downstream signalling cascades.

While p110α and p110β are ubiquitously expressed, the expression of the catalytic subunit p110δ is mainly restricted to leukocytes (Vanhaesebroeck et al., 1997), (Chantry et al., 1997). Studies using gene targeted mice suggest an essential role for p110δ in BCR signalling, as B cells from these mice proliferate poorly upon BCR stimulation and exhibit defective intracellular calcium flux (Okkenhaug et al., 2002), (Clayton et al., 2002), (Jou et al., 2002).

1.3.2.4 Phospholipase Cγ (PLCγ)

There are two PLCγ isoforms expressed in B cells: PLCγ1 and PLCγ2, the latter being most abundant, and both isoforms appear to participate in BCR signalling (Hempel et al., 1992), (Carter et al., 1991). Several molecules contribute to the activation of PLCγ upon BCR engagement. It is suggested that phosphorylation of B cell linker protein (BLNK), as well as recruitment of Btk to the plasma membrane are required for PLCγ phoshphorylation and activation of its effector function (Fu et al., 1998), (Kurosaki and Tsukada, 2000), (Rodriguez et al., 2001), (Hashimoto et al., 1999).

Activation of PLCγ results in the hydrolysis of PIP_2 and the production of soluble inositol-(1,4,5)-triphosphate (IP_3) and membrane-anchored diacylglycerol (DAG). The binding of IP_3 to IP_3-receptors on the endoplasmatic reticulum membrane

induces the release of calcium from intracellular stores, while DAG binds and activates several isoforms of protein kinase C (PKCs). Both, the elevation of intracellular calcium and the activation of PKCs contribute to the activation of transcription factors, including nuclear factor-κB (NF-κB) and nuclear factor of activated T cells (NF-AT).

1.3.3 The Immunological Synapse (IS)

1.3.3.1 Formation of the IS

On the membrane of a resting B cell or T cell, a variety of surface proteins are randomly distributed. However, recognition of specific antigen displayed on the surface of an antigen presenting cell (APC) triggers rapid reorganisation of these cell surface proteins, resulting in the formation of a specialised junction at the APC-T cell or APC-B cell interface known as immunological synapse (IS) (Dustin et al., 1998), (Grakoui et al., 1999), (Monks et al., 1998), (Batista et al., 2001), (Carrasco et al., 2004), (Carrasco and Batista, 2006).

Using fluorescently labelled antibodies to image the T cell receptor (TCR) and the integrin LFA-1 in fixed APC-T cell conjugates, Kupfer and colleagues were the first to observe a segregation of these two receptors into defined membrane compartments. Confocal microscopy imaging showed that the TCR accumulates into a central domain accompanied by its intracellular effector PKC-Θ. LFA-1 was restricted to the periphery of the TCR and co-localised with talin. These discrete domains were named supramolecular activation cluster (SMACs), whereby the TCR accumulates in a central SMAC (cSMAC) and LFA-1 segregates into the peripheral SMAC (pSMAC) (Monks et al., 1998).

In the early 1980s, the development of the glass-supported planar lipid bilayer technology made it possible to examine the interaction of immune cells with membranes by fluorescence microscopy. Since then, these artificial lipid bilayers have been extensively used to characterise the interactions of cell surface

receptors and their ligands and have become an invaluable tool for immunological studies (Groves and Dustin, 2003).

Using T cells interacting with artificial lipid bilayers, in which flurophore-conjugated peptide-MHC and ICAM-1 were anchored, the group of Dustin showed the reorganisation of receptors in real time by confocal microscopy. This particular study revealed a nascent IS within seconds of contact of the T cell with the lipid bilayer, whereby ICAM-1 accumulates in a central zone and peptide-MHC engagement by the TCR is detectable in the periphery. During the next minutes, this pattern inversed drastically and resembled a mature IS, as previously described by Kupfer and colleagues (Grakoui et al., 1999).

Also cytotoxic T cells (CTLs) show a pattern of TCR and integrin reorganisation at the IS that is similar to the one described for helper T cells. The TCR and proteins regulating TCR signalling accumulate in the cSMAC. LFA-1 and talin are excluded from the central zone and form a pSMAC (Stinchcombe et al., 2001), (Potter et al., 2001). However, in contrast to the originally described structure of the IS, the cSMAC of CTLs seems to be divided into a domain of TCR-signalling complexes next to a domain of clustered cytotoxic granules (Stinchcombe et al., 2001).

The interaction of B cells with APCs or planar lipid bilayers bearing specific antigen has recently been described as a two-step spreading and contraction mechanism (Fleire et al., 2006). Thereby, membrane-antigen recognition triggers B cell spreading over the APC, thus allowing BCR-antigen engagement. This is followed by a contraction of BCR/antigen complexes into a cSMAC. BCR engagement also triggers binding of the integrins LFA-1 and VLA-4 to their ligands ICAM-1 and VCAM-1, respectively. This results in their segregation into a pSMAC (Carrasco et al., 2004), (Carrasco and Batista, 2006) (Figure 1.6). Importantly, interaction of LFA-1 with ICAM-1 and VLA-4 with VCAM-1 supported antigen aggregation at limited antigen densities and facilitated B cell activation (Carrasco et al., 2004), (Carrasco and Batista, 2006).

Also other signalling molecules and receptors segregate into distinct areas at the IS, where they might contribute to membrane-bound antigen recognition. The phosphatase CD45 for example is excluded from the IS, probably forming a distal SMAC (dSMAC). In addition, PLCγ2 and Ganglioside (GM1), a marker for lipid rafts, are accumulated in the cSMAC, from which the negative regulators CD22 and SHP-1 are excluded (Batista et al., 2001) (Figure 1.6).

1.3.3.2 Mechanisms Supporting IS Formation

The observation that cell surface proteins localise into distinct areas upon antigen recognition raises questions about how this segregation is achieved. The exact processes leading to the formation of an IS are elusive, however several mechanisms are suggested to be involved in IS formation in B and T cells.

During formation of a mature IS, rearrangements of the actin cytoskeleton are critical for receptor redistribution towards the T cell/APC interface, as this process can be blocked by treatment with inhibitors of actin polymerisation (Wulfing and Davis, 1998), (Fleire et al., 2006).
In this respect, Vav1 regulates conjugate formation between $CD8^+$ T cells and APCs by contributing to LFA-1 activation and F-actin polarisation (Ardouin et al., 2003). Although structural aspects of the IS were not affected in this particular study, another report suggests that Vav may play an important role for IS formation in $CD4^+$ T cells (Wulfing et al., 2000).
Downstream of Vav, activation of Rac2 and the Abi/Wave complex are required for actin polymerization upon TCR stimulation (Yu et al., 2001), (Zipfel et al., 2006), (Nolz et al., 2006), however their contribution to IS formation is unclear.
Although there is evidence suggesting that PI3K may be involved in the regulation of the cytoskeleton (Bach et al., 2006), no difference in conjugate formation with APCs could be observed, when T cells were treated with the PI3K inhibitor Wortmannin (Costello et al., 2002), (Harriague and Bismuth, 2002).

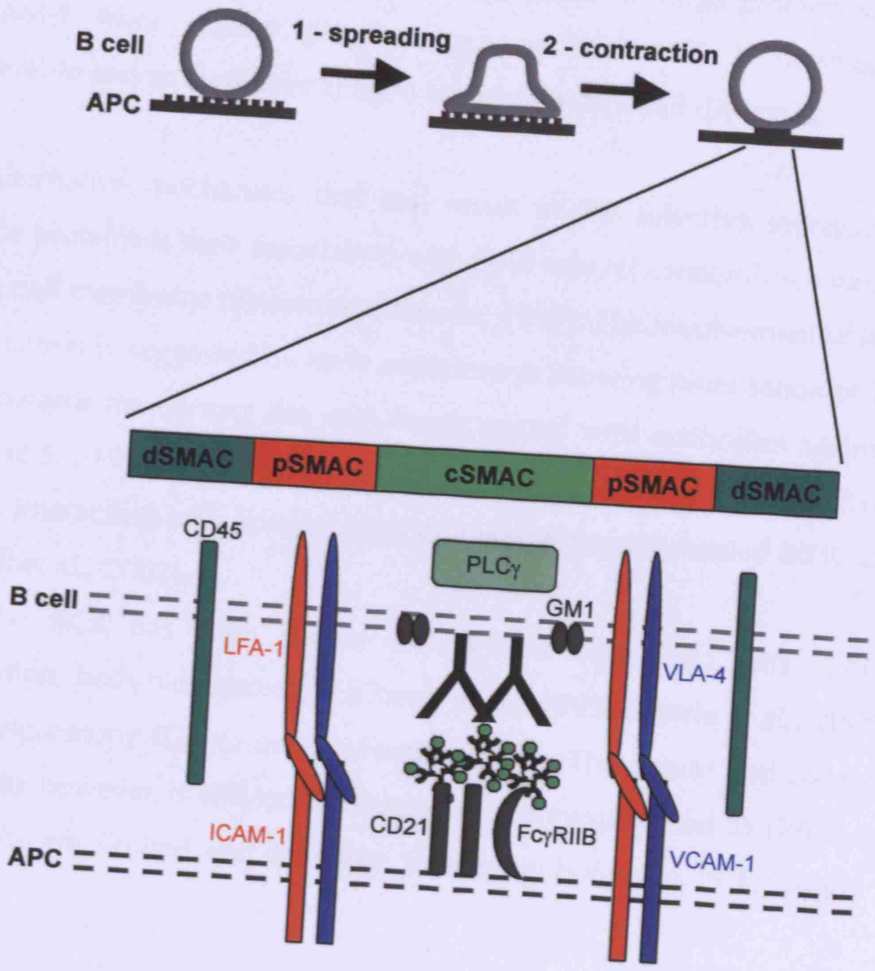

Figure 1.6 The Immunological Synapse (IS)
Recognition of membrane-bound antigen leads to the formation of an IS in a two step mechanism: The B cell spreads first over the antigen-presenting cell (APC) and this allows BCR-antigen engagement. The B cell then contracts BCR/antigen into a cSMAC. The integrins LFA-1 and VLA-4 bind to their ligands ICAM-1 and VCAM-1, respectively and form the pSMAC. PLCγ and Ganglioside 1 (GM1) are accumulated in the cSMAC. CD45 is excluded, probably forming a dSMAC. Adapted from Carrasco et al., 2006.

Another mechanism contributing to segregation of receptors at the IS was suggested by Chakraborty and colleagues, who predict the segregation of proteins of different sizes by mathematical modelling (Qi et al., 2001), (Chakraborty, 2002). According to this model, the segregation of large proteins such as LFA-1/ICAM-1 from smaller proteins such as TCR/MHC is thermodynamically favourable and so facilitates antigen recognition at small distances.

An alternative mechanism that can result in the selective segregation of cell surface proteins is their association with lipid rafts, cholesterol-rich microdomains in the cell membrane (Simons and Ikonen, 1997). The involvement of lipid rafts in IS formation is suggested by early experiments showing polarisation of T cell lipid rafts towards the contact site with beads coated with antibodies against the TCR (Viola et al., 1999). Furthermore, lipid rafts are enriched in the cSMAC of the IS in T cells interacting with lipid bilayers containing peptide-loaded MHC complexes (Burack et al., 2002).
Also the BCR has been shown to associate with lipid rafts upon antigen recognition, both biochemically (Cheng et al., 1999), (Petrie et al., 2000) and by using microscopy (Gupta and DeFranco, 2003). The nature and composition of lipid rafts however is still contradictory, as techniques used to detect or extract lipid rafts are limited and therefore their contribution to IS formation remains elusive.

Although cytoskeletal rearrangements, lipids raft and protein size may all contribute to the segregation of receptors at the T cell IS, the exact mechanism underlying its assembly remains unclear. It is also not know whether the same processes control B cell IS formation and this issue still needs to be investigated.

1.3.4 The Role of Other Receptors for B Cell Antigen Recognition

A mature IS forms several minutes after engagement of membrane-bound antigen. However, the initial mechanisms underlying antigen recognition by the BCR and the mechanisms contributing to functional B cell activation are to date unclear. It is likely that other receptors expressed by B cells can influence the antigen

recognition process and therefore modulate B cell activation, such as the complement-recognising B cell co-receptor complex CD19/CD21/CD81 or Toll-like receptors (TLRs).

Complement activation is essential for the early immune response to infection, whereby rapidly generated complement cleavage products are crucial for the elimination of pathogens. The complement receptor CD21 is expressed by B cells and recognises the iC3b, C3dg and C3d cleavage fragments of the C3 component of complement (Carroll, 1999). On the B cell surface, CD21 associates with the primary signalling component CD19 and the tetraspanin molecule CD81 (Poe et al., 2001). Several reports propose an important role for the CD19/CD21/CD81 complex for B cell activation and subsequent B cell responses (Fearon and Carroll, 2000), (Rickert, 2005). It has been shown that upon C3d-recognition, CD19 binds CD81 and CD21, as well as the BCR and augments B cell activation (Carter and Barrington, 2004). Although the significance of the engagement of CD19 or CD21 is not well understood, another report indicates that exposure to polymeric C3d results in BCR-induced proliferation (Carter and Fearon, 1989). Furthermore, co-engagement of CD21 and the BCR with C3d bound to antigen promotes CD19/CD21/CD81 translocation into lipid rafts, leading to augmentation and potentiation of B cell signal transduction events (Cherukuri et al., 2001).

TLRs are widely expressed on cells of the innate immune system. They recognize conserved microbial ligands such as bacterial lipopolysaccharide (LPS), lipopeptides or viral and bacterial RNA and DNA. In the last years, TLRs and their ligands have also emerged as important regulators of the adaptive immune responses. Some recent studies described TLR ligands, especially CpG-containing DNAs and LPS as critical modulators of B cell effector function, supporting B cell proliferation, differentiation and class switching (Pasare and Medzhitov, 2005), (Nemazee et al., 2006). Nevertheless, their function during B cell activation is not well understood and remains to be established in future studies.

1.4 Integrins

Integrins are cell surface receptors that control cellular interactions and cell migration. Because the ligands for integrins are widely expressed throughout the organism, cell adhesiveness has to be highly flexible and at the same time tightly regulated. In the immune system for example, B cells circulate through the body as non-adherent cells but rely on integrin function, whenever they transmigrate across the vasculature, recognise antigen in secondary lymphoid organs and form immunological synapses.

1.4.1 Integrin Structure

Integrins are heterodimeric integral membrane glycoproteins, which consist of non-covalently linked α and β subunits. At present, 18 α subunits and 8 β subunits have been identified in mammals, which give rise to 24 αβ pairs (Hemler, 1990). The two main integrins on B cells are LFA-1 ($\alpha_L\beta_2$) and VLA-4 ($\alpha_4\beta_1$). The ligands are ICAM-1, ICAM-2 and ICAM-3 for LFA-1 and VCAM-1 and fibronectin for VLA-4 (Springer, 1990).

A schema of the LFA-1 structure is depicted in Figure 1.7. Each α and β subunit consists of a large extracellular domain that together form a ligand-binding head region and two legs, which connect to a hydrophobic transmembrane domain and a short cytoplasmatic tail. The inserted (I) domain of the α_L subunit mediates binding to the ligand ICAM-1, and this requires the presence of a magnesium ion in the metal-ion-dependent adhesion site (MIDAS).

1.4.2 Affinity- / Avidity-Regulation of Integrins

Integrin activation is tightly regulated by a complex interplay between cation binding, intracellular signalling events and associations with the cell cytoskeleton. LFA-1 is perhaps the most widely studied integrin with respect to the mechanisms regulating integrin activation (Figure 1.7).

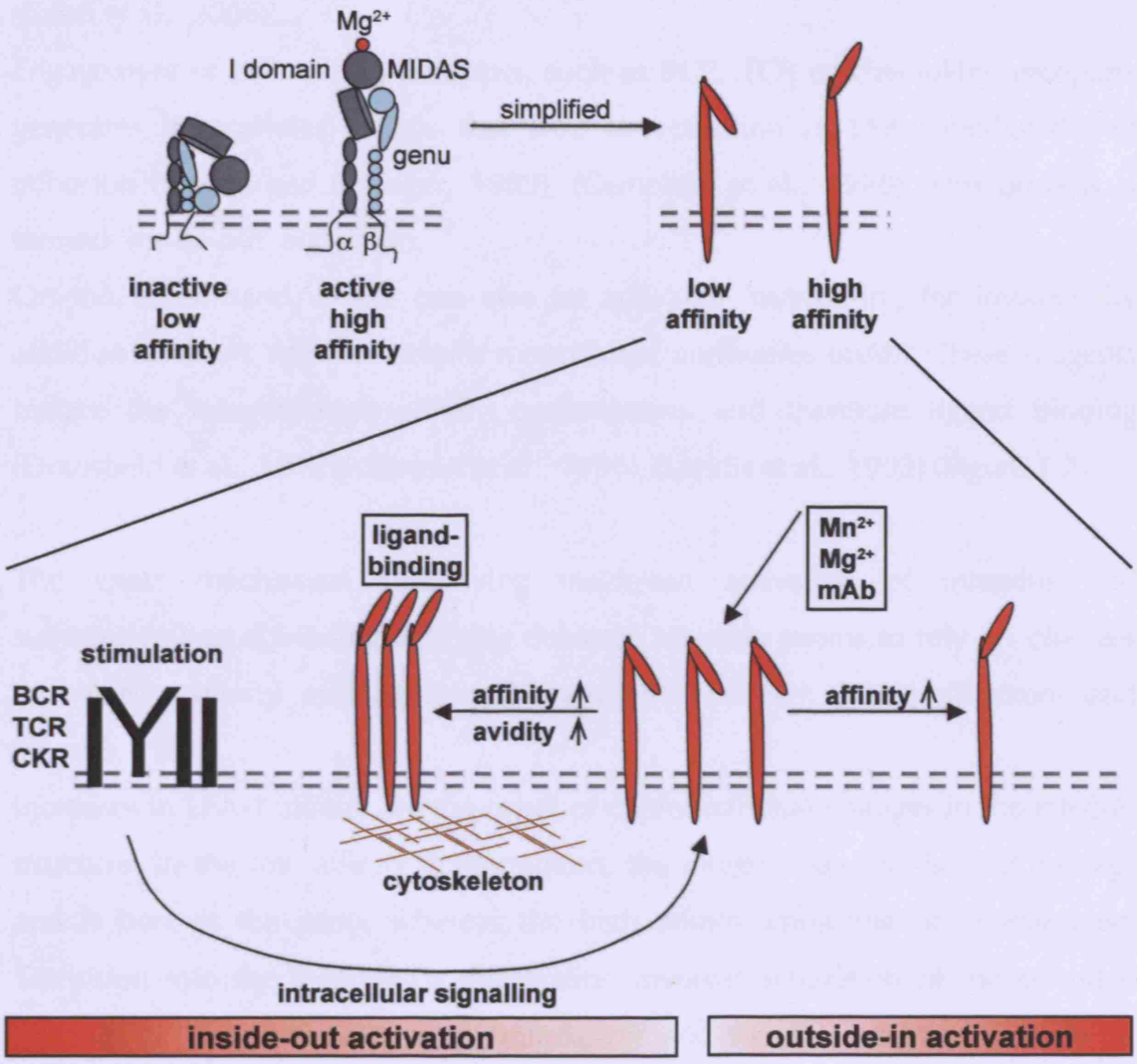

Figure 1.7 Regulation of LFA-1 activation
This figure summarises the processes leading to integrin activation, LFA-1 is used as example. On a resting B cell LFA-1 is maintained in an inactive, low affinity confomation. Stimulation of cell surface receptors, such as BCR, T cell receptor (TCR) or chemokine receptors (CKR), triggers inside-out activation of LFA-1 and ligand binding. Inside-out activation is a result of conformational changes in the LFA-1 structure leading to an increase in its affinity and cytoskeleton-dependent changes in the LFA-1 lateral distribution increasing its avidity. On the other hand, addition of Mn^{2+}, Mg^{2+} or certain monoclonal antibodies (mAb) induce the LFA-1 high affinity conformation by outside-in activation.

On resting lymphocytes LFA-1 is maintained in an inactive state, partially mobile or immobilized by interaction with the cortical cytoskeleton (Lu et al., 2001), (Cairo et al., 2006).

Engagement of cell surface receptors, such as BCR, TCR or chemokine receptors generates intracellular signals that lead to activation of LFA-1-mediated cell adhesion (Dustin and Springer, 1989), (Campbell et al., 1998). This process is termed 'inside-out' activation.

On the other hand, LFA-1 can also be activated 'outside-in', for instance by addition of Mn^{2+}, Mg^{2+} or certain monoclonal antibodies (mAb). These reagents induce the integrin high affinity conformation and therefore ligand binding (Dransfield et al., 1992), (Stewart et al., 1996), (Landis et al., 1993) (Figure 1.7).

The exact mechanism underlying inside-out activation of integrins and subsequent ligand binding is highly debated, however seems to rely on changes in integrin affinity and avidity (Carman and Springer, 2003), (Bazzoni and Hemler, 1998).

Increases in LFA-1 affinity are the result of conformational changes in the integrin structure. In the low affinity conformation, the integrin head folds over the legs and is bent at the genu, whereas the high affinity conformation is extended. Transition into the extended conformation involves separation of the α and β subunits at their transmembrane, cytoplasmic and leg domains, which might be regulated by the small cytoskeletal protein Talin (Takagi et al., 2002), (Kim et al., 2003). These events lead to the switchblade-like extension of the integrin and support ICAM-1 binding (Shimaoka and Springer, 2003) (Figure 1.7).

The high affinity conformation of LFA-1 is necessary for ligand binding (Kim et al., 2004), however under physiological conditions, such as cell-to-cell interactions, engaged integrins become aligned at the site of contact (Dustin et al., 1997). Therefore also LFA-1 avidity, e.g. its lateral mobility, contributes to cell adhesion. It is suggested that lateral mobility is regulated by interactions of the integrin cytoplasmatic domains with the cytoskeleton (Liu et al., 2000). In this line, addition of artificial agents that mimic intracellular signals, such as phorbolesters, increases LFA-1 mobility and this results in enhanced adhesion (Kucik et al., 1996), (Jin and Li, 2002). Furthermore, LFA-1 has been shown to cluster upon

binding to multivalent ICAM-1 (Kim et al., 2004) and ligand-bound integrin is constrained by cytoskeletal attachment (Peters et al., 1999). Although a lot of effort has been made in determining the role of the cytoskeleton to LFA-1 activation, the exact mechanism remains elusive.

On the basis of today's knowledge of integrin regulation and additional experiments, Cairo et al. now suggest the following model of LFA-1 activation (Cairo et al., 2006): On the resting lymphocyte, LFA-1 is maintained in an inactive state, partially mobile or immobilised by interaction with the cortical cytoskeleton. Activation of the cell results in release of the immobile fraction of LFA-1 from cytoskeletal constraints and reattachment to the cytoskeleton upon ligand binding.

The signalling molecules contributing to inside-out activation of integrins have mainly been investigated in T cells, however only recently they are starting to be examined in B cells. During the course of the here presented study, a number of molecules have been implicated in regulating VLA-4-mediated B cell adhesion, including Lyn and Syk, PI3K, Btk, PLCγ2, IP_3-receptor mediated calcium release and PKC (Spaargaren et al., 2003). Adhesion of B cells to ICAM-1 and VCAM-1 is unaffected in the absence of adhesion and degranulation promoting adaptor protein (ADAP), although ADAP is required for T cell adhesion (Griffiths et al., 2001), (Peterson et al., 2001). Furthermore, similar to Src-kinase-associated phosphoprotein of 55kDa (SKAP-55) in T cells, the SKAP-55 homologue (SKAP-HOM) is shown to regulate B cell adhesion to ICAM-1 and fibronectin (Togni et al., 2005). Recent reports also reveal the involvement of the Rap GTPases in regulating integrin activation downstream of BCR engagement (McLeod et al., 2004), (Duchniewicz et al., 2006) and it is tempting to speculate that this is mediated through the regulator of cell adhesion and polarisation enriched in lymphoid tissues (RAPL), as it has been described for T cells (Katagiri et al., 2003).

Although these studies reveal a partial picture of inside-out mechanism leading to integrin activation in B cells, it is unknown whether and how these events support the formation of a mature IS.

1.5 Aims

Our current knowledge of the signalling mechanisms leading to B cell activation mostly originates from biochemical studies and stimulation of B cells with soluble antigens. In recent years, however, the importance of membrane-tethered antigens became more and more clear, as these are more efficient in supporting B cell activation and may be the main form of antigen recognised *in vivo*. Membrane-bound antigen recognition triggers B cell spreading an the formation of the IS, which is characterised by a segregation of BCR and integrins into defined domains.

While much is known about the signalling mechanism initiated by antigen recognition in B cells, evidence linking these pathways to integrin activation, B cell spreading and the formation of the IS is missing.

The aims of this Thesis are:

- to dissect the signalling mechanism leading to integrin activation downstream of the BCR.
- to determine how BCR signalling mediates B cell spreading and formation of the IS.
- to assess the role of integrins during the initial phase of membrane-antigen recognition, e.g. B cell spreading.

Special Note

Page 42 missing from the original

2 Materials and Methods

2.1 Materials

2.1.1 Antibodies

Abbreviations: CRUK Cancer Research UK, BD Becton Dickinson, MP Molecular Probes, SC Santa Cruz, IF immunofluorescence, WB Western Blot, FACS Fluorescence Activated Cell Sorting

Antibody	Conjugate	Species	Stock (mg/ml)	Supplier	Usage/ Dilution
anti mouse icam-1 YN1/1.7	none	rat IgG2a	1	CRUK	IF 1:50
anti-mouse CD106	none	rat IgG2a, clone 429	n/a	BD	n/a
anti-mouse CD11a	FITC	rat IgG2a	0.5	BD	FACS 1:200
anti-mouse CD45R/B220	FITC	rat IgG2a	0.5	BD	FACS 1:200
anti-mouse CD45R/B220	PE	rat IgG2a	0.5	BD	FACS 1:200
anti-mouse CD49d	PE	rat IgG2a	0.5	BD	FACS 1:400
anti-mouse CD86	FITC	rat IgG2a	0.5	BD	FACS 1:200
anti-mouse IgG1	Alexa Fluor 488	rat IgG	0.5	MP	IF 1:200
anti-mouse IgG-HRP	HRP	goat IgG	0.8	Pierce	WB 1:5000
anti-mouse IgM	PE	goat IgG	0.5	BD	FACS 1:400
anti-mouse IgM (μ chain)	none	goat IgG $F(ab')_2$	1.3	Jackson	5μg/ml
anti-mouse IgMa	biotin	goat IgG	1	BD	ELISA 1:1000
anti-Vav2	none	goat IgG (P-18)	0.2	SC	FACS 1:100
anti-Vav3	none	goat IgG (K-19)	0.2	SC	FACS 1:100
anti-Vav1	none	rabbit IgG (C-14)	0.2	SC	FACS 1:100

Antibody	Conjugate	Species	Stock (mg/ml)	Supplier	Usage/ Dilution
anti-rabbit IgG (H+L)-HRP	HRP	goat IgG	0.8	Pierce	WB 1:10000
anti-Rac1 (23A8)	none	mouse IgG2b	1	Upstate	WB 1:2000
anti-goat IgG (H+L)	Alexa Fluor 488	donkey IgG	2	MP	FACS 1:500
anti-Rac2	none	rabbit antiserum	n/a	Upstate	WB 1:2000
anti-Rap1 (sc-65)	none	rabbit IgG	0.2	SC	WB 1:1000
anti-rat IgG	Alexa Fluor 488	goat IgG	0.5	MP	IF 1:200
anti-mouse kappa (α-κ)	none	Rat IgG1	1	CRUK	IF 1:50
anti-pTyr (IG2)	none	mouse IgG1	0.5	CRUK	IF 1:200
anti-pTyr (PY7)	none	mouse IgG1	0.5	CRUK	IF 1:200

2.1.2 Inhibitors

Reagent	Supplier	Stock Solution	Storage
PP1 analog	Calbiochem	3.2mM in DMSO	4°C
PP2	Calbiochem	3.3mM in DMSO	4°C
LY294002	Calbiochem	3.2mM in DMSO	-20°C
Wortmannin	Sigma	2mM in DMSO	4°C
Protease Inhibitor Cocktail EDTA free Tablets	Roche	1 tablet was used for 50ml	4°C
Phalloidin-TRITC	Sigma	0.5mg/ml in methanol	-20°C

2.1.3 Reagents and Buffers

All chemicals were obtained from Sigma, unless otherwise indicated.

Buffer/Solutions	Composition
stacking gel (14%)	3.5ml 40% Acrylamide, 2.5ml stacking gel buffer, 0.1ml 10% SDS, 50µl 10% APS, 5µl TEMED, 3.9ml dH_2O

Buffer/Solutions	Composition
resolving gel (14%)	3.5ml 40% Acrylamide, 2.5ml resolving gel buffer, 0.1ml 10% SDS, 50µl 10% APS, 5µl TEMED, 3.9ml dH_2O
stacking gel buffer	0.5M Tris-HCl, pH6.8
resolving gel buffer	1.5M Tris-HCl, pH8.8
PBS/Tween	1xPBS, 1% Tween-20
$ELISA_{block}$	2% BSA, 0.01% Tween-20, 0.1% NaN_3 in 1xPBS
5x MLB	125mM HEPES pH7.5, 750mM NaCl, 5% Igepal CA-630, 50mM $MgCl_2$, 5mM EDTA, 10% glycerol, dH_2O
$FACS_{block}$	2% FCS, 0.1% NaN_3 in 1xPBS
LB medium	for 10 litres: 100g Bacto-Tryptone, 50g Yeast extract, 100g NaCl, 100 µg/ml ampiclillin, dH_2O
GST buffer	25mM Tris, pH8, 10% Glycerol, 1mM EDTA, 100mM NaCl, 1mM DTT, protease inhibitor, dH_2O
lysis buffer	25mM Tris-HCl pH8, 150mM NaCl, 0.1% NaN_3, 1% Triton-X-100, dH_2O
pre-elution buffer	25mM Tris-HCl pH8, 150mM NaCl, 2% octylglucoside, dH_2O
elution buffer	100mM Glycine pH3, 150mM NaCl, 2% octylglucoside, dH_2O
1x PBS	for 10litres: 80g NaCl, 2.5g KCl, 14.3g Na_2HPO_4, 2.5g KH_2PO_4, dH_2O, pH7.2
labelling buffer	100mM $NaHCO_3$ pH8.4, 150mM NaCl, 1% Triton-X-100, dH_2O
permeabilisation buffer	1x PBS, 0.2% Triton-X-100
Tris/NaCl	25mM Tris-HCl pH8, 150mM NaCl, dH_2O
$slide_{block}$	1x PBS, 1% BSA, 0.5% FCS, 0.5% goat serum, 0.05% Tween-20, 0.1% NaN_3
TAE, 50x	2M Tris, 1M acetic acid, 50mM EDTA, dH_2O
chambers blocking buffer	1xPBS pH7.4, 2mM Mg^{2+}, 0.5mM Ca^{2+}, 2% FCS, 1g/l D-glucose

Buffer/Solutions	Composition
adhesion buffer	1xPBS pH7.4, 2mM Mg^{2+}, 0.5mM Ca^{2+}, 0.5% FCS, 1g/l D-glucose
$RPMI_{complete}$	RPMI 1640 with Glutamax (Gibco), 10% FCS, 10mM HEPES (Gibco), 10units/ml penicillin/streptomycin (Gibco), 50µM 2-mercaptoethanol
Tail Juice	100mM NaCl, 50mM Tris-HCl pH8, 100mM EDTA, 1% SDS, dH_2O
DNA loading dye, 6x	10mM Tris-HCl pH8.5, 1mM EDTA, 0.25% Bromphenol blue, 40% Sucrose, dH_2O
SDS-PAGE buffer, 4x	10% glycerol, 62.5mM Tris-HCl pH6.8, 2% SDS, 0.01mg/ml Bromphenol blue, 2% 2-mercaptoethanol, dH_2O
Running buffer	for 1 litre: 144g Glycine, 30g Tris, 10g SDS, dH_2O
Blotting buffer	for 1 litre: 144g Glycine, 30g Tris, dH_2O

2.2 Mice

2.2.1 Transgenic Mouse Lines

Naïve B cells isolated from the spleen of the following transgenic mouse lines were used for this study:

Mouse Line	Background	Reference
WT	C57BL/6	www.criver.com
$CD19^{cre/+}$ WT	C57BL/6	(Rickert et al., 1997)
$Lyn^{-/-}$	C57BL/6	(Hibbs et al., 1995)
MD4 WT	C57BL/6	(Goodnow et al., 1988)
$p110\delta^{-/-}$	C57BL/6 or MD4	(Clayton et al., 2002)
$Rac1^{fx/fx}$	$CD19^{cre/+}$, C57BL/6	(Walmsley et al., 2003)
$Rac2^{-/-}$	$CD19^{cre/+}$, C57BL/6	(Roberts et al., 1999)
$SKAP\text{-}HOM^{-/-}$	C57BL/6	(Togni et al., 2005)
$Vav1^{-/-}$	C57BL/6 or MD4	(Turner et al., 1997)

Mouse Line	Background	Reference
$Vav1^{-/-}$ $Vav2^{-/-}$	C57BL/6 or MD4	(Doody et al., 2001)
$Vav1^{-/-}$ $Vav2^{-/-}$ $Vav3^{-/-}$	C57BL/6 or MD4	(Fujikawa et al., 2003)
$Vav2^{-/-}$	C57BL/6 or MD4	(Doody et al., 2001)
$Vav3^{-/-}$	C57BL/6 or MD4	(Fujikawa et al., 2003)

2.2.2 Animal Husbandry

All animal care and breeding was carried out at the Biological Resource Unit Cancer Research UK.
Mice were maintained in accordance with UK Home Office guidelines.

MD4 mice were maintained as heterozygous for MD4 on a C57BL/6 background.

$Vav1^{-/-}$, $Vav2^{-/-}$ and $Vav1^{-/-}Vav2^{-/-}$ mice were imported from Dr. Martin Turner (Babraham Institute, Camebridge, UK), crossed into the MD4 C57BL/6 background and maintained as heterozygous for MD4 and homozygous for the deletion of Vav1, Vav2 or Vav1/Vav2.

Spleens from the following mice were provided at the day of the experiment:

- $Lyn^{-/-}$: Dr. Edina Schweighoffer / Dr. Victor Tybulewicz (NIMR, London, UK)
- $CD19^{cre/+}$ WT, $Rac1^{fx/fx}$, $Rac2^{-/-}$: Dr. Robert Henderson / Dr. Victor Tybulewicz (NIMR, London, UK)
- SKAP-$HOM^{-/-}$: Dr. Mauro Togni / Dr. Burkhart Schraven (Otto von Guerike University, Magdeburg, Germany)
- $p110\delta^{-/-}$ (C57BL/6 or MD4): Dr. Martin Turner (Babraham Institute, Cambridge, UK)
- $Vav3^{-/-}$, $Vav1^{-/-}Vav2^{-/-}Vav3^{-/-}$ (C57BL/6 or MD4): Dr. Elena Vigorito / Dr. Martin Turner (Babraham Institute, Cambridge, UK)

2.2.3 Genotyping $Vav1^{-/-}$, $Vav2^{-/-}$ and $Vav1^{-/-}Vav2^{-/-}$ Mice by Polymerase Chain Reaction (PCR)

2.2.3.1 Purification of DNA from Mouse-Tail

5mm of mouse-tail was incubated at 37°C over night with 750µl tail juice containing 200µg/ml Proteinase K (20mg/ml stock solution, Qiagen) in Eppendorf tubes. 250µl of a saturated NaCl solution was added and mixed gently. Tubes were centrifuged in a microfuge at 13000rpm for 10 minutes at 4°C. The supernatant was transferred into a new tube and mixed gently with 500µl isopropanol. DNA was pelleted by centrifugation at 13000rpm in a microfuge for 10 minutes at 4°C. Pellet was washed with 800µl 70% ice-cold ethanol and centrifuged at 13000rpm at 4°C. Ethanol was removed and the pellet left to air dry prior to being dissolved in 100µl dH_2O.

2.2.3.2 Primers

Vav1F1	T_m 57.5°C - GAGCTGTTCTCTGTGCATAC
Vav1R1	T_m 60.1°C - CTAGAATTCCCCAAGTCCTG
Vav2F1	T_m 54.1°C - CTAGACACACCTGCTAGAAG
Vav2R1	T_m 65.0°C - CCATCATGGACACATCGATG
PGK3	T_m 53.4°C – AGACTAGTGAGACGTGCTAC

2.2.3.3 PCR Progamm

2 minutes - 95°C

REPEAT THE FOLLOWING STEPS FOR 30 CYCLES

30 seconds - 95°C

30 seconds - 54°C

1 minute - 72°C

FINISHING

5 minutes - 72°C and hold at 4°C

2.2.3.4 PCR Protocol

PCR reactions were set up in PCR strips (ABgene). The PCR reaction mix consisted of: 1µl purified mouse-tail DNA, 200ng of each primer, 1unit PicTaq Polymerase (Cancer Research UK), 1x Thermophilic Polymerase DNA Buffer (Promega), 1.5mM $MgCl_2$ (Promega), 200µM dATP/dGTP/dCTP/dTTP (Promega) in a final volume of 20µl. PCR programs were run on a Peltier Thermal Cycler (Biorad).

2.2.3.5 Agarose Gel Electrophoresis

1xTAE buffer containing 1.5% agarose (Life Technologies) was heated in a microwave, with intermittent mixing, to dissolve the agarose. The solution was allowed to cool down prior to addition of ethidium bromide (4µl in 100ml). The solution was then cast in a mould (Jencons) and allowed to set. DNA loading dye was added to PCR reactions at a 1:5 dilution and 20µl of each sample was loaded per agarose well. DNA was electrophoresed at 120V in 1xTAE buffer.

2.2.4 Genotyping MD4 Mice by Enzyme-Linked Immunosorbent Assay (ELISA)

MD4 mice and MD4 $Vav1^{-/-}$, MD4 $Vav2^{-/-}$ and MD4 $Vav1^{-/-}Vav2^{-/-}$ mice were genotyped by detecting antigen-specific antibodies in blood samples of the mice using ELISA. 96-well immunoplates (Maxisorp Immuno Plate, Nunc) were coated with 90µl per well of a 1mg/ml hen egg lysozyme (HEL) solution for 1 hour at 37°C and blocked with 200µl per well $ELISA_{block}$ for 1 hour at room temperature (RT). Blood samples were centrifuged in a microfuge at 13000rpm for 10 minutes at 4°C to separate the serum and 1:10 and 1:100 dilutions of the serum were prepared. 80µl per well of these dilutions were incubated in the plates for 1 hour at RT. Specific antibodies captured by the HEL were detected by incubating sequentially with a biotinylated anti-mouse IgMa antibody, streptavidin-alkaline phosphatase conjugate (Extravidin-AP, Sigma) and the substrate (alkaline phosphatase yellow (pNPP) susbstrate tablets, Sigma).

2.3 Cell Culture

2.3.1 Cell Culture Conditions

Primary naïve B cells, B cell lines and transient transfected B cell lines were cultured in $RPMI_{complete}$ at 37°C and 5% CO_2. Stably transfected B cell lines were grown in $RPMI_{complete}$ and 0.5mg/ml HygromycinB (Invitrogen).

2.3.2 Isolation of Naïve B Cells from Mouse Spleens

Naïve B cells were isolated by negative selection from the spleens of at least 3 months old mice on the day of the experiment. Spleens were disrupted on a cell strainer (70µm, BD Falcon) with a syringe plunger and total splenocytes were washed with 10ml 1xPBS. Lymphocytes from the splenocyte suspension were enriched with Lympholyte-M (Cedarlane Laboratories), remaining red blood cells were in lysed in 1ml Tris/ammonium buffer, T cells were depleted by incubation with Dynabeads mouse pan-T (Dynal Biotech ASA, Oslo, Norway) for 30 minutes at 4°C. The B cells were then incubated in 15ml of $RPMI_{complete}$ in 10mm round plates (Falcon) for 1 hour at 37°C to allow settling of the macrophages on the plastic. The obtained population contained 90-95% B cells as assessed by FACS using anti-mouse B220 and anti-mouse IgM specific antibodies (Figure 2.1)

2.3.3 Cell Lines

2.3.3.1 Cell Lines

- A20: B cell lymphoma (Kim et al., 1979)
- A20-1158: A20 B cells expressing a HEL-specific BCR (Williams et al., 1994).
- H2: A20 B cells expressing a HEL-specific BCR that consists of the mIg fused to the transmembrane domain of the MHC molecule. mIg cannot associate with Igα and Igβ and the B cells are therefore signalling deficient (Williams et al., 1994).

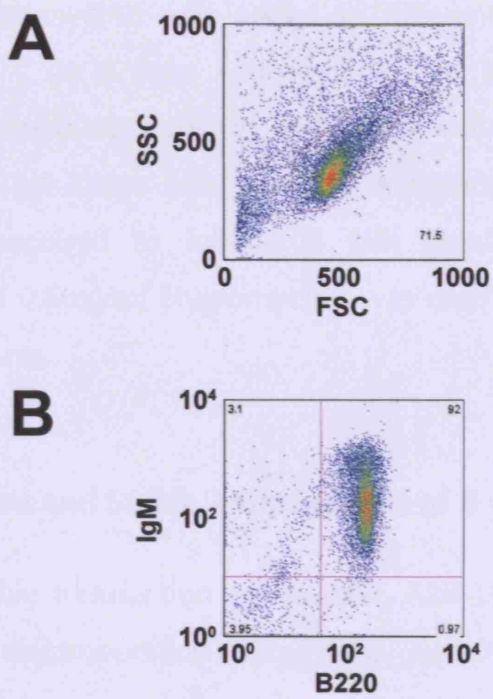

Figure 2.1 Purification of B cells from mouse spleen
(A) Flow cytometric analysis of the cell population obtained from a MD4 mouse spleen. **(B)** Analysis of B220 and IgM expression levels from cells falling into the gate shown in **(A)**. Numbers show percentages of cells falling into the indicated gates. Mature naive B cells are IgM^+ and $B220^+$ (92%).

2.3.3.2 Optimisation of the HygromycinB Concentration for B Cell Selection

To obtain the optimal concentration of HygromycinB for the selection of stably transfected A20 or H2 B cells (see section 2.3.3.3 below), $3x10^4$ A20-1158 B cells were plated into each well of a 6-well tissue culture plate (Falcon) in 5ml $RPMI_{complete}$. HygromycinB was added in different amounts and B cells were incubated at 37°C for 8 days. A dose-dependent killing curve was obtained by counting the remaining cells in the wells with different concentrations of HygromycinB. This curve was used to determine the minimal HygromycinB concentration required to induce B cell dead (Figure 2.2). The optimal concentration of 0.5mg/ml HygromycinB was used for the selection of B cells in further experiments.

2.3.3.3 Transient and Stable Transfections of B Cell Lines

Transient or stable transfection of the A20, A20-1158 and H2 B cell lines was facilitated by electroporation using the transfection system from Amaxa Biosystems, which permeabilizes the cells with an electrical pulse, allowing uptake of the DNA.

$2x10^6$ A20 B cells were centrifuged at 200xg for 10 minutes at 4°C and resuspended in 100µl of Nucleofector Solution V (Amaxa Biosystems) containing DNA. The cells were then placed in an electroporation cuvette (Amaxa Biosystems) and subjected to electroporation using the Nucleofector device (Amaxa Biosystems) according to manufacturer's instructions (program L-13).

For transient transfections, the cells were then plated into a 10mm round plate (Falcon) in $RPMI_{complete}$ and used 8-24 hours later in experiments.

For stable transfections, the cells were mixed with 50ml $RPMI_{complete}$ and plated into 5 96-well tissue culture plates (Falcon) at 100µl per well. After 24 hours, another 100µl $RPMI_{complete}$ containing 1mg/ml HygromycinB (Invitrogen) were

added to each well to obtain a final concentration of 0.5mg/ml HygromycinB. Single clones were selected after 3 weeks of culture, screened for expression of GFP by FACS and positive clones were expanded.

2.3.4 Cell Treatment with Inhibitors

B cells were treated with the Src-family tyrosine kinase inhibitors PP1 analog (PP1) and PP2 (both 100µM), the PI3K inhibitors Wortmannin (100nM) and LY294002 (50µM) in adhesion buffer for 30 minutes at 37°C. B cells were used for experiments in the presence of the inhibitor.

2.3.5 Fluorescence Activated Cell Sorting (FACS) Analysis

B cells or B cell lines were incubated with the indicated antibodies in $FACS_{block}$ for 20 minutes on ice. Cells were then washed twice with 1xPBS and subjected to FACS analysis using FACSCalibur cytometer (Becton, Dickinson and Company) and the Flowjo software (Tree Star). Unstained and single-fluorochrome controls were used to set voltages and compensation for each experiment.

2.4 Lipid Bilayer Technology

2.4.1 Preparation of Liposomes

Liposomes were prepared from 1,2-dioleoyl-sn-glycero-3-phosphocholine (DOPC) and 1,2-dioleoyl-sn-glycero-3-phosphoethanolamine-N-(Cap Biotinyl) (N-biotinyl Cap-PE). Both lipids were purchased from Avanti Polar Lipids as 10mg/ml stock solutions dissolved in chloroform. The DOPC solution was either mixed in a 1:50 molar ratio with N-biotinyl Cap-PE solutions or was not mixed and chloroform was evaporated using N_2. Remaining traces of chloroform were removed by application of a high vacuum for 4 hours. The dried lipids were then resuspended in Tris/NaCl buffer containing 2% octylglucoside to obtain 4mM (10x stock) lipid solutions and sonicated until clear.

The lipid solutions were then diluted 1:10 with Tris/NaCl buffer containing 2% octylglucoside, filtered (0.22 µm, Millipore) and dialysed against octylglucoside-free buffer Tris/NaCl buffer for 36 hours with buffer exchange every 12 hours to remove the detergent and to generate the liposomes.

2.4.2 Purification of GPI-linked ICAM-1 and VCAM-1

ICAM-1 and VCAM-1 were produced as GPI-linked proteins on the cell membranes of L cells as previously described (Carrasco et al., 2004), (Carrasco and Batista, 2006).

Approximately 5g of L cells expressing GPI-linked ICAM-1 or GPI-linked VCAM-1 were solubilised in lysis buffer in the presence of protease inhibitors (Complete EDTA-free tablets, Roche Diagnostics). The lysate was incubated with mild rotation for 1 hour at 4°C and particulate matter were eliminated by centrifugation at 1000xg for 10 minutes. The supernatant was then incubated for another 1 hour at 4°C in the presence of 0.5% deoxycholate and cleared by ultracentrifugation at 100000xg for 1 hour.

In the meantime 1-2mg of anti-ICAM-1 (YN1/1.7) or anti-VCAM-1 (CD106) antibody were coupled in a NHS-activated HiTrap 1 ml column according to manufacturer's instructions (Amersham Bioscience). The lysate was then loaded onto this column using the Aekta (Amersham Bioscience) at a flow rate of 0.1-0.3ml/minute at 4°C.

Labelling of the proteins was carried out at this point (see section 2.4.3 below).

The column was washed with 15 column volumes of lysis buffer containing 0.5% deoxycholate and equilibrated with pre-elution buffer. Elution was performed with an acidic elution buffer and the fractions (10 x 1 ml each) were collected in 1M Tris (pH8) to neutralize the pH.

Fractions containing the protein were pooled, reconstituted with the 10x stock of DOPC liposomes in a ratio of 10:1, and detergent was removed by dialysis (see section 2.4.1 above).

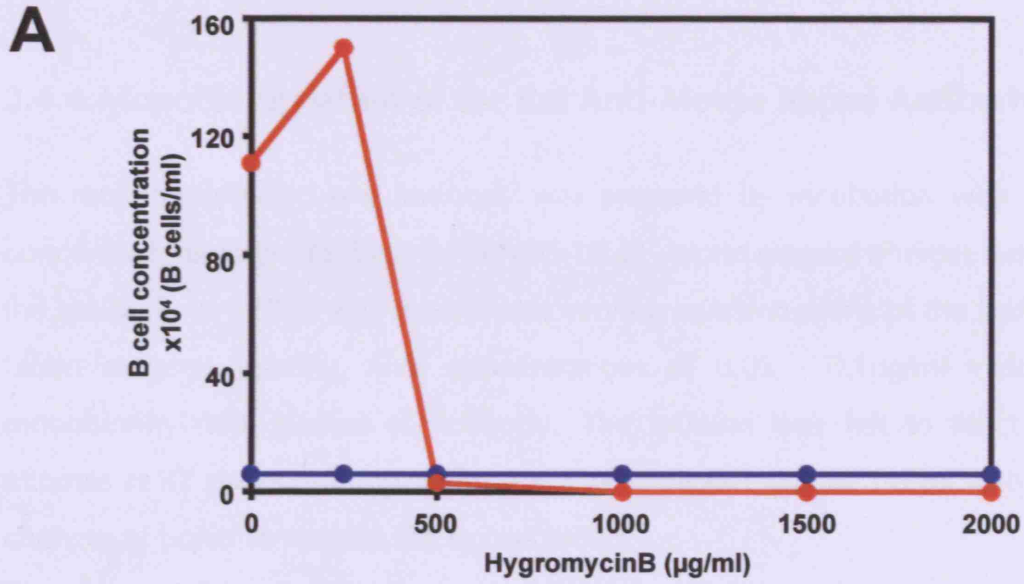

Figure 2.2 HygromycinB Killing Curve
(A) $6x10^4$ A20-1158 B cells per milliliter were plated into a 6-well tissue culture plate (blue line). B cells were treated with different concentrations of HygromycinB and incubated for 8 days. Remaining cells were counted (red line). Concentration used for further experiments is 0.5mg/ml HygromycinB.

2.4.3 Labelling of GPI-linked ICAM-1 and VCAM-1

The column, described in section 2.4.2 above, was equilibrated with labeling buffer. 200-400μg of Alexa Fluor 532 succinimidyl ester (5mg/ml stock in DMSO, Molecular Probes) were injected into the column using syringes at both ends, mixed and incubated for 1 hour at RT. The protein-labeling reagent was then washed out with labeling buffer and then the column was equilibrated with lysis buffer.

2.4.4 Monobiotinylation of the Rat Anti-Mouse Kappa Antibody, α-κ

The monobiotinylated α-κ antibody was prepared by incubation with limiting concentrations of the EZ-Link sulfo-NHS-LC-LC-biotin reagent (Pierce). 1mg/ml of the antibody in 1xPBS was mixed with varying concentrations of the sulfo-NHS-biotin reagent. Usually, final concentrations of 0.03 - 0.1μg/ml yielded the monobiotinylated species of antibody. The mixture was left to react for 30 minutes at RT protected from light, and then dialyzed against 1xPBS with several changes of buffer to remove the excess biotin.

The degree of biotinylation was evaluated by FACS, using streptavidin-coated beads (Bangs Laboratories, Inc.). Briefly, 1μl of beads were mixed with 100μl of a dilution 1:50 of the biotinylated α-κ antibody. The mixture was incubated for 20 minutes at RT with agitation, to prevent the beads from settling in the bottom of the tube, and then washed once. The beads were then incubated with 100 μl of Alexa Fluor 633-conjugated streptavidin and an Alexa Fluor 488-conjugated goat anti-rat IgG antibody for 20 minutes at RT with agitation. After washing, the beads were analyzed by FACS. The monobiotinylated α-κ antibody can be distinguished from a polybiotinylated one by the levels of Alexa Fluor 633-conjugated streptavidin staining (Figure 2.3).

This method was also used for the preparation of monobiotinylated HEL (Sigma).

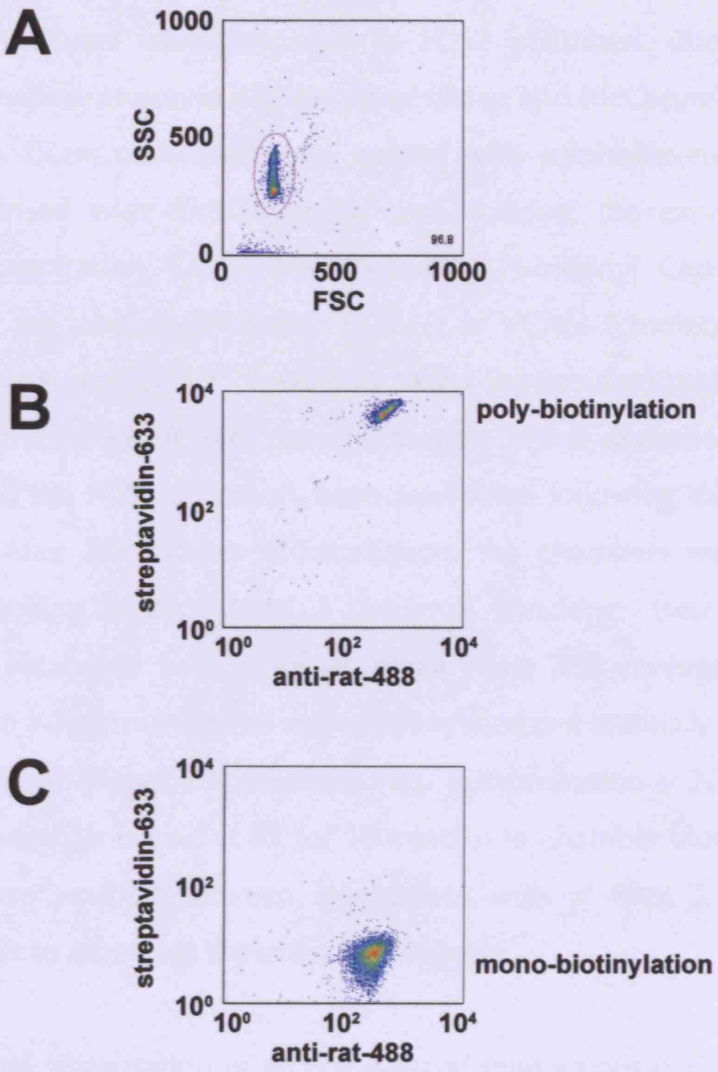

Figure 2.3 Testing the biotinylation of the α-κ antibody
(A) Flow cytometric analysis of the population of streptdavidin-coated beads. Beads were incubated with **(B)** a poly-biotinylated and **(C)** a mono-biotinylated α-κ antibody, followed by detection of the α-κ with a Alexa Fluor 488 goat anti-rat IgG and the free biotin with Alexa Fluor 633 streptavidin. **(B)** and **(C)** show the analysis of the anti-rat-488 and streptdavidin-633 staining of beads falling into the gate shown in **(A)**.

2.4.5 Assembling of Lipid Bilayers in FCS2 Chambers

Planar lipid bilayers were prepared in FCS2 chambers (Bioptechs Inc.) by liposome spreading as previously described (Brian and McConnell, 1984), (Dustin et al., 1996). Glass coverslips were treated with sulphochromic solution over night, and rinsed with distilled water and acetone; the excess acetone was removed by aspiration. Liposomes containing N-biotinyl Cap-PE (biotinylated lipids) and/or the labeled GPI-linked ICAM-1 or VCAM-1 molecules were mixed at different ratios with DOPC liposomes to get the required molecular densities. Then, liposome drops (0.8µl per membrane) were deposited on the glass coverslips and the FCS2 chambers were assembled following the manufacturer's instructions. After 20 minutes of incubation, the chambers were flushed with chamber blocking buffer. After 1 hour of blocking, the chambers were successively incubated with 1 ml of Alexa Fluor 633-conjugated streptavidin (concentration ≈ 1µg/ml), 1 ml of monobiotinylated α-κ antibody (concentration ≈ 50µg/ml) or 1 ml of monobiotinylated HEL (concentration ≈ 200ng/ml). All the incubations were performed at RT for 20 minutes in chamber blocking buffer. The chambers were washed between incubations with at least 3 ml of chamber blocking buffer to eliminate the excess of reagents.

For the optimal visualisation of receptor-ligand interactions during the contact of B cells with the lipid bilayers, it is essential that all proteins can freely diffuse. Monobiotinylation of the α-κ antibody or HEL is necessary to keep the lipid bilayer in a fluid state. A polybiotinylated α-κ antibody or HEL molecule would cross-link several molecules of Alexa Fluor 633-conjugated streptavidin resulting in the formation of static protein clusters and the decrease of free diffusion of proteins.

2.4.6 Experiments on Lipid Bilayers

2.4.6.1 Determining the Density of Molecules

The density of antigen was estimated as the density of monobiotinylated α-κ antibody on the surface of the artificial lipid bilayers. This was determined with a fluorometric assay using calibrated beads (Bangs Laboratories). These beads have 5 populations with different antibody binding capacities (ABC, 4 plus the negative control); this value represents the number of molecules of mouse or rat IgG that each population binds. To estimate the density, the beads were incubated in $FACS_{block}$ with saturating concentrations of the α-κ (20μg of antibody/drop of beads, final volume = 100μl) for 20 minutes. The beads were then washed and incubated with an Alexa Fluor 488-conjugated goat anti-rat antibody (10μg of antibody, final volume = 100μl). In parallel, lipid bilayers containing biotinylated lipids were prepared and loaded with Alexa Fluor 633-conjugated streptavidin and α-κ antibody according to section 2.4.5 above. Then the α-κ was labeled with the Alexa Fluor 488-conjugated goat anti-rat antibody for 20 minutes and washed out. The fluorescence intensity of the beads and the artificial bilayers were then measured by confocal microscopy. A calibration curve was obtained from the fluorescence intensity of the different populations of the calibrated beads. The fluorescence intensity of the lipid bilayer was compared with this calibration curve to determine the density of the α-κ in the bilayer. An example of the 5 populations of beads upon incubation with primary and secondary antibody is shown in Figure 2.4.

This method was also used for the quantification of ICAM-1 and VCAM-1 densities in the bilayers using anti-ICAM-1 (YN1/1.7) or anti-VCAM-1 (CD106) antibodies, respectively.

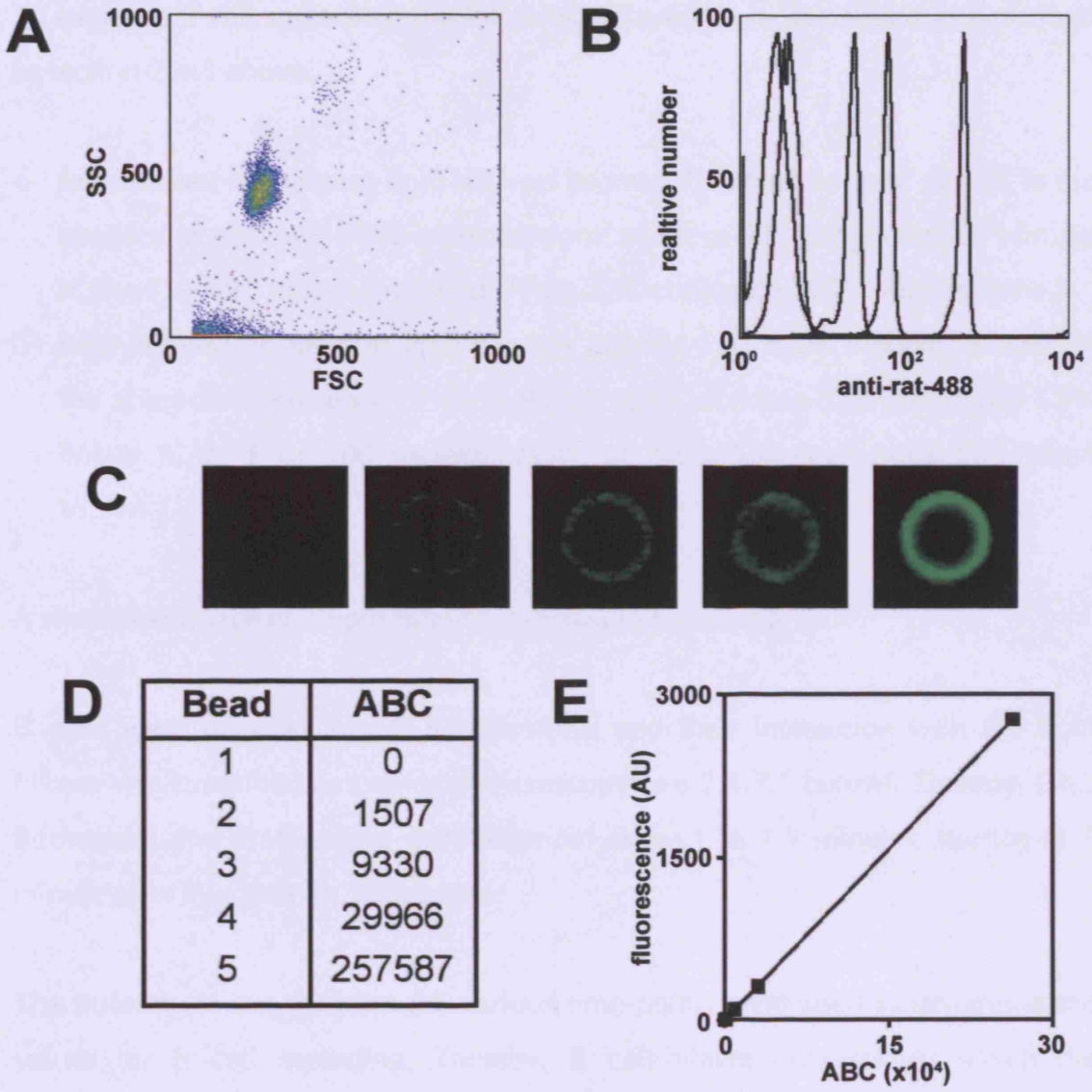

Bead	ABC
1	0
2	1507
3	9330
4	29966
5	257587

Figure 2.4 Determining the density of molecules in lipid bilayers with calibrated beads
(A) Flowcytometric analysis of calibrated beads population. **(B)** Calibrated beads from **(A)** were loaded with the α-κ, followed by the Alexa Fluor 488 goat anti-rat IgG. The resulting 5 populations of calibrated beads are shown by flowcytometric analysis. **(C)** Examination of the 5 populations of beads by confocal microscopy **(D)** Antibody binding capacity (ABC) of the beads used to estimate the density of the antigen. **(E)** Calibration curve derived from the fluorescene intensity of the different bead populations measured by confocal microscopy and their respective ABC.

2.4.6.2 B Cell Spreading Assay

To examine B cell spreading, the following bilayers were assembled as described in section 2.4.5 above.

- ***low amount of antigen:*** lipid bilayers bearing 35 molecules/μm^2 of HEL in the absence or presence of 80 molecules/μm^2 of Alexa-532-conjugated GPI-linked ICAM-1 or 100 molecules/μm^2 of Alexa-532-conjugated GPI-linked VCAM-1
- ***high amount of antigen:*** lipid bilayers bearing 150 molecules/μm^2 of HEL in the absence or presence of 80 molecules/μm^2 of Alexa-532-conjugated GPI-linked ICAM-1 or 100 molecules/μm^2 of Alexa-532-conjugated GPI-linked VCAM-1

A simplified image of a lipid bilayer is shown in Figure 2.5.

B cells were injected into FCS2 chambers and their interaction with the lipid bilayer was examined by confocal microscopy (see 2.4.7.1 below). Thereby, DIC, fluorescent and IRM images were acquired every 1 to 1.5 minutes, starting at 1 minute after injection for 10 minutes.

The fluorescent images from the various time-points were used to determine the values for B cell spreading. Thereby, B cell-bilayer contacts, in which the fluorescence due to antigen accumulation exceeded the average fluorescence of the lipid bilayer by 120% were selected with the Volocity software (Improvision, UK). The utilisation of this program also allowed calculating the value of the area of B cell-bilayer contacts, which defined the spreading area.

The fluorescent images were also used to quantify the total number of accumulated antigen molecules. These values were obtained by multiplying the accumulated density (molecules/μm^2) by the selected area (μm^2) in each cell or time-point. The accumulated density (molecules/μm^2) was estimated as [intensity in the selected area (fluorescence units/μm^2) - intensity in neighbouring area

(fluorescence units/μm^2)] / [specific activity (fluorescence units/molecule)]. All quantifications were done after synchronizing the cells for their initial contacts with the lipid bilayer.

2.4.6.3 B Cell Adhesion Assay

To examine B cell adhesion, lipid bilayers bearing 80 molecules/μm^2 of Alexa-532-conjugated GPI-linked ICAM-1 or 100 molecules/μm^2 of Alexa-532-conjugated GPI-linked VCAM-1 were prepared as described in section 2.4.5 above.

B cells were treated with 5μg/ml anti-IgM $(Fab')_2$ for 30 minutes at 37°C, before injection into the chamber. B cells were incubated inside the chamber for 20 minutes and their interaction with the lipid bilayer was examined by interference reflection microscopy (IRM), which shows B cell/bilayer contacts as dark areas. B cell adhesion frequency was defined as the percentage of B cells showing dark contacts of the total amount of B cells present in one image.

2.4.6.4 B Cell IS Formation Assay

To examine B cell IS formation, lipid bilayers bearing 150 molecules/μm^2 of HEL or α-κ and 80 molecules/μm^2 of Alexa-532-conjugated GPI-linked ICAM-1 or 100 molecules/μm^2 of Alexa-532-conjugated GPI-linked VCAM-1 were assembled as described in section 2.4.5 above.

B cells were injected into FCS2 chambers and their interaction with the lipid bilayer was examined by confocal microscopy after 20 min. IS frequency was defined as the percentage of B cells showing a cSMAC and a pSMAC of the total amount of B cells present in one image.

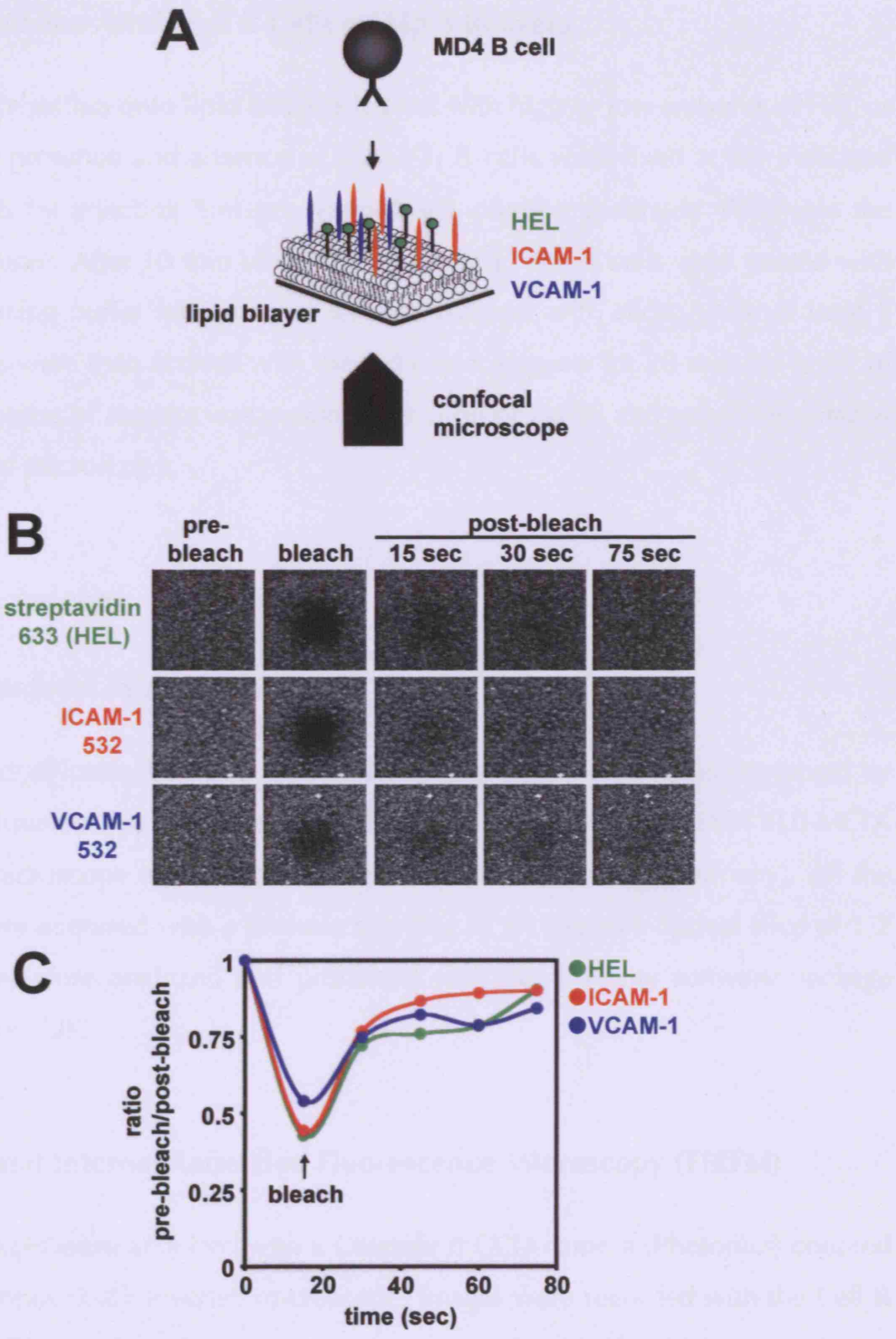

Figure 2.5 Lipid bilayer technology
(A) Simplified image of a lipid bilayer containing HEL (green), ICAM-1 (red) and VCAM-1 (blue). MD4 B cells are settled onto those bilayers and their interaction is followed by confocal microscopy. **(B)** Fluorescence recovery after photobleaching (FRAP) of bilayers bearing HEL, ICAM-1 and VCAM-1. **(C)** Fluorescence recovery of bilayers bearing HEL, ICAM-1 and VCAM-1, expressed as ratio of mean intensity at time n after bleach divided by mean intensity before bleach.

2.4.6.5 Immunostaining of B Cells on Lipid Bilayers

B cells were settled onto lipid bilayers loaded with high or low amounts of HEL or α-κ in the presence and absence of ICAM-1. B cells were fixed at the indicated time points by injecting 1ml pre-warmed 4% paraformaldehyde (PFA) into the FCS2 chamber. After 10 min of incubation at 37°C, the B cells were treated with permeabilizing buffer for 5 min at RT and blocked with $slide_{block}$ for at least 1 hour. Cells were then stained with the indicated reagents for 20 minutes at RT in $slide_{block}$. Excess of reagent was washed with 3 ml of 1xPBS and cells were imaged by confocal microscopy.

2.4.7 Microscopy

2.4.7.1 Confocal Microscopy

The kinetics of interaction of B cells with artificial lipid bilayers was monitored by confocal fluorescence microscopy and IRM with a Zeiss Axiovert LSM 510-META inverted microscope equipped with the Zeiss software (Zeiss, Germany). All the images were acquired with a pinhole resulting in an effective optical slice of 1-2 μm. Images were analyzed and processed with the Volocity software package (Improvision, UK).

2.4.7.2 Total Internal Reflection Fluorescence Microscopy (TIRFM)

TIRFM images were acquired with a Cascade II CCD camera (Photonics) coupled to an Olympus IX-81 inverted microscope. Images were recorded with the Cell R software (Olympus) and analysed and processed with the Volocity software package (Improvision).

2.5 Protein Analysis

2.5.1 Expression of Proteins in Competent Bacteria

Escherichia coli (*E.coli*) were transformed according to section 2.6.2 below with the following constructs:

- glutathione-S-transferase (GST)-tagged fusion protein comprised of the Cdc42/Rac interactive binding domain of Pak1 (GST-CRIB): gift from Dr. Tomohiro Kurosaki (RIKEN Research Centre, Japan)
- GST-tagged fusion protein comprised of the Rap1-binding domain of RalGDS (GST-RalGDS-RBD): gift from Dr. Doreen Cantrell (School of Life Science Research, UK)

Colonies were grown on agar plates containing 100μg/ml ampicillin over night at 37°C. The following day, cultures of single colonies were grown in 100ml LB medium containing 100μg/ml ampicillin at 37°C, 220rpm, over night. 3ml of this culture were transferred to 500ml LB medium containing 100μg/ml ampicillin and grown until culture reached an OD600 of 0.5 at 37°C, 220rpm. Addition of 1mM IPTG (1ml of 500mM IPTG stock) induced protein expression. After another 2 hours of culture, *E. coli* were pelleted at 3500rpm for 20 minutes at 4°C. Pellets were frozen at -20°C or GST-tagged proteins were purified directly as explained in section 2.5.2 below.

2.5.2 Purification of GST-Tagged Proteins

GST fusion proteins were purified from a 500 ml IPTG-induced *E.coli* culture. Pellets were resuspended in 10 ml GST buffer and sonicated 6x 20 seconds at medium power. 500μl of 20% Triton-X-100 were added and incubated for 10 minutes on ice. Solution was centrifuged at 15000xg for 20 minutes at 4°C and supernatant was recovered. 1.5ml Glutathione beads (Pharmacia Biotech) were prewashed twice with GST buffer prior to being added to the supernatant. For efficient coupling of GST-tagged proteins to beads, mixture was incubated

rotating for 1 hour at 4°C. Beads were then washed 3x with GST buffer. 1ml GST buffer and 4ml 100% Glycerol was added and mixed well. In this form beads were stored for up to 1 month at -20°C.

2.5.3 Preparation of Detergent Soluble B Cell Extracts

Naïve B cells were suspended at $1x10^7$ (for Rac1 and Rap1 activation assays) or $2x10^6$ (for Rac2 activation assays) in 750µl ice-cold 1.5x MLB. The lysate was incubated for 3 minutes on ice and then centrifuged in a microfuge at 13000rpm for 3 minutes to remove insoluble material. The supernatant was used for the Rac and Rap1 activation assays, see section 2.5.4 below.

2.5.4 Rac1, Rac2 and Rap1 Activation Assays

B lymphocytes were stimulated with 10µg/ml anti-IgM $F(ab')_2$ for the indicated times or left unstimulated. Lysates were prepared as described in 2.5.3 above. Supernatants were incubated with GST fusion protein-coupled Glutathione beads (15µg protein) for 30 minutes at 4°C under gentle rotation. The beads were then collected by centrifugation in a microfuge at 13000rpm for 1 minute and washed by re-suspension and re-pelleting in 1.5x MLB three times. The sepharose was then boiled in SDS-PAGE buffer for 10 minutes.

2.5.5 SDS Polyacrylamide Gel Electrophoresis (SDS-PAGE)

Activation of Rac and Rap GTPases, as well as protein purification was assessed by SDS-page performed on 14% acrylamide gels, composed of a stacking gel layered over a separating gel. Electrophoresis was performed in a Mini Protean 3 Cell (Biorad) with Running buffer at 200V and 60mAmp per gel. A dual coloured protein standard (Biorad) was run under identical conditions in the same gel to allow calibration by molecular weight. Samples that were not analysed by Western blot were visualized using a commercial colloidal Comassie Blue dye (Pierce) according to manufacturer's instructions.

2.5.6 Western Blot

Following SDS-PAGE, proteins were transferred onto a PVDF membrane (Biorad) at 400 mAmps for 45 minutes at 4°C in a Mini Protean 3 Cell (Biorad) containing Blotting buffer. The membrane was blocked with PBS/Tween containing 5% milk powder for 1 hour at RT with gentle agitation. The membrane was then incubated with the primary antibody diluted in PBS/Tween containing 5% milk over night at 4°C with gentle agitation. After washing 4 times 15 minutes each with PBS/Tween containing 5% milk, the HRP-conjugated secondary antibody was applied in PBS/Tween 5% milk for 1 hour at RT. The membrane was then washed 8 times for 5 minutes each with PBS/Tween and visualised using chemiluminescent substrate (ECL detection reagent, Amersham Bioscience) according to manufacturer's instructions. Excess substrate was blotted from the membrane onto clean tissue and membrane was exposed to film (Hyperfilm ECL, Amersham Bioscience) to visualize protein levels.

2.6 Molecular Biology

2.6.1 DNA Constructs

- Vav1-EGFP: gift from Dr. Martin Turner (Babraham Institute, Cambridge, UK)
- Rac1-EGFP: gift from Dr. Chad E. Harris / David A. Williams (Cincinnati Children's Hospital Medical Centre, USA)
- Rac2-EGFP: gift from Dr. Chad E. Harris / David A. Williams (Cincinnati Children's Hospital Medical Centre, USA)
- EGFP-Rac2V12: gift from Dr. Eloisa Arana (Cancer Research UK, London, UK)

2.6.2 Transformation of *E.coli*

Competent *E. coli* bacteria were prepared by Kathy Howe. The transformation was performed by incubating bacteria and plasmid on ice for 20 min, which was followed by heat shock at 42°C for 45 seconds. Bacteria were again placed on ice

for 2 minutes, shaken for 1 hour at 37°C and plated onto agar plates containing 100μg/ml ampicillin to form colonies.

2.6.3 Plasmid Purification

Colonies were picked and grown in 250ml LB medium containing 100μg/ml ampiclillin at 37°C, 220rpm, over night. Maxi preparations of plasmids were performed with the Qiagen maxi kit according to manufacturer's instructions (Qiagen).

3 The Role of BCR-signalling for B Cell Spreading, LFA-1 Activation and pSMAC Formation

At the early stage of membrane-antigen recognition BCR-engagement triggers B cell spreading and contraction, a two-phase process critical for maximal antigen engagement and gathering into a cSMAC (Fleire et al., 2006). As a result a mature immunological synapse (IS) is formed, at which the integrin LFA-1 bound to its ligand ICAM-1 segregates into the pSMAC, surrounding the antigen cluster (Carrasco et al., 2004). At low antigen availability LFA-1/ICAM-1 binding assists antigen aggregation and promotes B cell activation (Carrasco et al., 2004). However, the contribution of this pair of adhesion molecules to B cell spreading has not been established yet.

B cell spreading, LFA-1 activation and the formation of the pSMAC are processes that depend on signalling triggered upon BCR engagement (Carrasco et al., 2004; Fleire et al., 2006). Nevertheless, the signalling pathways regulating these events are still unknown.

The following chapter describes the contribution of the LFA-1/ICAM-1 interaction to initial B cell spreading and antigen accumulation upon membrane-bound antigen recognition. It further describes how BCR-triggered signalling regulates B cell spreading, LFA-1 activation and pSMAC formation.

3.1 BCR-Mediated LFA-1/ICAM-1 Binding Supports B Cell Spreading and Antigen Aggregation by Promoting B Cell Attachment

To establish the role of the LFA-1/ICAM-1 interaction during the B cell spreading phase upon membrane-bound antigen recognition, naïve MD4 B cells expressing a hen egg lysozyme (HEL)-specific BCR were purified and settled onto lipid bilayers containing a low or high amount of HEL (35 and 150 molecules/μm^2, respectively) in the presence or absence of ICAM-1 (see section 2.4.6.2 above for a detailed description of the bilayer system). B cell behavior on these bilayers was

evaluated during a 10-minutes time course by using confocal microscopy (Figure 3.1 A). B cell spreading was measured by the gathered antigen area and showed a 6μm^2 increase on lipid bilayers bearing a low amount of HEL in the presence of ICAM-1. This also resulted in higher antigen accumulation (Figure 3.1 B, C). However, no difference in B cell spreading and antigen aggregation could be observed at high HEL amounts, whether ICAM-1 was present or not (Figure 3.1 B, C).

At the same time, B cell attachment to the lipid bilayer was quantified by interference reflection microscopy (IRM), showing B cell contacts as dark areas. IRM analysis revealed large tight contacts in the presence of ICAM-1 and smaller scattered contacts in its absence (Figure 3.1 A, D). No B cell attachment could be observed when B cells were incubated on lipid bilayers containing only ICAM-1, thus the difference in contact area and tightness was due to BCR-triggered LFA-1/ICAM-1-interaction (Figure 3.1 A, D).

In conclusion, antigen recognition through the BCR triggers LFA-1 activation and ICAM-1 binding during the early stage of membrane-bound antigen recognition. This promotes B cell adhesion, which in turn assists B cell spreading and antigen accumulation at low antigen densities.

3.2 Signalling Mechanisms Contributing to B Cell Spreading, LFA-1 Activation and IS Formation

B cell spreading and antigen aggregation have recently been reported to depend on BCR signalling (Fleire et al., 2006). Also activation of LFA-1 and binding to ICAM-1 requires BCR signals (see 3.1 and (Carrasco et al., 2004)). However, the signalling molecules that mediate B cell spreading and LFA-1 activation upon antigen engagement by the BCR are not known. To identify the mechanism that regulates the early B cell response upon membrane-bound antigen recognition, several signalling molecules that are activated downstream of the BCR were tested for their ability to regulate B cell spreading and LFA-1 activation.

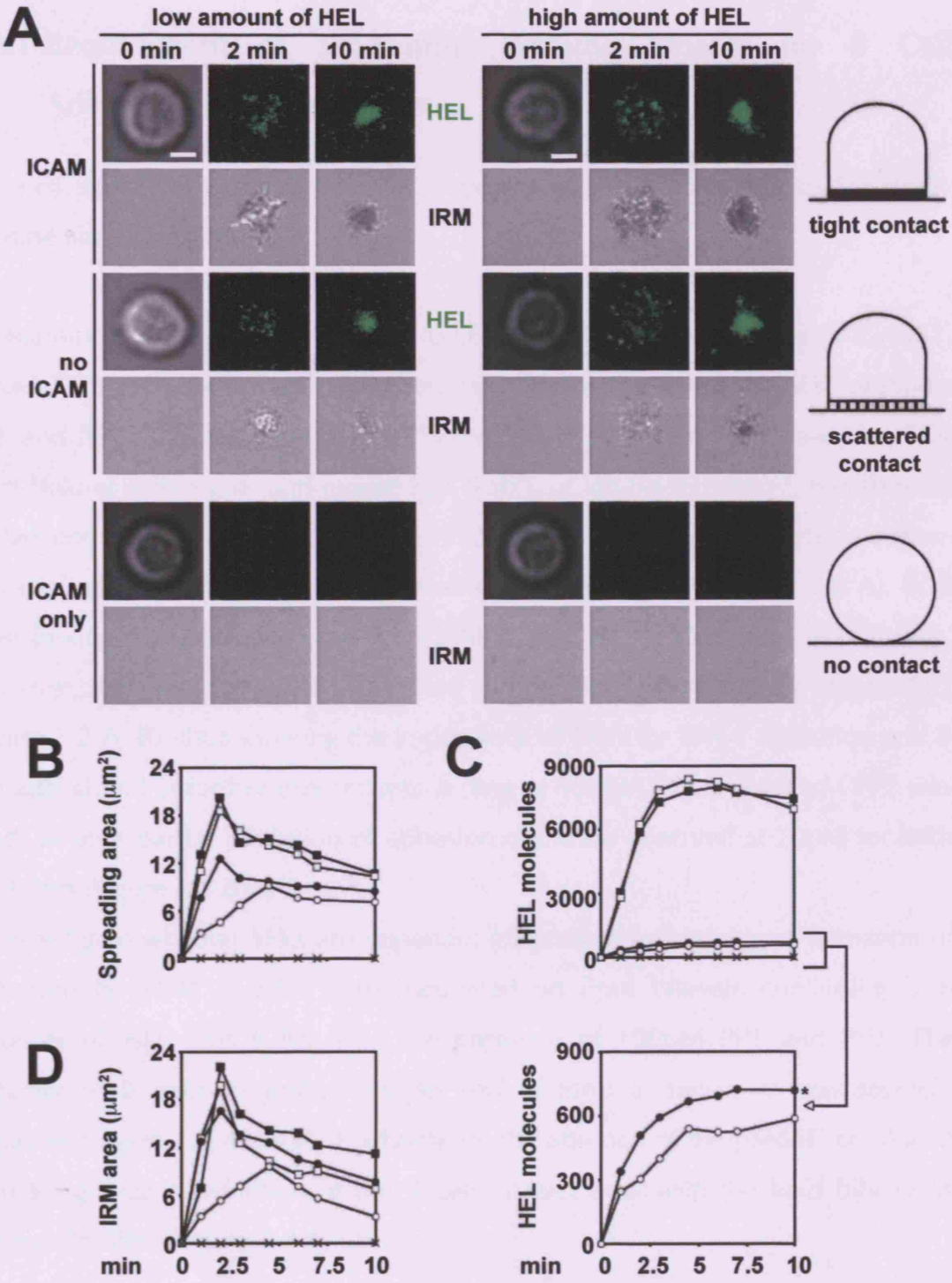

Figure 3.1 LFA-1/ICAM-1 promotes B cell spreading and antigen aggregation at low antigen amounts

(A) MD4 B cells were settled onto lipid bilayers containing a high and low amount of HEL in the presence and absence of ICAM-1 and the kinetic of interaction was followed by confocal microscopy for 10min. DIC, HEL fluorescence and IRM images of representative B cells at the indicated time points are shown. Scale bar: 1μm. Quantification of **(B)** the area of HEL (spreading), **(C)** the number of accumulated HEL molecules and **(D)** the IRM area. Symbols: ■ high HEL + ICAM-1, □ high HEL no ICAM-1, ● low HEL + ICAM-1, ○ low HEL no ICAM-1, × ICAM-1 only. Values are a mean of 10-20 cells each. t-test: * $p \leq 0.01$. Data are representative of two independent experiments.

3.2.1 Requirement of Src-Family Tyrosine Kinases for B Cell Adhesion and IS Formation

The first signalling event upon BCR engagement is the activation of Src-family tyrosine kinases (SFKs).

To examine the contribution of SFKs to LFA-1 activation and binding to ICAM-1, naïve C57BL/6 B cells were pre-treated with various doses of the SFK inhibitors PP1 and PP2. Un-treated and PP1/PP2-treated B cells were stimulated by BCR cross-linking with a goat anti-mouse IgM $(Fab')_2$ or left un-stimulated. B cells were settled onto lipid bilayers containing ICAM-1 only and their capacity to adhere was evaluated by counting B cell-bilayer contacts using IRM (Figure 3.2 A). BCR cross-linking induced adhesion to ICAM-1 in 85% of the untreated B cells. However, this was completely abolished at a dose of 100μM PP1 or 100μM PP2 (Figure 3.2 A, B), thus showing the importance of SFKs for LFA-1 activation and B cell adhesion. For further experiments, a dose of 100μM PP1 and 100μM PP2 was used, as only partial inhibition of adhesion could be observed at 10μM for both inhibitors (Figure 3.2 B).
To investigate whether SFKs are important for antigen gathering and formation of a mature IS, MD4 B cells were incubated on lipid bilayers containing high amounts of HEL plus ICAM-1 in the presence of 100μM PP1 and PP2. The capacity of B cells to gather antigen and to form a mature IS was severely impaired (Figure 3.3 A, B, C). Furthermore, the absence of the pSMAC correlated with a significant reduction of the B cell contact area with the lipid bilayer as assessed by IRM (Figure 3.3 A, D).

These results are in agreement with previous observations demonstrating SFK-transduced signalling as a requirement for B cell spreading and antigen aggregation (Fleire et al., 2006). These data also show that SFKs mediate LFA-1 activation and pSMAC formation at the IS.

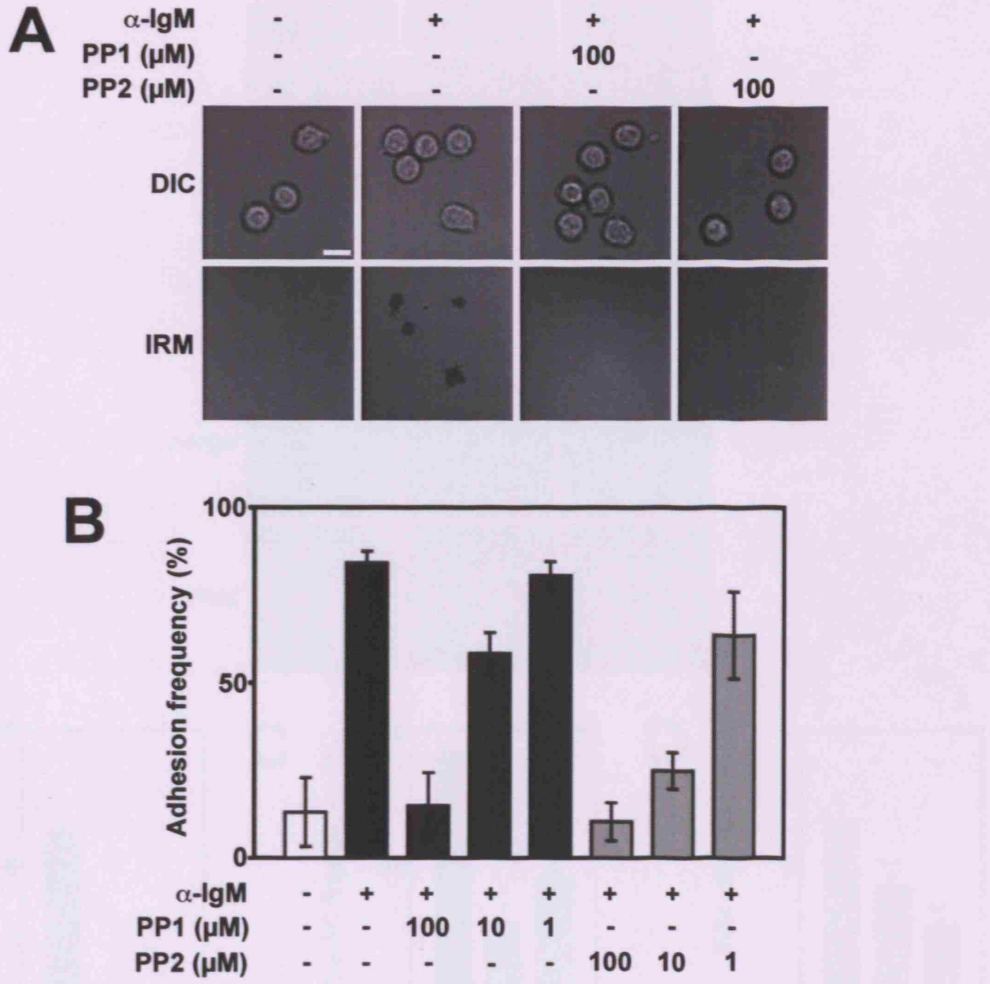

Figure 3.2 Inhibition of SFKs blocks B cell adhesion to ICAM-1
Not stimulated or α-IgM stimulated WT B cells were settled onto lipid bilayers containing ICAM-1 and adhesion capacity was assessed by IRM. B cells were pre-treated with different doses of PP1 or PP2. **(A)** DIC and IRM images of a representative field of B cells treated as indicated are shown. Scale bar: 5μm. **(B)** Quantification of the B cell adhesion frequency by counting B cell-bilayer contacts in 4 different IRM images containing 20-30 cells each. The mean percentage (±se) is shown. Data are representative of 3 independent experiments.

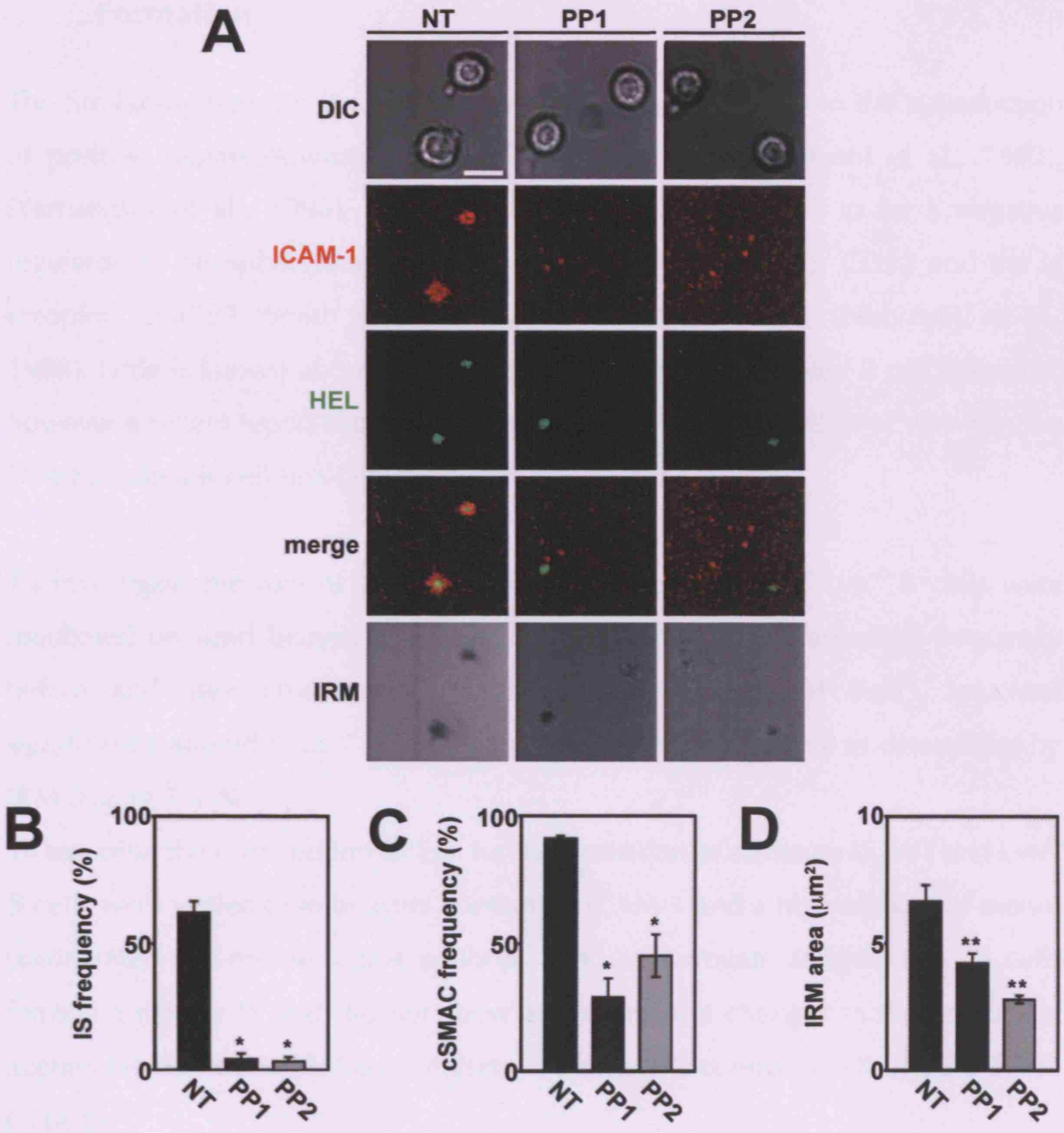

Figure 3.3 Inhibition of SFKs blocks IS formation
(A) Not treated (NT), PP1-treated (100µM) and PP2-treated (100µM) MD4 B cells were settled onto lipid bilayers containing a high amount of HEL and ICAM-1 and imaged by confocal microscopy after 20min. DIC, fluorescent, merged and IRM images of representative B cells are shown. Scale bar: 5µm. Quantification of **(B)** the IS frequency, **(C)** the frequency of B cells forming a cSMAC and **(D)** the IRM area. In each condition 4 different fields containing 10-20 cells each were analysed. The mean value (±se) is shown. t-test: * $p \leq 0.01$, ** $p \leq 0.001$. Data are representative of 2 independent experiments.

3.2.2 The Role of the Lyn Tyrosine Kinase for B Cell Adhesion and IS Formation

The Src-family tyrosine kinase Lyn is suggested to participate in the transduction of positive signals downstream of BCR engagement (Yamanashi et al., 1992), (Yamanashi et al., 1993). Nevertheless, Lyn mainly appears to be a negative regulator by phosphorylation of ITIMs of the BCR co-receptor CD22 and the Ig receptor FcγRIIB1 (Smith et al., 1998), (Chan et al., 1998), (Nishizumi et al., 1998). Little is known about the role of Lyn for integrin-mediated B cell adhesion, however a recent report suggests that Lyn contributes to activation of VLA-4 in the DT40 chicken B cell line (Spaargaren et al., 2003).

To investigate the role of Lyn for LFA-1 activation, WT and $Lyn^{-/-}$ B cells were incubated on lipid bilayes containing only ICAM-1. B cell adhesion frequency before and after cross-linking of the BCR with anti-IgM $(Fab')_2$ was not significantly altered in $Lyn^{-/-}$ B cells compared to the WT control as determined by IRM (Figure 3.4 A).
To examine the contribution of Lyn for the formation of a mature IS, WT and $Lyn^{-/-}$ B cells were settled onto bilayers containing ICAM-1 and a high amount of mono-biotinylated anti-mouse kappa antibody (α-κ) as surrogate antigen. $Lyn^{-/-}$ B cells formed a mature IS and did not show any significant changes in the amount of accumulated α-κ and IRM area in comparison to WT control B cells (Figure 3.4 B, C, D, E).

These data show that Lyn is not required for BCR-mediated antigen aggregation, LFA-1 activation and pSMAC formation and indicate a redundant role for other SFKs that are expressed in B cells.

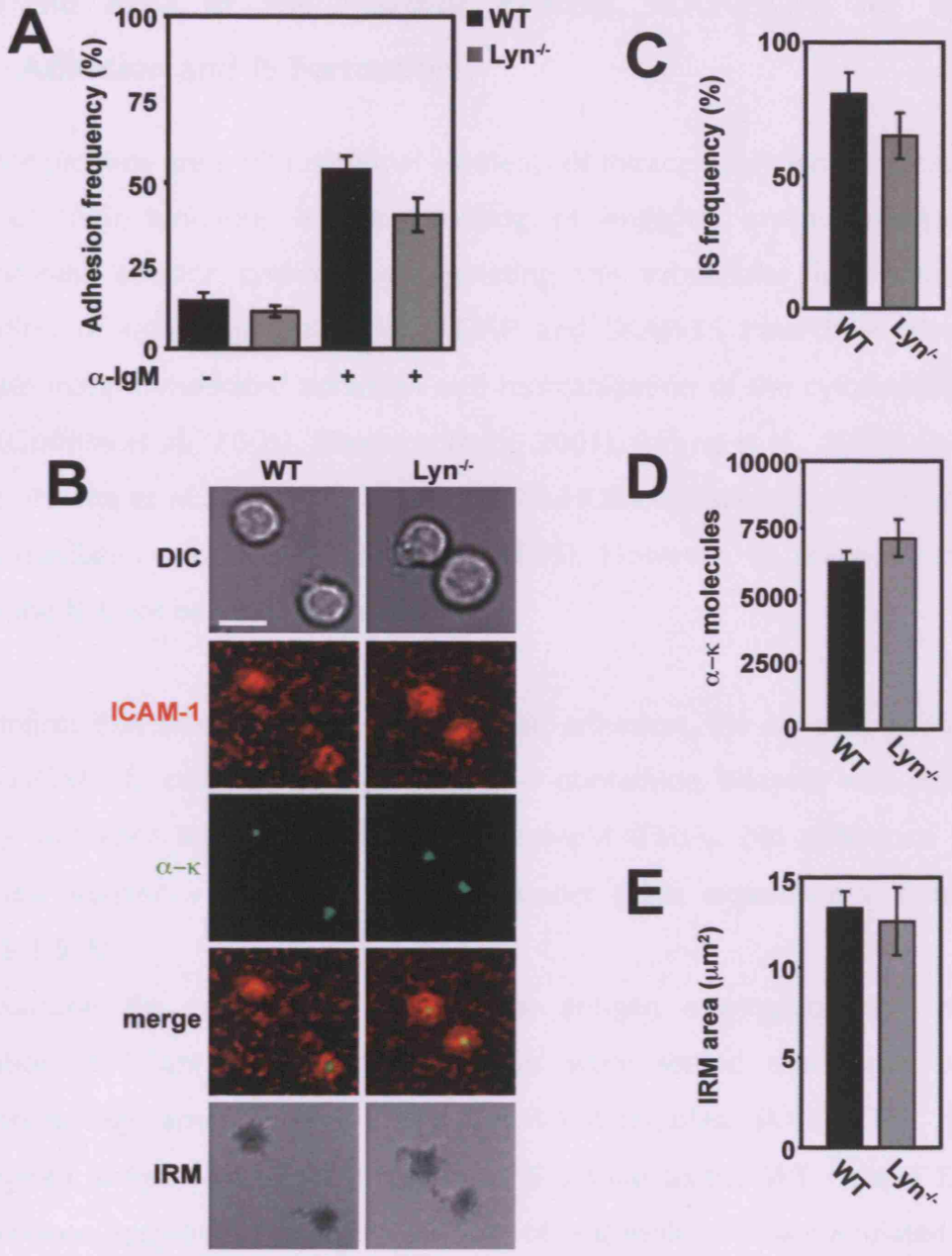

Figure 3.4 Normal adhesion and IS formation in Lyn$^{-/-}$ B cells
(A) Not stimulated or α-IgM stimulated WT and Lyn$^{-/-}$ B cells were settled onto lipid bilayers containing ICAM-1 and adhesion frequency was quantified by counting B cell-bilayer contacts in 4 different IRM images containing 20-30 cells each. The mean percentage (±se) is shown. Data are representative of 2 independent experiments. **(B)** WT and Lyn$^{-/-}$ B cells were settled onto lipid bilayers containing a high amount of α-κ and ICAM-1 and imaged by confocal microscopy after 20min. DIC, fluorescent, merged and IRM images of representative B cells are shown. Scale bar: 5μm. Quantification of **(C)** the IS frequency, **(D)** the number of accumulated α-κ molecules and **(E)** the IRM area of 4 different fields containing 10-20 cells each. The mean value (±se) is shown. Data are representative of 2 independent experiments.

3.2.3 The Role of the Adaptor Protein SKAP-HOM for B Cell Adhesion and IS Formation

Adaptor proteins are multifunctional elements of intracellular signalling cascades. One of their functions is the coupling of engaged antigen receptors to downstream effector systems by regulating the subcellular localisation and activation of signalling molecules. ADAP and SKAP-55 have been shown to regulate integrin-mediated adhesion and reorganization of the cytoskeleton in T cells (Griffiths et al., 2001), (Peterson et al., 2001), (Wang et al., 2003), (Jo et al., 2005), (Kliche et al., 2006). In B cells, SKAP-HOM is also suggested to regulate LFA-1-mediated adhesion (Togni et al., 2005). However, its contribution to IS formation has not been established.

To confirm that SKAP-HOM mediates B cell adhesion, the capacity of WT and SKAP-HOM$^{-/-}$ B cells to adhere to ICAM-1-containing bilayers was evaluated before and after BCR stimulation with anti-IgM $(Fab')_2$. No difference in the adhesion frequency could be observed under these experimental conditions (Figure 3.5 A).

To examine the role of SKAP-HOM for antigen aggregation and pSMAC formation, WT and SKAP-HOM$^{-/-}$ B cells were settled onto lipid bilayers containing high amounts of α-κ and ICAM-1 molecules. SKAP-HOM$^{-/-}$ B cells aggregated antigen and formed a mature IS similar to the WT control B cells. Furthermore, quantification of the amount of α-κ molecules accumulated in the cSMAC and the IRM area did not reveal any differences (Figure 3.5 B, C, D, E).

Thus, these data suggest that the adaptor SKAP-HOM is dispensable for LFA-1-mediated adhesion, antigen aggregation and pSMAC formation in B cells.

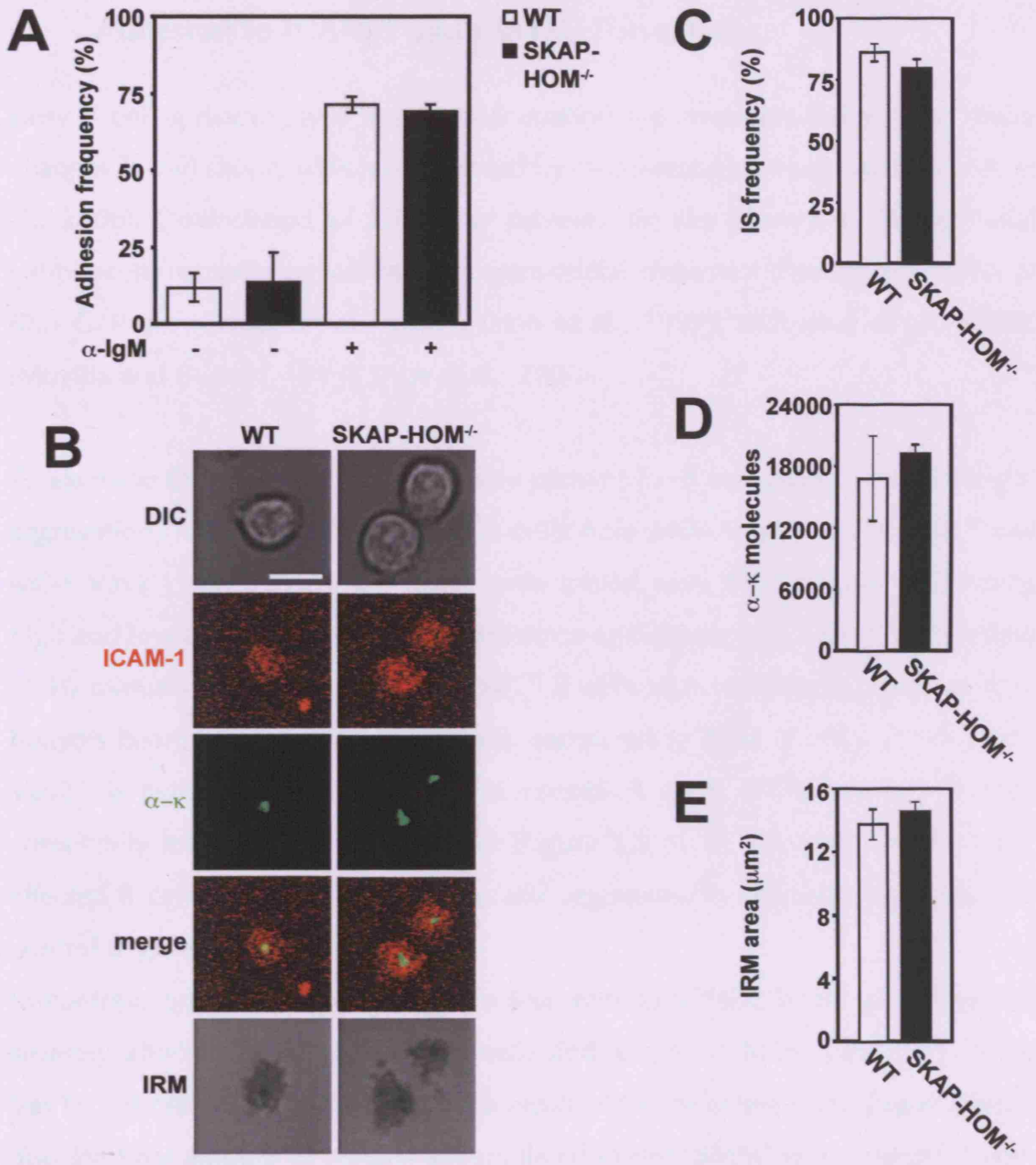

Figure 3.5 Normal adhesion and IS formation in SKAP-HOM$^{-/-}$ B cells
(A) Not stimulated or α-IgM stimulated WT and SKAP-HOM$^{-/-}$ B cells were settled onto lipid bilayers containing ICAM-1 and adhesion frequency was quantified by counting B cell-bilayer contacts in 4 different IRM images containing 20-30 cells each. The mean percentage (±se) is shown. Data are representative of 2 independent experiments. **(B)** WT and SKAP-HOM$^{-/-}$ B cells were settled onto lipid bilayers containing a high amount of α-κ and ICAM-1 and imaged by confocal microscopy after 20min. DIC, fluorescent, merged and IRM images of representative B cells are shown. Scale bar: 5μm. Quantification of **(C)** the IS frequency, **(D)** the number of accumulated α-κ molecules and **(E)** the IRM area of 4 different fields containing 10-20 cells each. The mean value (±se) is shown. Data are representative of 2 independent experiments.

3.2.4 The Role of the Family of Vav Proteins for B Cell Spreading, Adhesion to ICAM-1 and pSMAC Formation

Early B cell spreading and mature IS formation are processes that require major changes in cell shape, which is mediated by cytoskeletal rearrangements (Fleire et al., 2006). Downstream of SFKs, Vav proteins are key players in linking initial lymphocyte receptor signalling with cytoskeletal dynamics through activation of Rho GTPases (Crespo et al., 1997), (Han et al., 1997), (Schuebel et al., 1998), (Movilla and Bustelo, 1999), (Abe et al., 2000).

To examine the role of the family of Vav proteins for B cell spreading and antigen aggregation, naïve MD4 B cells and B cells from MD4 Vav1$^{-/-}$, MD4 Vav2$^{-/-}$ and MD4 Vav1$^{-/-}$/Vav2$^{-/-}$ (Vav1/2$^{-/-}$) mice were settled onto lipid bilayers containing high and low amounts of HEL in the presence and absence of ICAM-1 over a time of 10 minutes. Spreading of MD4 Vav1$^{-/-}$ B cells was severely reduced on lipid bilayers bearing a high amount of HEL compared to MD4 B cells. While MD4 Vav2$^{-/-}$ B cells spread comparably to control B cells, MD4 Vav1/2$^{-/-}$ B cells completely lost their ability to spread (Figure 3.6 A, B). Although loss of Vav1 affected B cell spreading, antigen was still aggregated as efficiently as in the WT control (Figure 3.6 C).

In contrast, on lipid bilayers bearing a low amount of HEL, B cell spreading was severely affected in MD4 Vav2$^{-/-}$ B cells and absent in MD4 Vav1$^{-/-}$ and MD4 Vav1/2$^{-/-}$ B cells (Figure 3.7 A, B). As a result of the defective spreading response, also the final amount of antigen accumulated in the cSMAC was reduced (Figure 3.7 C). The loss of spreading of MD4 Vav1$^{-/-}$, Vav2$^{-/-}$ and Vav1/2$^{-/-}$ B cells correlated with a reduction of the B cell contact area with the bilayer as observed by IRM (Figure 3.6 A, D and Figure 3.7 A, D). Furthermore contacts appeared scattered, similar to spreading in the absence of ICAM-1 (see Figure 3.6 A right panel and Figure 3.7 A right panel), which suggests that LFA-1 activation and in turn, ICAM-1 binding might be affected by the loss of Vav1 and/or Vav2.

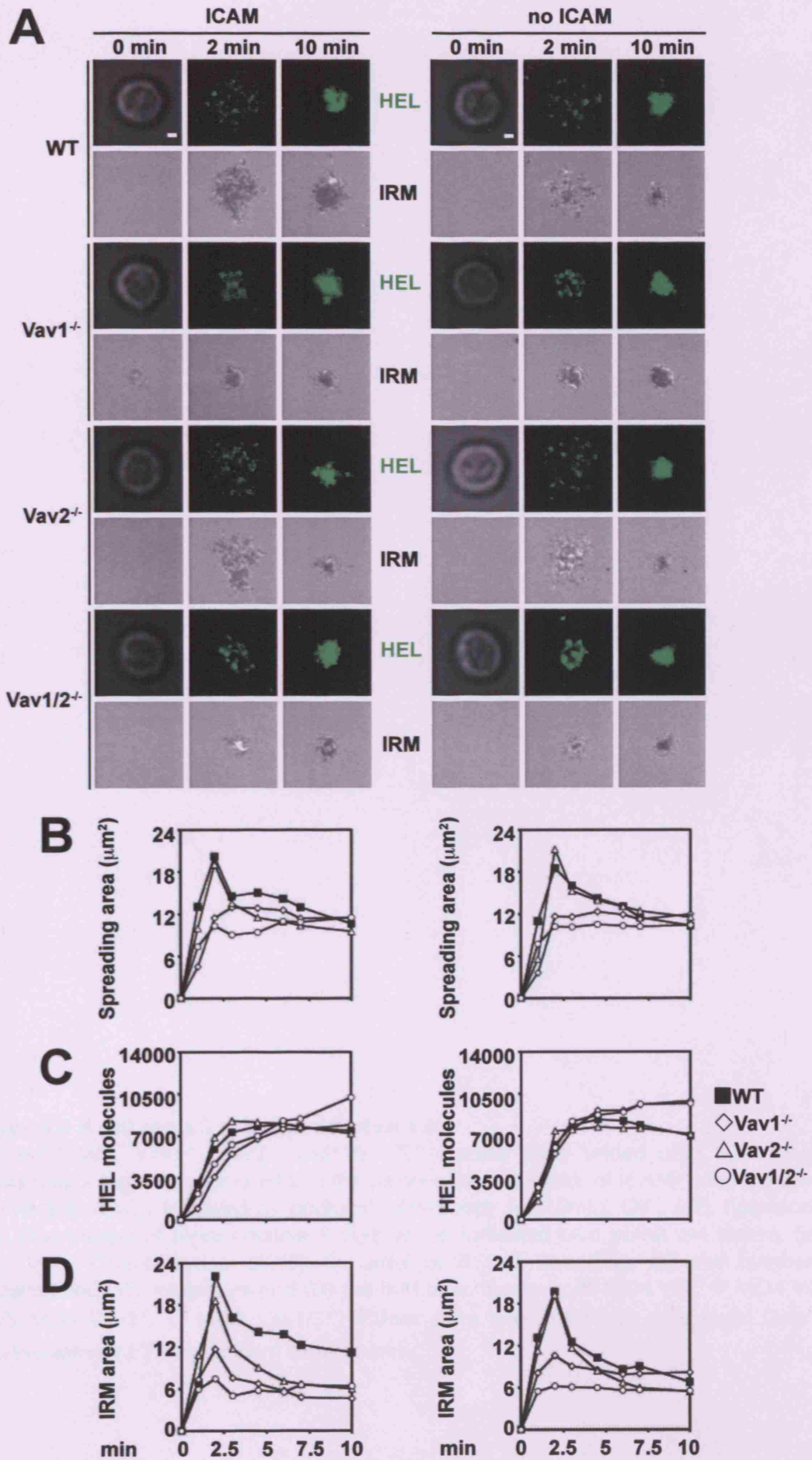
A
ICAM
no ICAM
0 min
2 min
10 min
WT
Vav1-/-
Vav2-/-
Vav1/2-/-
HEL
IRM
B
Spreading area (μm²)
C
HEL molecules
WT
Vav1-/-
Vav2-/-
Vav1/2-/-
D
IRM area (μm²)
min
0
2.5
5
7.5
10

Figure 3.6 B cell spreading is dependent on Vav1
(A) MD4 WT, Vav1$^{-/-}$, Vav2$^{-/-}$ and Vav1/2$^{-/-}$ B cells were settled onto lipid bilayers containing a high amount of HEL in the presence and absence of ICAM-1 and the kinetic of interaction was followed by confocal microscopy for 10min. DIC, HEL fluorescence and IRM images of representative B cells at the indicated time points are shown. Scale bar: 1µm. Quantification of **(B)** the area of B cell spreading, **(C)** the number of accumulated HEL molecules and **(D)** the IRM area. Symbols: ■ MD4 WT, ◇ MD4 Vav1$^{-/-}$, △ MD4 Vav2$^{-/-}$, ○ MD4 Vav1/2$^{-/-}$. Values are a mean of 10-20 cells each. Data are representative of 2 independent experiments.

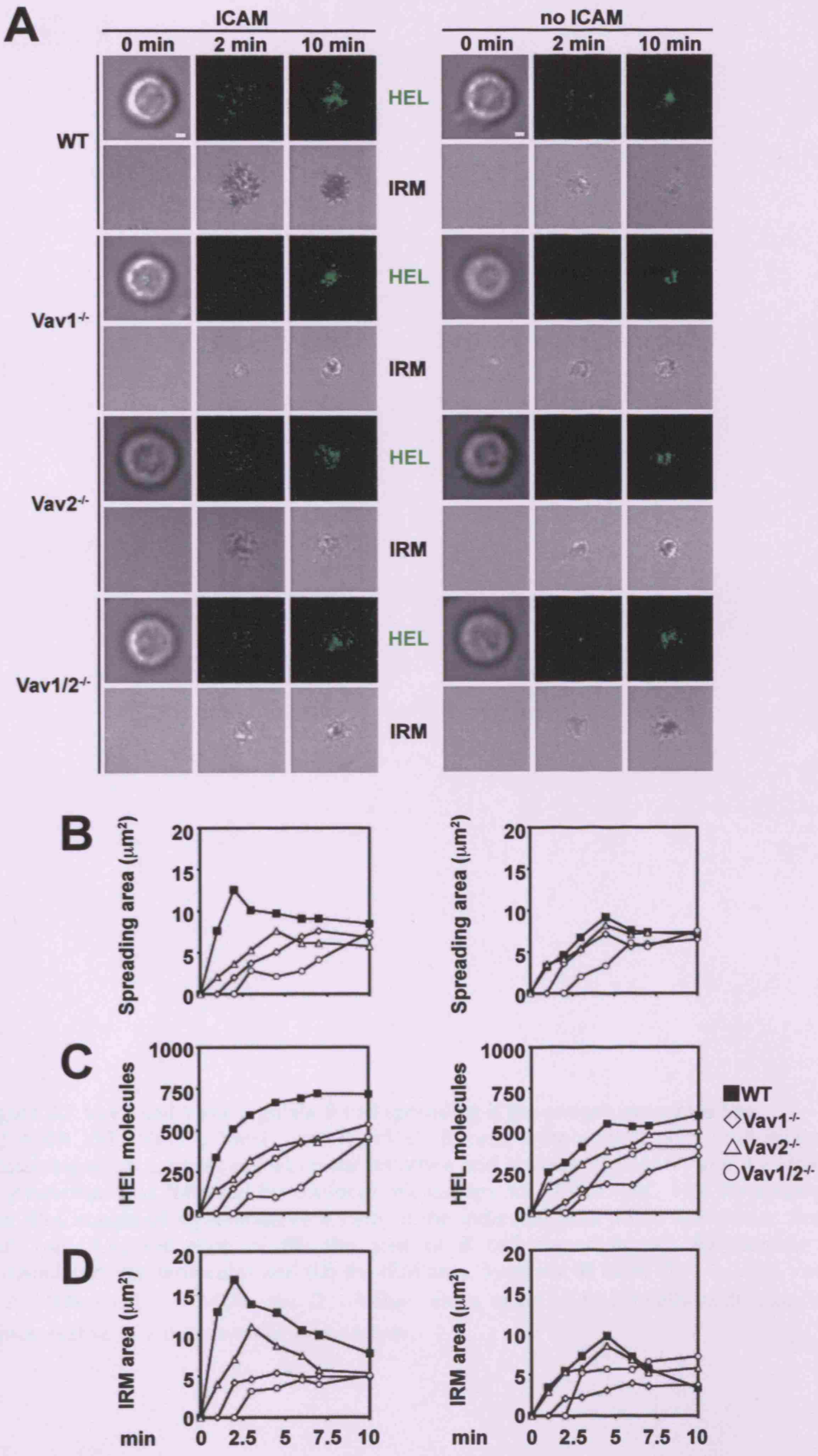
A
ICAM
no ICAM
0 min
2 min
10 min
WT
Vav1-/-
Vav2-/-
Vav1/2-/-
HEL
IRM
B
Spreading area (μm²)
C
HEL molecules
D
IRM area (μm²)
min
0
2.5
5
7.5
10
WT
Vav1-/-
Vav2-/-
Vav1/2-/-

Figure 3.7 Vav1 and Vav2 regulate B cell spreading if the antigen amount is low
(A) MD4 WT, Vav1$^{-/-}$, Vav2$^{-/-}$ and Vav1/2$^{-/-}$ B cells were settled onto lipid bilayers containing a low amount of HEL in the presence and absence of ICAM-1 and the kinetic of interaction was followed by confocal microscopy for 10min. DIC, HEL fluorescence and IRM images of representative B cells at the indicated time points are shown. Scale bar: 1µm. Quantification of **(B)** the area of B cell spreading, **(C)** the number of accumulated HEL molecules and **(D)** the IRM area. Symbols: ■ MD4 WT, ◇ MD4 Vav1$^{-/-}$, △ MD4 Vav2$^{-/-}$, O MD4 Vav1/2$^{-/-}$. Values are a mean of 10-20 cells each. Data are representative of 2 independent experiments.

Therefore, the capacity of C57BL/6 WT, Vav1$^{-/-}$, Vav2$^{-/-}$ and Vav1/2$^{-/-}$ B cells to adhere to bilayers containing only ICAM-1 was evaluated by IRM analysis before and after BCR stimulation with the anti-IgM $(Fab')_2$ fragment. B cell adhesion of Vav1$^{-/-}$ and Vav2$^{-/-}$ B cells to ICAM-1 was significantly reduced to 30% and 45%, respectively, compared to the WT control (Figure 3.8 A). This defect was even more pronounced in Vav1/2$^{-/-}$ B cells, indicating that Vav1 and Vav2 regulate LFA-1 activation (Figure 3.8 A).

Furthermore, on bilayers containing a high amount of HEL and ICAM-1 molecules, pSMAC formation was strongly reduced in MD4 Vav1$^{-/-}$ and Vav2$^{-/-}$ B cells and completely abolished in MD4 Vav1/2$^{-/-}$ B cells (Figure 3.8 B, C). As a result, the B cell contact with the bilayer was significantly reduced as assessed by IRM (Figure 3.8 B, D).

Interestingly, loss of Vav3 (MD4 Vav3$^{-/-}$ B cells) did neither affect B cell adhesion to ICAM-1, cSMAC and pSMAC formation nor the contact area with the bilayer (Figure 3.8 A, B, C, D). This suggests that LFA-1 activation and pSMAC formation may occur independently of Vav3.

These results show that Vav1 is necessary for efficient B cell spreading and antigen accumulation. Signalling via Vav2 is not required for B cell spreading when the amount of available antigen is high, suggesting that Vav1 can overtake Vav2 function under those conditions. At lower antigen availability, however, Vav2 is required for spreading and antigen accumulation. Furthermore, Vav1 and Vav2 mediate B cell adhesion and pSMAC formation by contributing to LFA-1 activation downstream of BCR engagement, while Vav3 is not required.

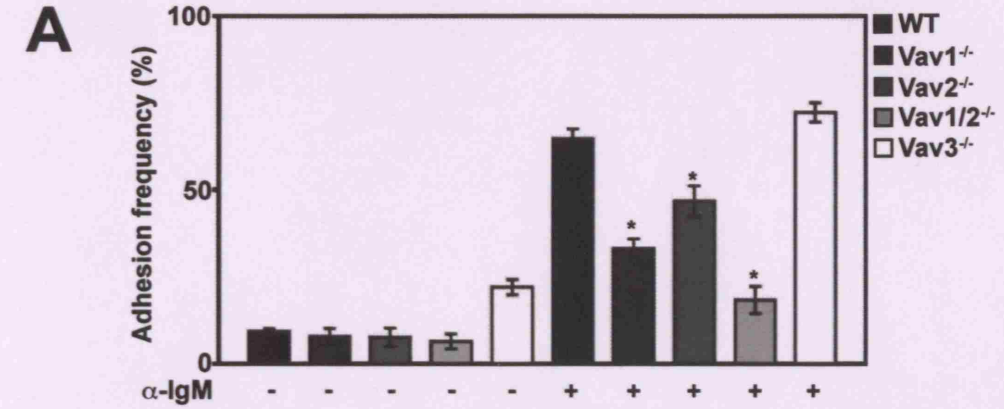
A
Adhesion frequency (%)
100
50
0
WT
Vav1-/-
Vav2-/-
Vav1/2-/-
Vav3-/-
α-IgM
- - - - - + + + + +

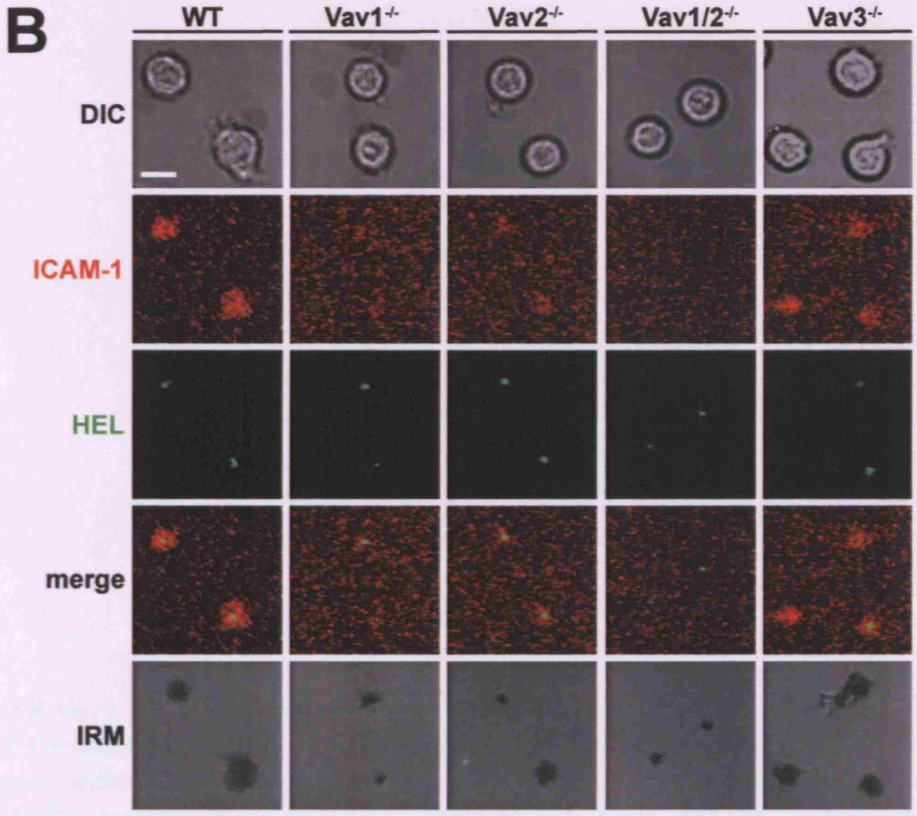
B
WT
Vav1-/-
Vav2-/-
Vav1/2-/-
Vav3-/-
DIC
ICAM-1
HEL
merge
IRM

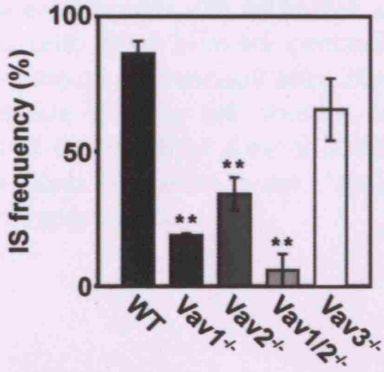
C
IS frequency (%)
100
50
0
WT
Vav1-/-
Vav2-/-
Vav1/2-/-
Vav3-/-

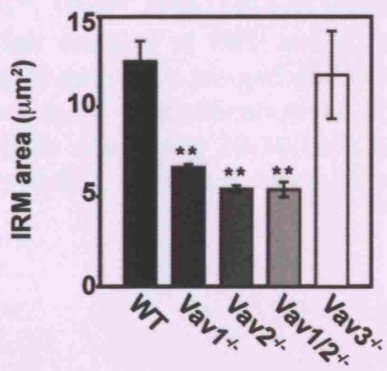
D
IRM area (μm²)
15
10
5
0
WT
Vav1-/-
Vav2-/-
Vav1/2-/-
Vav3-/-

Figure 3.8 Vav1 and Vav2, but not Vav3 regulate B cell adhesion and pSMAC formation
(A) Not stimulated or α-IgM stimulated WT and Vav1$^{-/-}$, Vav2$^{-/-}$, Vav1/2$^{-/-}$ and Vav3$^{-/-}$ B cells were settled onto lipid bilayers containing ICAM-1 and adhesion frequency was quantified by counting B cell-bilayer contacts in 3 different IRM images containing 30-40 cells each. The mean percentage (±se) is shown. Data are representative of 2 independent experiments. **(B)** MD4 WT and Vav1$^{-/-}$, Vav2$^{-/-}$, Vav1/2$^{-/-}$ and Vav3$^{-/-}$ B cells were settled onto lipid bilayers containing a high amount of HEL and ICAM-1 and imaged by confocal microscopy after 20min. DIC, fluorescent, merged and IRM images of representative B cells are shown. Scale bar: 5μm. Quantification of **(C)** the IS frequency and **(D)** the IRM area of 3 different fields containing 20-30 cells each. The mean value (±se) is shown. t-test: *$p \leq 0.01$, **$p \leq 0.001$. Data are representative of 3 independent experiments.

3.2.5 The Role of the GTPases Rac1 and Rac2 for B Cell Spreading, B Cell adhesion and IS Formation

The defective spreading and pSMAC formation in Vav-deficient B cells implicated a deregulation of downstream signalling due to absence of Vav GEF activity. Two proteins that are activated downstream of Vav by guanine nucleotide exchange are the small GTPases Rac1 and Rac2 (Crespo et al., 1997), (Movilla and Bustelo, 1999), (Schuebel et al., 1998), (Abe et al., 2000).

To test whether Rac1 or Rac2 are required for B cell spreading, naïve B cells from $CD19^{cre/+}$ WT, $CD19^{cre/+}$ $Rac1^{fx/-}$ ($Rac1^{-/-}$) and $CD19^{cre/+}$ $Rac2^{-/-}$ mice were incubated on bilayers containing high and low amounts of α-κ in the presence or absence of ICAM-1. Loss of either Rac1 or Rac2 did not affect B cell spreading or antigen aggregation at high amounts of antigen as compared to WT B cells, independently of the ICAM-1 presence (Figure 3.9 A, B, C).
However, at low densities, B cell spreading and antigen aggregation was decreased in $Rac2^{-/-}$ B cells, while no reduction could be observed $Rac1^{-/-}$ B cells in the presence of ICAM-1 (Figure 3.10 A, B, C). Furthermore, $Rac2^{-/-}$ B cells showed a reduction of the contact area with lipid bilayers bearing ICAM-1 independently of the amount of α-κ as shown by IRM in Figure 3.9 A, D and Figure 3.10 A, D.
The observed decrease in spreading and antigen accumulation of $Rac2^{-/-}$ B cells in the presence of ICAM-1 matched the values obtained for WT and $Rac1^{-/-}$ B cells in the absence of ICAM-1. This suggested that BCR-mediated LFA-1 activation might be affected by the loss of Rac2.
Therefore the adhesion capacity of $Rac1^{-/-}$ and $Rac2^{-/-}$ B cells to ICAM-1 containing lipid bilayers was examined. The frequency of adhering $Rac2^{-/-}$ B cells to ICAM-1 upon BCR cross-linking was significantly decreased, indicating a defective LFA-1 activation in those B cells. In contrast, no defect in $Rac1^{-/-}$ B cell adhesion was observed (Figure 3.11 A).

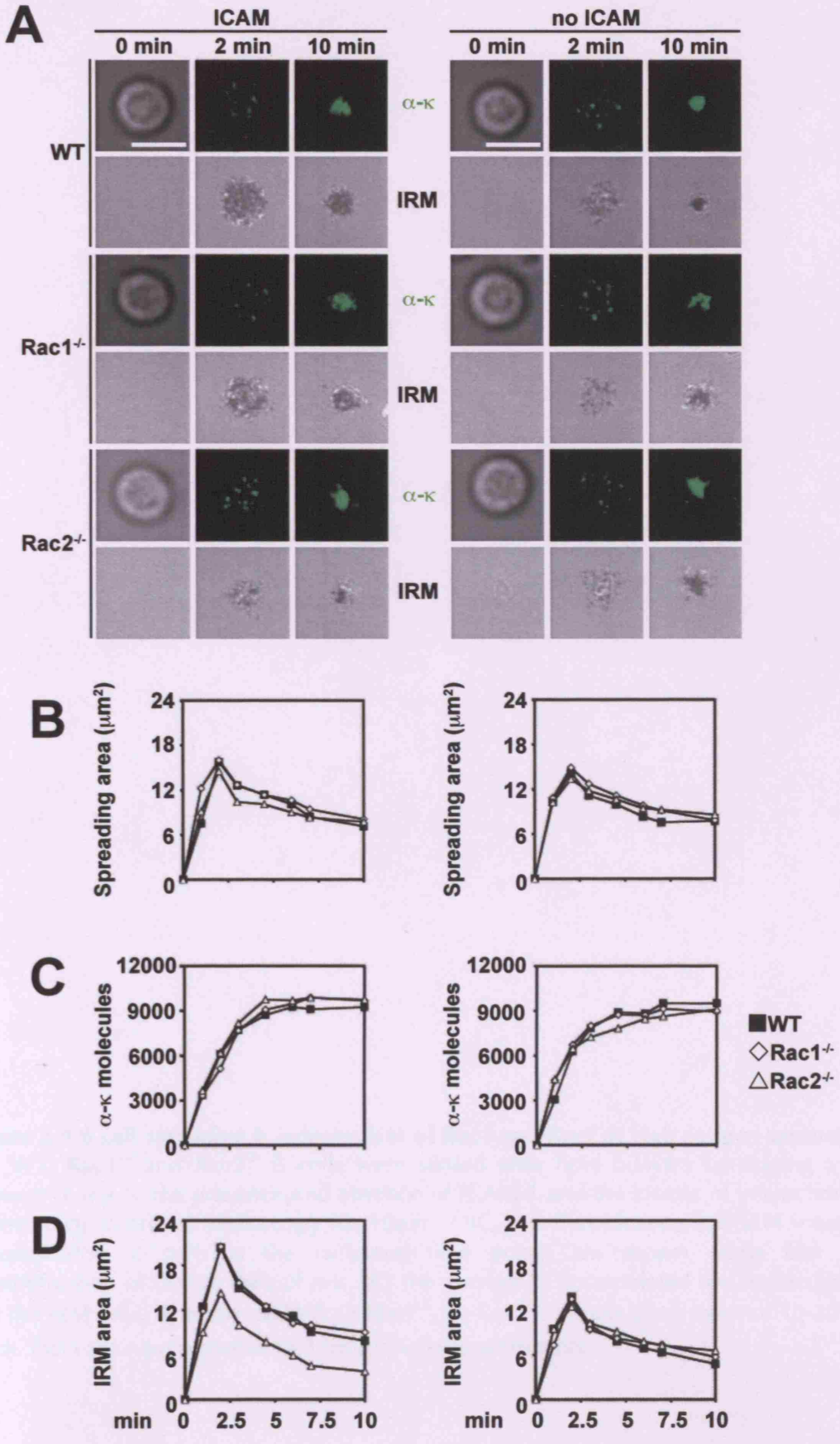
A
ICAM
no ICAM
0 min
2 min
10 min
WT
Rac1-/-
Rac2-/-
α-κ
IRM
B
Spreading area (μm²)
C
α-κ molecules
■WT
◇Rac1-/-
△Rac2-/-
D
IRM area (μm²)
min
0
2.5
5
7.5
10

Figure 3.9 B cell spreading is independent of Rac1 and Rac2 at high antigen amounts
(A) WT, $Rac1^{-/-}$ and $Rac2^{-/-}$ B cells were settled onto lipid bilayers containing a high amount of α-κ in the presence and absence of ICAM-1 and the kinetic of interaction was followed by confocal microscopy for 10min. DIC, α-κ fluorescence and IRM images of representative B cells at the indicated time points are shown. Scale bar: 5μm. Quantification of **(B)** the area of α-κ, **(C)** the number of accumulated α-κ molecules and **(D)** the IRM area. Symbols: ■ WT, ◇ $Rac1^{-/-}$, △ $Rac2^{-/-}$. Values are a mean of 10-20 cells each. Data are representative of 3 independent experiments.

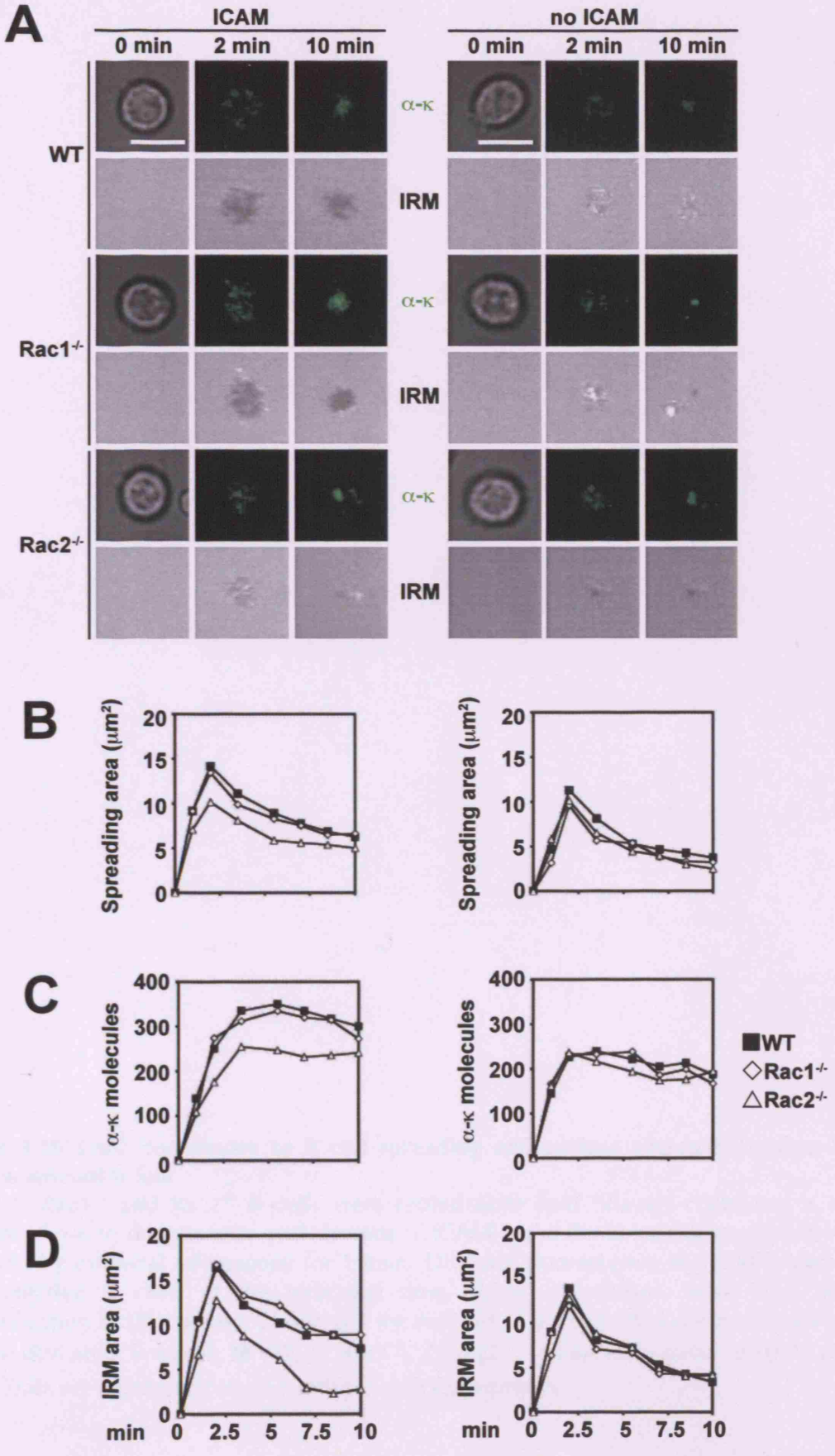
A
ICAM
no ICAM
0 min
2 min
10 min
WT
Rac1-/-
Rac2-/-
α-κ
IRM
B
Spreading area (μm²)
C
α-κ molecules
D
IRM area (μm²)
min
0
2.5
5
7.5
10
■WT
◇Rac1-/-
△Rac2-/-

Figure 3.10 Rac2 contributes to B cell spreading and antigen aggregation when the antigen amount is low

(A) WT, $Rac1^{-/-}$ and $Rac2^{-/-}$ B cells were settled onto lipid bilayers containing a low amount of α-κ in the presence and absence of ICAM-1 and the kinetic of interaction was followed by confocal microscopy for 10min. DIC, α-κ fluorescence and IRM images of representative B cells at the indicated time points are shown. Scale bar: 5μm. Quantification of **(B)** the area of α-κ, **(C)** the number of accumulated α-κ molecules and **(D)** the IRM area. Symbols: ■ WT, ◇ $Rac1^{-/-}$, △ $Rac2^{-/-}$. Values are a mean of 10-20 cells each. Data are representative of 3 independent experiments.

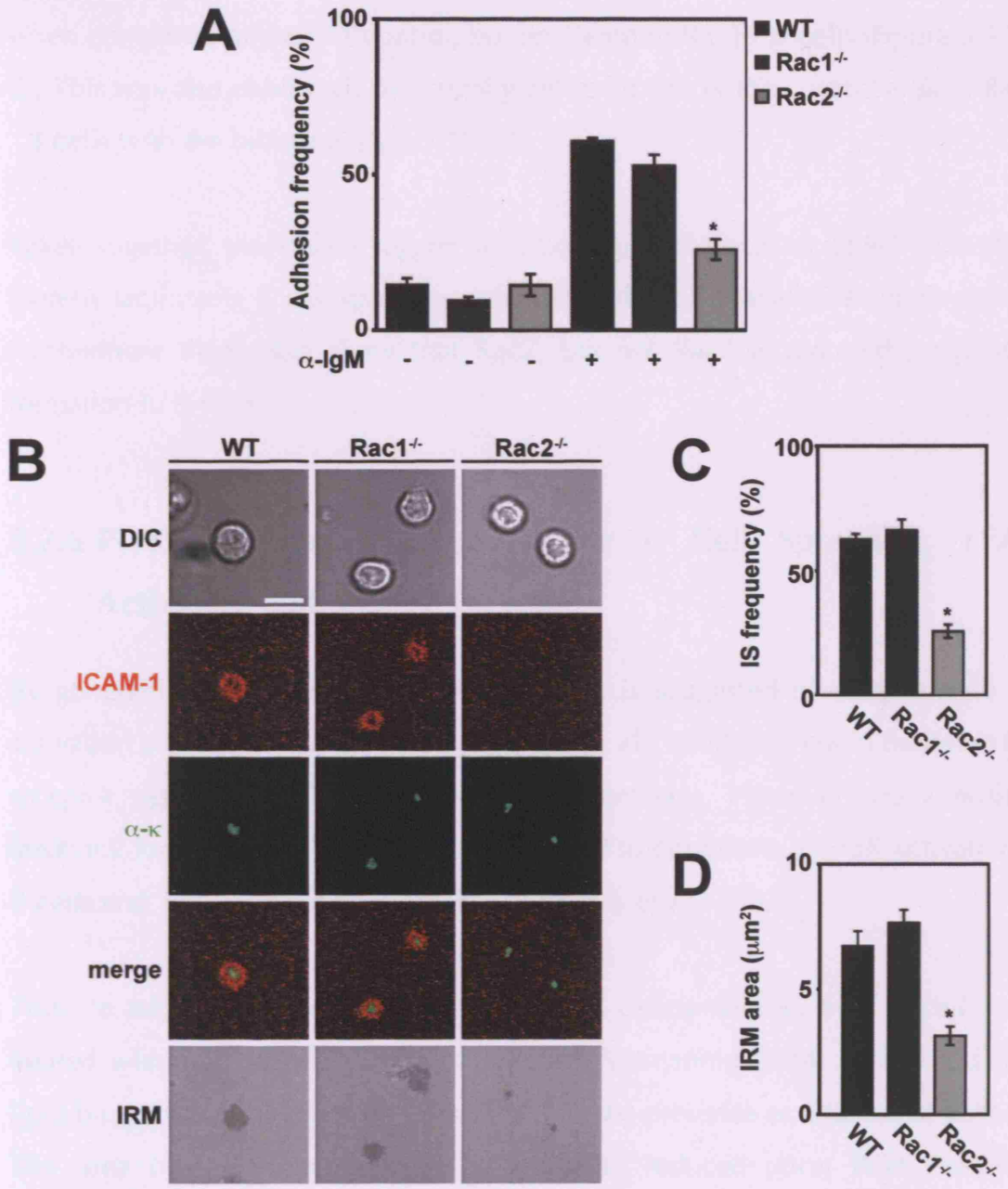

Figure 3.11 Rac2 regulates B cell adesion and pSMAC formation
(A) Not stimulated or α-IgM stimulated WT, Rac1$^{-/-}$ and Rac2$^{-/-}$ B cells were settled onto lipid bilayers containing ICAM-1 and adhesion capacity was assessed by IRM. Quantification of the B cell adhesion frequency by counting B cell-bilayer contacts in 4 different IRM images containing 30-40 cells each. The mean percentage (±se) is shown. Data are representative of 3 independent experiments. **(B)** WT, Rac1 and Rac2$^{-/-}$ B cells were settled onto lipid bilayers containing a high amount of α-κ and ICAM-1 and imaged by confocal microscopy after 20min. DIC, fluorescent, merged and IRM images of representative B cells are shown. Scale bar: 5μm. Quantification of **(C)** the IS frequency and **(D)** the IRM area of 4 different fields containing 10-20 cells each. The mean value (±se) is shown. t-test: * $p \leq 0.01$. Data are representative of 3 independent experiments.

Furthermore, the ability of $Rac2^{-/-}$ B cells to form a pSMAC was reduced 2.5-fold when compared to the WT control, but unaltered in $Rac1^{-/-}$ B cells (Figure 3.11 B, C). This was also confirmed by a significant reduction of the contact area of $Rac2^{-/-}$ B cells with the bilayer (Figure 3.11 D).

Taken together, these data suggest a critical role of Rac2 for LFA-1 activation, thereby facilitating B cell spreading when the amount of available antigen is low. Furthermore these data show that Rac2, but not Rac1 is required for pSMAC formation in B cells.

3.2.6 PI3K Function is Required for B Cell Spreading, LFA-1 Activation and pSMAC Formation

By generating second messenger lipids, PI3K is suggested to contribute to the activation of Vav (Han et al., 1998), (Palmby et al., 2002) and could therefore link receptor signalling with cytoskeletal rearrangements. However, via a positive feedback loop Vav and Rac are also suggested to contribute to PI3K activation in B cells and T cells (Inabe et al., 2002), (Reynolds et al., 2002).

Thus, to address the importance of PI3K for B cell spreading, MD4 B cells were treated with 100nM of the PI3K inhibitior Wortmannin (WM) and settled onto lipid bilayers bearing a low amount of HEL in the presence or absence of ICAM-1. The area of B cell spreading was markedly reduced upon WM treatment. Furthermore, antigen was less efficiently aggregated compared to untreated MD4 B cells, which suggested a role of PI3K for B cell spreading. However, the observed difference matched spreading and antigen aggregation of untreated B cells in the absence of ICAM-1 (Figure 3.12 A, B, C), indicating that PI3K might be required for LFA-1 activation. This notion was supported by the fact that the decrease in spreading was accompanied by a reduction of the B cell contact area with the lipid bilayer as assessed by IRM (Figure 3.12 A, D).

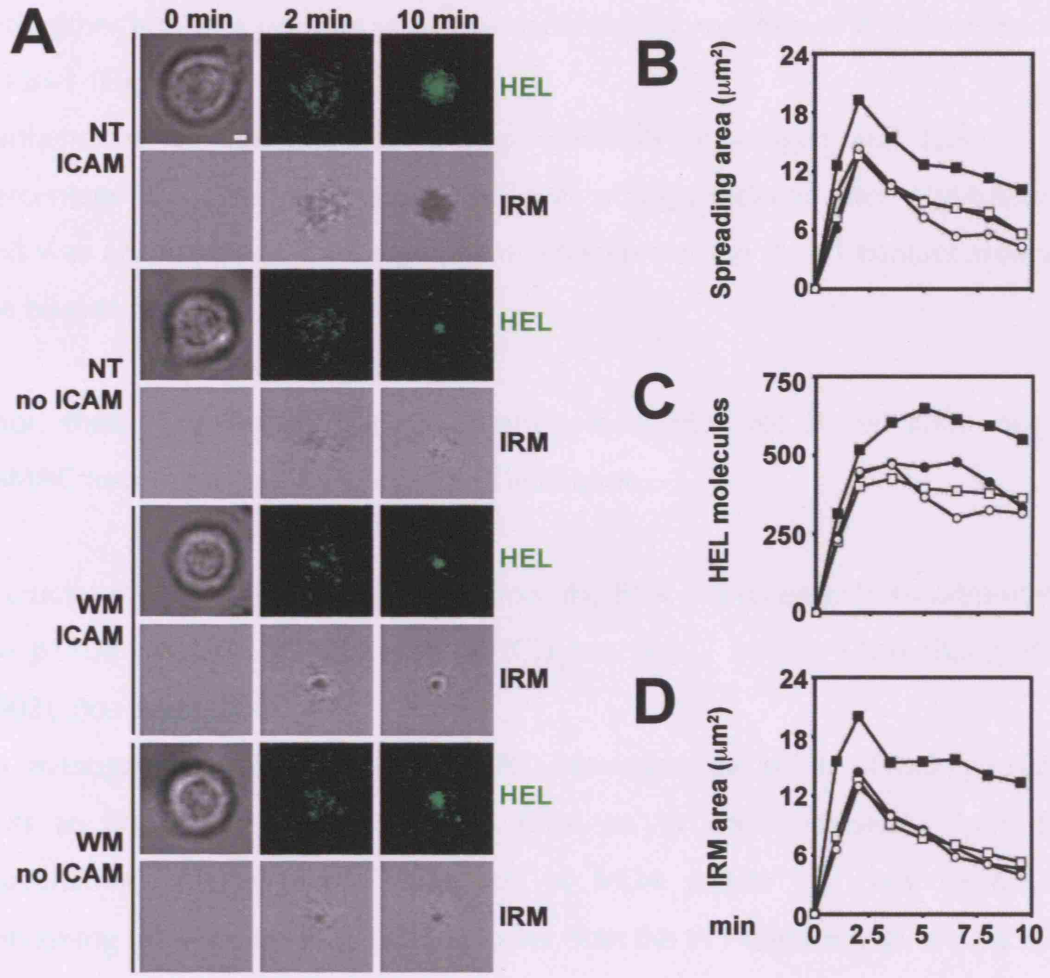

Figure 3.12 PI3K contributes to B cell spreading and antigen aggregation at a low antigen amount

(A) MD4B cells, not treated (NT) and pre-treated with 100nM WM, were settled onto lipid bilayers containing a low amount of HEL in the presence and absence of ICAM-1 and the kinetic of interaction was followed by confocal microscopy for 10min. DIC, HEL fluorescence and IRM images of representative B cells at the indicated time points are shown. Scale bar: 1μm. Quantification of **(B)** the area of HEL (spreading), **(C)** the number of accumulated HEL molecules and **(D)** the IRM area. Symbols: ■ NT + ICAM-1, □ NT no ICAM-1, ● WM + ICAM-1, ○ WM no ICAM-1. Values are a mean of 20-30 cells each. Data are representative of 2 independent experiments.

Therefore the role of PI3K for LFA-1 activation was tested. C57BL/6 (WT) B cells were pre-treated with different doses of WM and LY294002 (LY), another inhibitor for PI3K, and activated by BCR cross-linking with anti-IgM $(Fab')_2$. Their adhesion frequency on bilayers bearing ICAM-1 was determined by IRM. Pre-treatment with either inhibitor resulted in a dose-dependent abrogation of B cell adhesion to ICAM-1 (Figure 3.13 A).
Furthermore, in the presence of high amounts of antigen and ICAM-1, the percentage of B cells forming a pSMAC was strongly reduced after WM-treatment and was accompanied by a significant reduction of the B cell contact area with the bilayer (Figure 3.13 B, C, D).

Thus, these data indicate an important role of PI3K for B cell adhesion and pSMAC formation by mediating LFA-1 activation.

A crucial role for signal transduction from the BCR has recently been attributed to the p110δ catalytic subunit of PI3K (Clayton et al., 2002), (Okkenhaug et al., 2002), (Jou et al., 2002).
To investigate the role of p110δ for LFA-1 activation, the ability of MD4 $p110\delta^{-/-}$ B cells to adhere to ICAM-1 and to form an IS was evaluated. Upon BCR crosslinking, the adhesion frequency of MD4 $p110\delta^{-/-}$ B cells to ICAM-1 containing bilayers was significantly lower than the WT control (Figure 3.14 A).
Furthermore, on lipid bilayers bearing a high amount of HEL and ICAM-1 $p110\delta^{-/-}$ B cells aggregated a similar amount of antigen while pSMAC formation at the IS was abrogated. This also correlated with a decreased B cell contact area with the lipid bilayer (Figure 3.14 B, C, D, E).

Taken together, these data show that PI3K regulates LFA-1 activation and B cell adhesion to ICAM-1 and therefore contributes to B cell spreading and antigen aggregation at low antigen concentration. The p110δ catalytic subunit is required for LFA-1 activation. However, it is likely that also other subunits contribute to B cell adhesion to ICAM-1 and pSMAC formation at the IS.

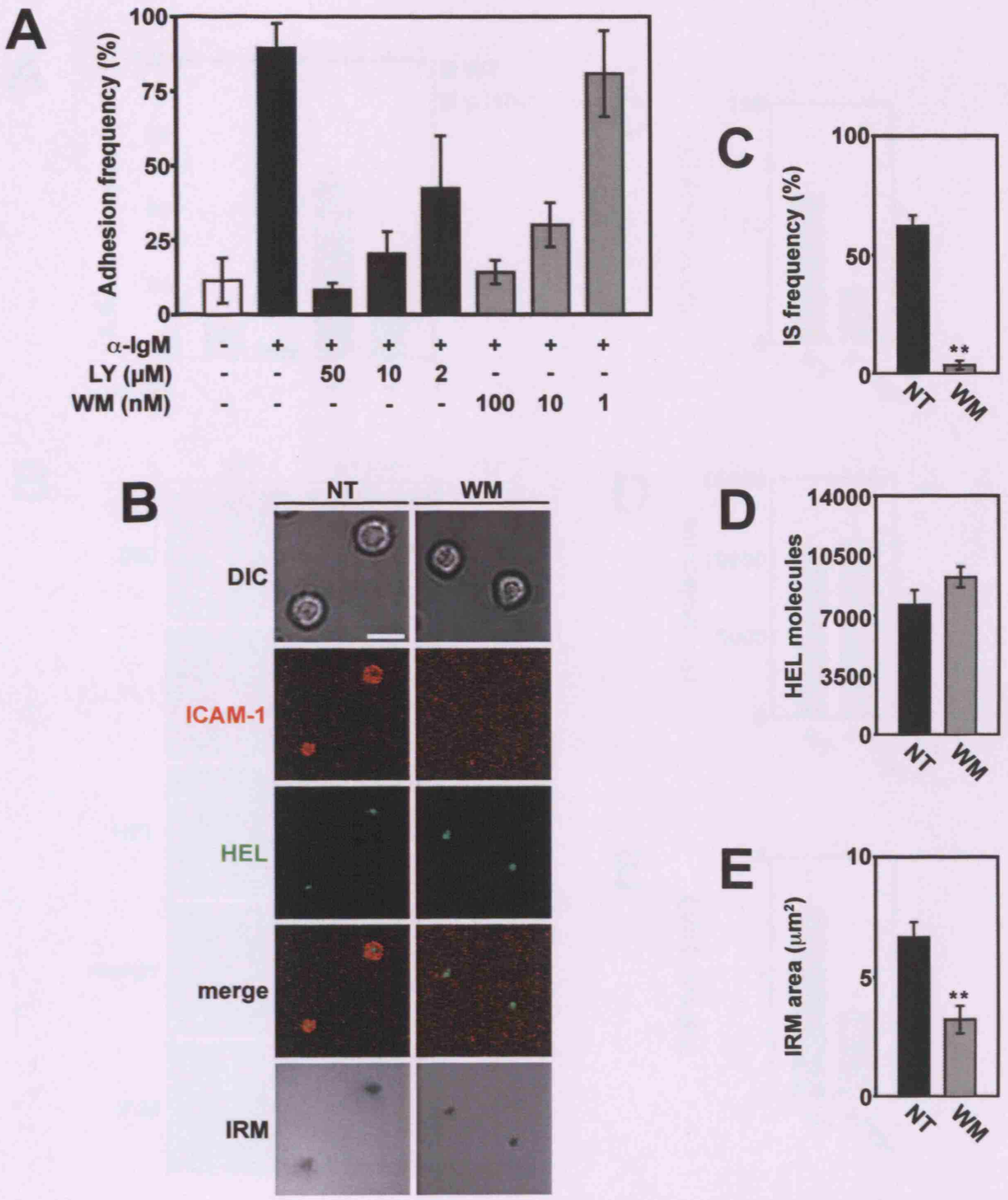

Figure 3.13 Inhibition of PI3K blocks B cell adhesion and pSMAC formation
(A) Not stimulated or α-IgM stimulated WT B cells were settled onto lipid bilayers containing ICAM-1 and adhesion capacity was assessed by IRM. B cells were pre-treated with different doses of WM or LY. Quantification of the B cell adhesion frequency by counting B cell-bilayer contacts in 4 different IRM images containing 20-30 cells each. The mean percentage (±se) is shown. Data are representative of at least 3 independent experiments. **(B)** Not treated (NT) and WM-treated (100nM) MD4 B cells were settled onto lipid bilayers containing a high amount of HEL and ICAM-1 and imaged by confocal microscopy after 20min. DIC, fluorescent, merged and IRM images of representative B cells are shown. Scale bar: 5μm. Quantification of **(C)** the IS frequency, **(D)** the number of accumulated HEL molecules and **(E)** the IRM area of 4 different fields containing 20-30 cells each. The mean value (±se) is shown. t-test: ** $p \leq 0.001$. Data are representative of at least 3 independent experiments.

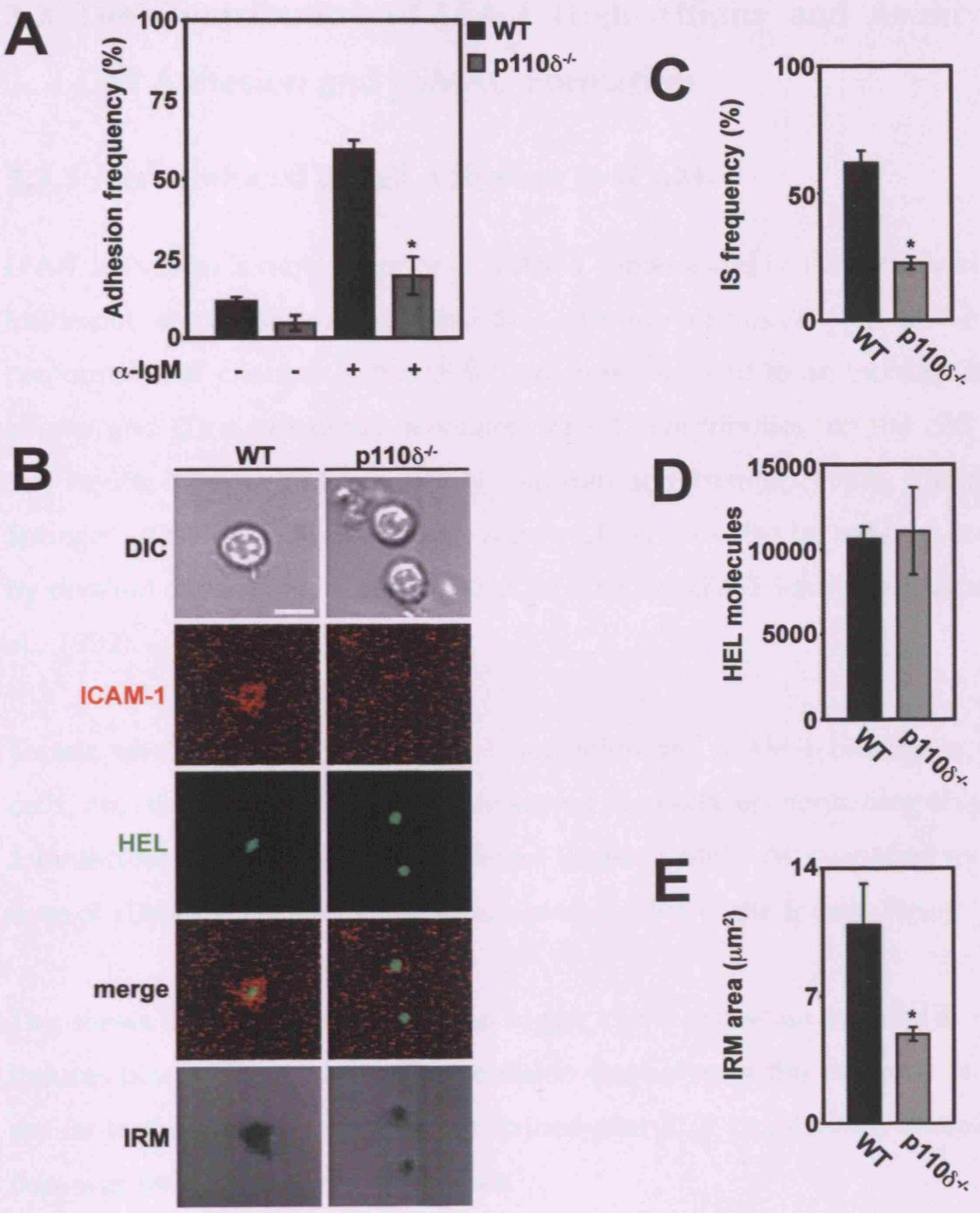

Figure 3.14 p110δ regulates B cell adhesion and pSMAC formation
(A) Not stimulated or α-IgM stimulated WT and p110δ$^{-/-}$ B cells were settled onto lipid bilayers containing ICAM-1 and adhesion capacity was assessed by IRM. Quantification of the B cell adhesion frequency by counting B cell-bilayer contacts in 4 different IRM images containing 20-30 cells each. The mean percentage (±se) is shown. Data are representative of 2 independent experiments. **(B)** MD4 WT and p110δ$^{-/-}$ B cells were settled onto lipid bilayers containing a high amount of HEL and ICAM-1 and imaged by confocal microscopy after 20min. DIC, fluorescent, merged and IRM images of representative B cells are shown. Scale bar: 5μm. Quantification of **(C)** the IS frequency, **(D)** the number of accumulated HEL molecules and **(E)** the IRM area of 4 different fields containing 10-20 cells each. The mean value (±se) is shown. t-test: * $p \leq 0.01$. Data are representative of 2 independent experiments.

3.3 The Contribution of LFA-1 High Affinity and Avidity to B Cell Adhesion and pSMAC Formation

3.3.1 Mn^{2+} Induced B Cell Adhesion to ICAM-1

LFA-1 activation is required prior to ICAM-1-binding and can be achieved by two inside-out signalling mechanisms that are non-exclusive: (1) BCR-triggered conformational changes in the LFA-1 structure that lead to an increase in LFA-1 affinity and (2) cytoskeleton-dependent LFA-1 redistribution on the cell surface that results in a high LFA-1 avidity (Bazzoni and Hemler, 1998), (Carman and Springer, 2003). Additionally, high affinity LFA-1 can also be induced outside-in by divalent cations, such as Mn^{2+} that bind to the LFA-1 I-domain (Dransfield et al., 1992).

To test whether Mn^{2+} induces LFA-1 activation and ICAM-1 binding in naïve B cells, not stimulated WT B cells were settled onto bilayers containing only ICAM-1 molecules in the presence of different doses of Mn^{2+}. As quantified by IRM, a dose of 10mM Mn^{2+} induced adhesion in up to 75% of the B cells (Figure 3.15A).

This shows that addition of Mn^{2+} can trigger LFA-1 activation in naïve B cells and induces binding to ICAM-1. The adhesion frequency in the presence of Mn^{2+} is similar to the adhesion frequency obtained after BCR crosslinking. Therefore this dose was used for further experiments.

3.3.1.1 Mn^{2+} Restores B Cell Adhesion upon WM-Treatment and in Vav-Deficient B Cells

To test whether the defective adhesion of WM-treated, $Vav1^{-/-}$, $Vav2^{-/-}$, $Vav1/2^{-/-}$ or $Rac2^{-/-}$ B cells was due to a defect in triggering LFA-1 high affinity, the adhesion of those B cells to lipid bilayers bearing only ICAM-1 was examined in the presence of 10mM Mn^{2+}. As shown in Figure 3.16 A, Mn^{2+} addition restored adhesion to ICAM-1 in 50% WM-treated B cells. The adhesion frequency of $Vav1^{-/-}$, $Vav2^{-/-}$

and Vav1/2$^{-/-}$ B cells to ICAM was comparable to WT B cells in the presence of Mn^{2+} (Figure 3.16 B). The defective adhesion of Rac2$^{-/-}$ B cells however, could not be restored using Mn^{2+} and showed a 5-fold decrease compared to WT or Rac1$^{-/-}$ B cells (Figure 3.16 C).

These data show that the Mn^{2+}-induced LFA-1/ICAM-1 interaction is sufficient to induce B cell adhesion in WM-treated as well as in Vav1$^{-/-}$, Vav2$^{-/-}$, and Vav1/2$^{-/-}$ B cells. In contrast, Mn^{2+} was not sufficient to restore adhesion of Rac2$^{-/-}$ B cells.

3.3.2 Mn^{2+} does not Restore pSMAC Formation upon WM-Treatment and in Vav- and Rac2-Deficient B Cells

To test whether the loss of pSMAC formation in WM-treated, Vav1$^{-/-}$, Vav2$^{-/-}$, Vav1/2$^{-/-}$ and Rac2$^{-/-}$ B cells can also be restored using Mn^{2+}, they were incubated on bilayers containing a high amount of antigen and ICAM-1 in the presence of Mn^{2+}.

As examined by confocal microscopy, WM-treated, Vav1$^{-/-}$, Vav2$^{-/-}$, Vav1/2$^{-/-}$ and Rac2$^{-/-}$ B cells did not recover pSMAC formation in the presence of Mn^{2+} (Figure 3.17 A, B). An increased number of Vav1$^{-/-}$ and Vav2$^{-/-}$ B cells showed ICAM accumulation, this appeared to localise predominantly only at one side of the cSMAC instead of forming a peripheral ring (Figure 3.17 B).

These data suggest that although LFA-1 in its high affinity state is able to induce B cell adhesion, this is not sufficient for pSMAC formation and implicate other mechanisms in the regulation of this process.

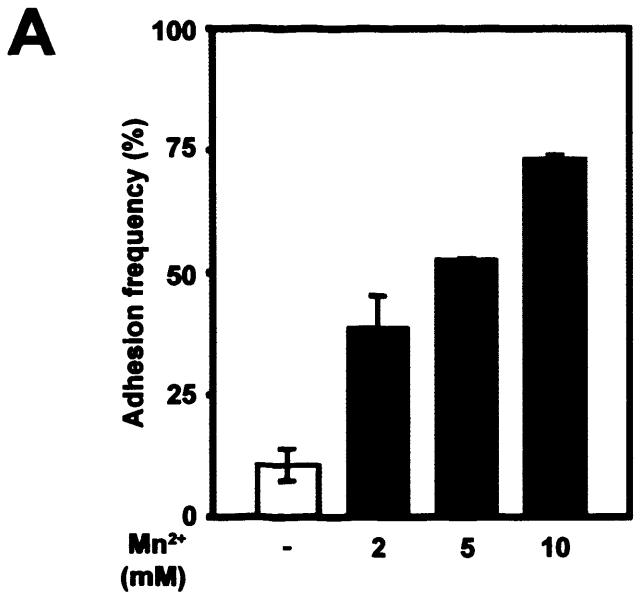

Figure 3.15 Mn^{2+} induced B cell adhesion to ICAM-1
(A) WT B cells were settled onto lipid bilayers containg only ICAM-1 molecules in the presence and absence of different amounts of Mn^{2+}. B cell adhesion frequency was quantified by counting the number of contacts of B cells with the bilayer by IRM in 4 different fields containing 20-30 B cells each.

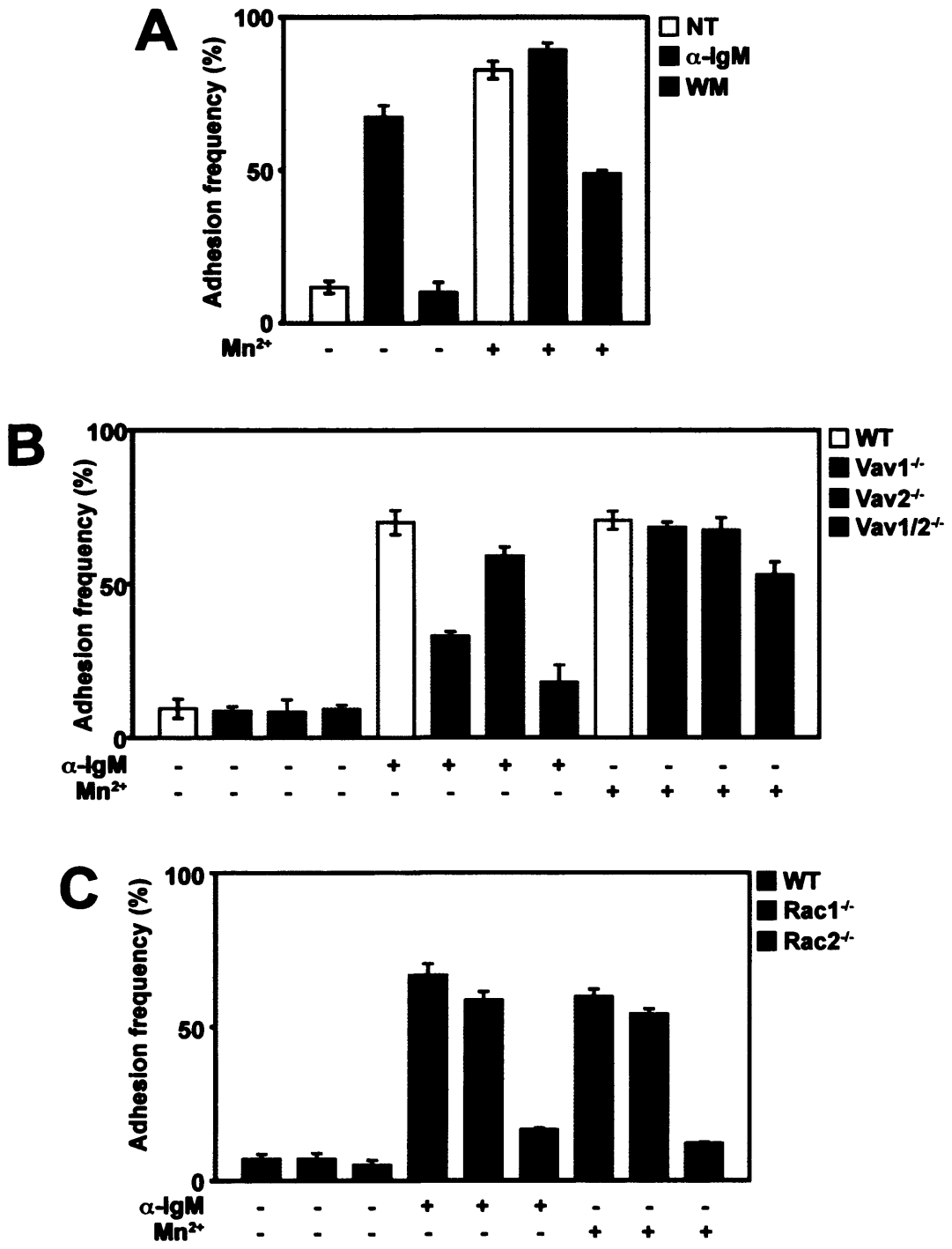

Figure 3.16 B cell adhesion is restored by Mn^{2+} in WM-treated, $Vav1^{-/-}$, $Vav2^{-/-}$ and $Vav1/2^{-/-}$ B cells

The following B cells were settled onto lipid bilayers containg only ICAM-1 molecules in the presence and absence of α-IgM or 10mM Mn^{2+} and adhesion frequency was quantified by counting B cell contacts with the bilayer using in 3 different fields containing 20-30 B cells each. **(A)** NT B cells and B cells treated with 100nM WM. **(B)** WT, $Vav1^{-/-}$, $Vav2^{-/-}$ and $Vav1/2^{-/-}$ B cells. **(C)** WT, $Rac1^{-/-}$ and $Rac2^{-/-}$ B cells. Data are representative of 2 independent experiments.

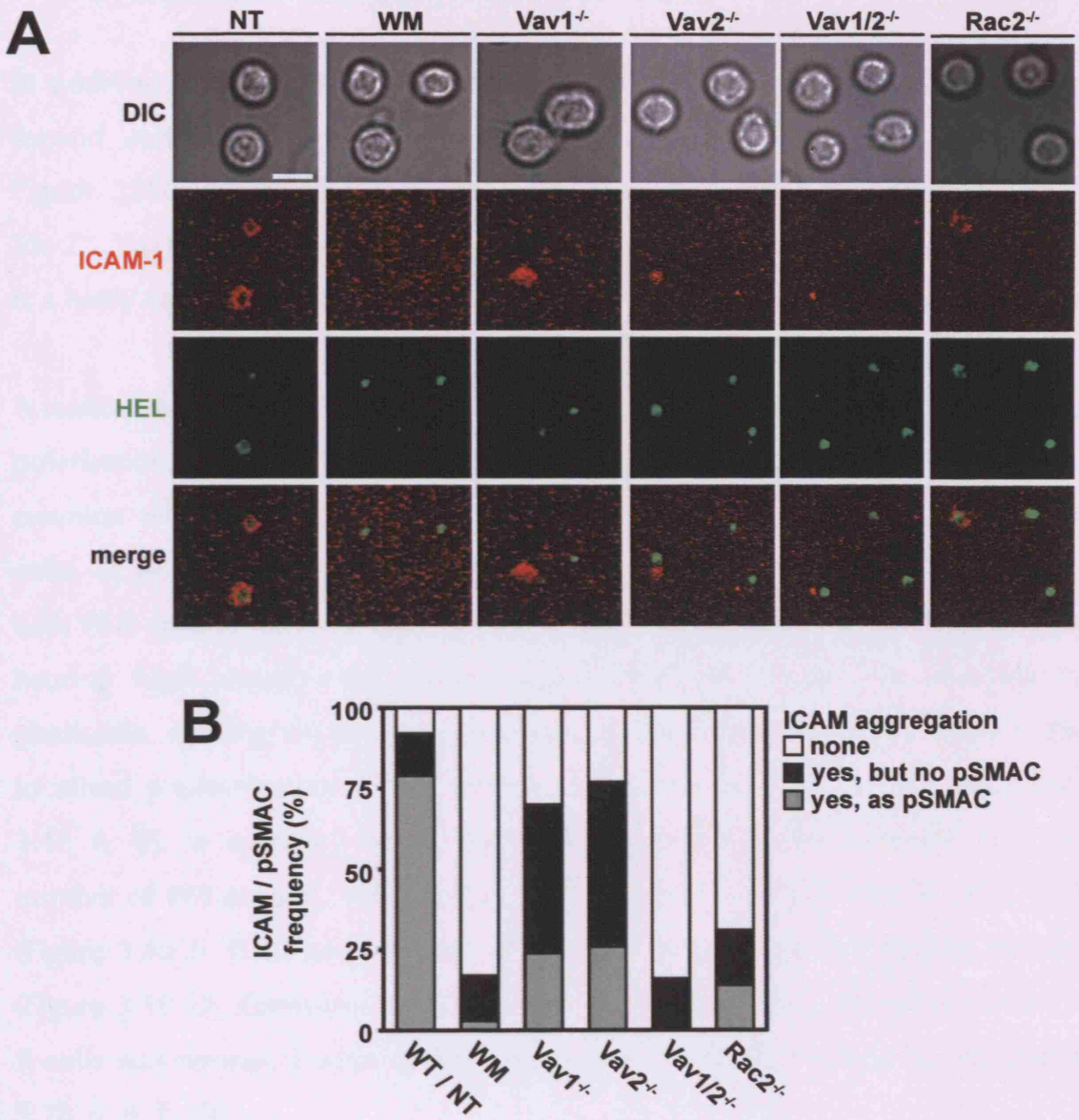

Figure 3.17 Mn^{2+} does not restore pSMAC formation in WM-treated and Vav- and Rac-deficient B cells

WT B cells, B cells treated with 100nM WM, MD4 Vav1$^{-/-}$, MD4 Vav2$^{-/-}$, MD4 Vav1/2$^{-/-}$ and Rac2$^{-/-}$ B cells were incubated on bilayers containing a high amount of antigen and ICAM-1 molecules for 20 min in the presence of 10mM Mn^{2+}. **(A)** DIC, fluorescent and merged images from representative B cells are shown. Scale bar: 5µM. **(B)** The percentage of B cells accumulating ICAM-1, forming a pSMAC or do not accumulate ICAM-1 is shown. Quantification was done on 4 different fields containing 10-20 cells each. The mean value (±se) is shown. Data are representative of at least 2 independent experiments.

3.4 SFKs, Vav1, Vav2, Rac2 and PI3K are Required for Cytoskeletal Rearrangements at the IS

In addition to conformational changes, rearrangement of the cytoskeleton is a second mechanism that supports LFA-1 binding to ICAM-1 (van Kooyk and Figdor, 2000). As Mn^{2+} failed to restore pSMAC formation in WM-treated, $Vav1^{-/-}$, $Vav2^{-/-}$, $Vav1/2^{-/-}$ and $Rac2^{-/-}$ B cells (3.3.2), misregulation of cytoskeletal dynamics is a likely cause of the defects observed in those B cells.

A readout for cytoskeletal rearrangements induced upon antigen recognition is the polarisation of F-actin at the IS (Ardouin et al., 2003), (Fleire et al., 2006). To examine whether F-actin accumulation was affected, PP1- and WM-treated B cells, as well as $Vav1^{-/-}$, $Vav2^{-/-}$, $Vav1/2^{-/-}$, $Rac1^{-/-}$ and $Rac2^{-/-}$ B cells were fixed with PFA upon mature IS formation after 20 minutes incubation on lipid bilayers bearing high amounts of antigen and ICAM-1 molecules. As revealed by phalloidin staining F-actin was polarised towards the IS in WT B cells and localised predominantly at the pSMAC region surrounding the antigen (Figure 3.18 A, B). In contrast, F-actin polarisation could only be observed in a low number of PP1-treated, WM-treated, $Vav1^{-/-}$, $Vav2^{-/-}$, $Vav1/2^{-/-}$ and $Rac2^{-/-}$ B cells (Figure 3.18 A, B, C) and the area of polarised F-actin was significantly reduced (Figure 3.18 D). Consistent with the observation that pSMAC formation in $Rac1^{-/-}$ B cells was normal, F-actin polarisation was not affected in those B cells (Figure 3.18 A, B, C, D).

These data demonstrate that antigen recognition by the BCR triggers cytoskeletal rearrangements, e.g. F-actin polarisation, through a signalling cascade involving subsequent activation of SFKs, Vav1 and Vav2, PI3K and Rac2. This, in turn, might support LFA-1 activation and pSMAC formation at the IS.

In addition, the amount of actin polymerisation could be determined in future experiments to support the morphological data of F-actin polarisation obtained from these experiments. To do this, WT, PP1-treated, WM-treated, $Vav1^{-/-}$, $Vav2^{-/-}$, $Vav1/2^{-/-}$ and $Rac2^{-/-}$ B cells could be stimulated by BCR cross-linking and the amount of F-actin could be measured upon phalloidin staining by FACS analysis.

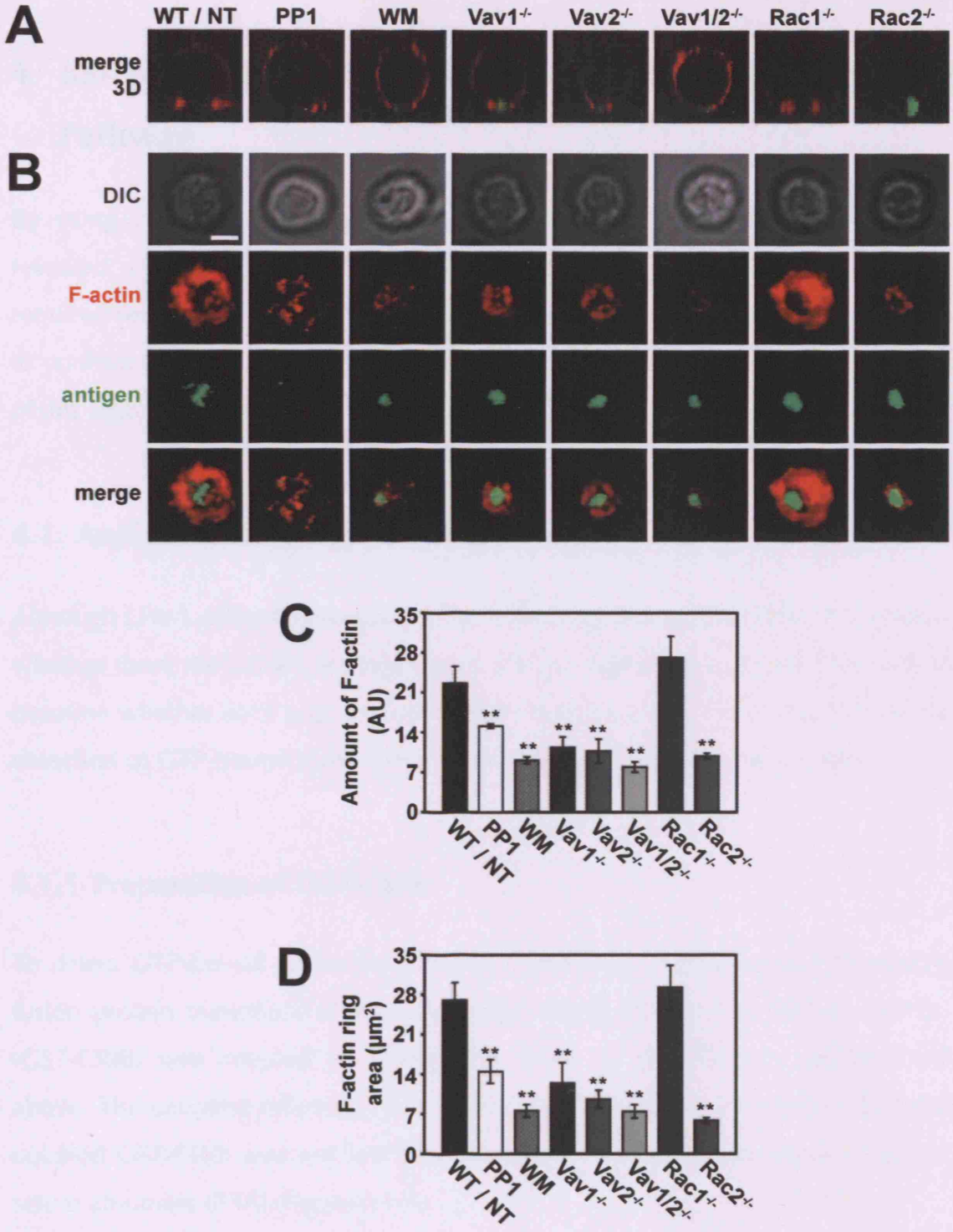

Figure 3.18 F-actin polarisation at the IS depends on SFKs, PI3K, Vav1, Vav2 and Rac2
WT B cells, B cells treated with 100µM PP1 or 100nM WM, Vav1$^{-/-}$, Vav2$^{-/-}$, Vav1/2$^{-/-}$ and Rac2$^{-/-}$ B cells were incubated on bilayers containing a high amount of antigen and ICAM-1 molecules for 20 min. B cells were fixed with 4% PFA and F-actin was stained with phalloidin-TRITC. **(A)** F-actin polarisation towards the IS for a representative B cells is shown by an axial projection. **(B)** DIC, fluorescent and merged images from representative B cells show amount and area of F-actin at the IS. Scale bar: 2.5µM. **(C)** Quantification of the amount of F-actin and (**D**) quantification of the area of F-actin of 4 different fields containing 10-20 cells each. The mean value (±se) is shown. t-test: ** $p \leq 0.001$. Data are representative of 3 independent experiments.

4 Biochemical Analysis of the Vav1/2-Rac2-PI3K Signalling Pathway

By using confocal microscopy, the results presented in the previous chapter revealed a signalling mechanism involving SFKs, Vav1, Vav2, Rac2 and PI3K, required for activation of the integrin LFA-1 in B cells. However, it was important to confirm these results using a different approach, such as biochemical analysis of this signalling pathway.

4.1 Analysis of Rac1 and Rac2 Activation

Although LFA-1 activation requires SFKs, Vav1, Vav2, Rac2 and PI3K, it is unclear whether these molecules act together in a linear signalling cascade. One way to examine whether Rac1 and Rac2 activation requires SFK, Vav1/2 and PI3K, is the detection of GTP-bound forms of Rac1 and Rac2 upon antigen recognition.

4.1.1 Preparation of GST-CRIB

To detect GTP-bound active forms of Rac1 and Rac2, a glutathione-S-transferase fusion protein comprised of the Cdc42/Rac interactive binding domain of Pak1 (GST-CRIB) was coupled to Glutathione beads as described in section 2.5.2 above. The coupling efficiency was determined by SDS-PAGE and the amount of coupled GST-CRIB was estimated by comparison to different amounts of bovine serum albumine (BSA) (Figure 4.1 A).

To test, whether GST-CRIB binds to active Rac1- and Rac2-GTP, naïve WT B cells were stimulated with anti-IgM $(Fab')_2$ for the indicated times or left unstimulated. B cells were lysed and incubated with the GST-CRIB beads. Binding of Rac1- and Rac2-GTP to the GST-CRIB beads at the different time points was examined by SDS-PAGE and Western Blot (WB) analysis (described in section 2.5 above). As shown in Figure 4.1 B, C, GTP-bound Rac1 can be observed at 1 minute after

BCR cross-linking, while Rac2 activation peaks at 30 seconds. Moreover, the amount of GTP-bound Rac1 and -Rac2 declines shortly after their initial activation (Figure 4.1 B, C).

Thus, GST-CRIB can be used to precipitate GTP-bound active forms of Rac1 and Rac2 in lysates of naïve B cells upon stimulation by BCR crosslinking.

4.1.2 Regulation of Rac1 and Rac2 Activation Downstream of the BCR

To determine how Rac1 and Rac2 activation is regulated downstream of antigen recognition, naïve WT B cells were treated with the SFK inhibitor PP1 or the PI3K inhibitor WM before stimulation by BCR crosslinking. Furthermore the role of Vav proteins for Rac1 and Rac2 activation was examined in Vav1/2$^{-/-}$ B cells.
Inhibition of SFKs resulted in a loss of GTP-bound Rac1 and Rac2 (Figure 4.2 A, B). While activation of Rac1 was also abolished upon inhibition of PI3K activity, Rac2 activation was partially affected (Figure 4.3 A, B). Rac1 activation was almost abrogated in Vav1/2$^{-/-}$ B cells (Figure 4.2 C) and this is in agreement with a previous report by Johmura et al. (Johmura et al., 2003). Rac2-GTP levels were also diminished in Vav1/2$^{-/-}$ B cells and residual Rac2 activation was delayed in comparison to the WT control B cells (Figure 4.3 C).

These results demonstrate that upon antigen recognition early SFK-mediated signalling triggers activation of the small GTPases Rac1and Rac2 via a Vav1/Vav2 and partially PI3K-dependent mechanism. Nevertheless, a residual activation of Rac2 could be observed in Vav1/2$^{-/-}$ B cells, which suggests that other GEFs might partly regulate Rac2 activation.

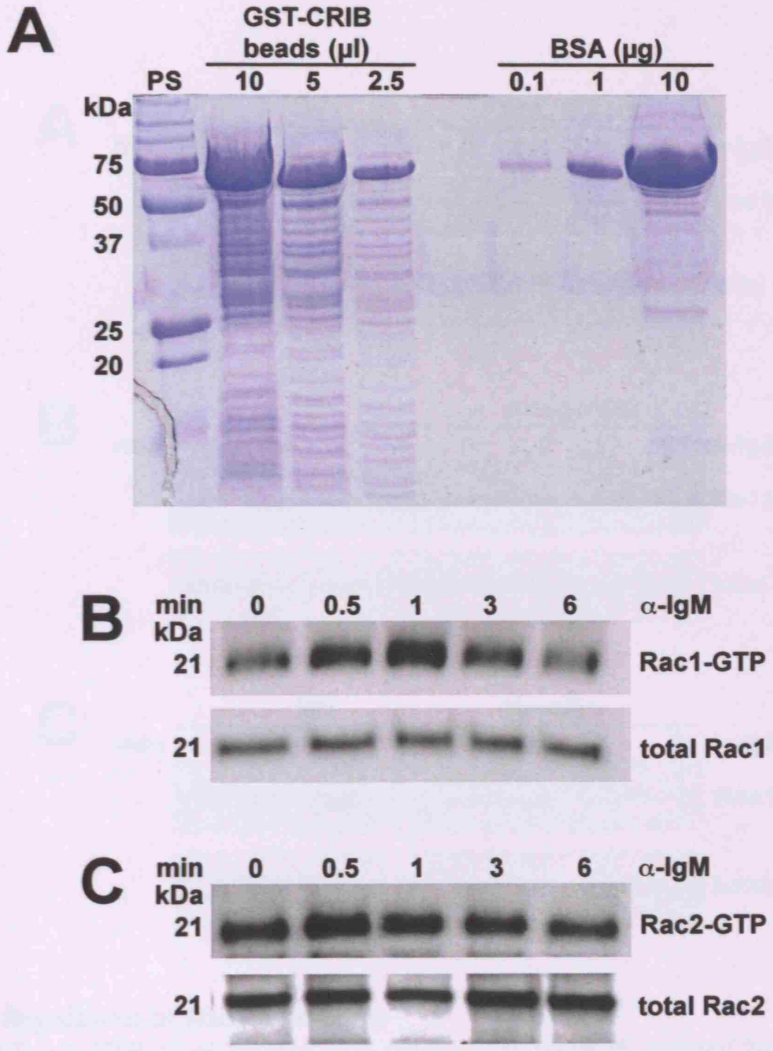

Figure 4.1 Biochemical analysis of Rac1 and Rac2 activation
(A) SDS page analysis of a GST-CRIB preparation, compared to BSA. Analysis of **(B)** Rac1-GTP and **(C)** Rac2-GTP from lysates of B cells,which were stimulated by BCR cross-linking with anti-IgM $(Fab')_2$ for the indicated times, using GST-CRIB. Samples for the detection of total Rac1 and Rac2 were taken from the same lysates prior to beeing incubated with GST-CRIB. Blots were probed with **(B)** mouse anti-Rac1 IgG2b and goat anti-mouse IgG-HRP and **(C)** rabbit anti-Rac2 IgG and goat anti-rabbit IgG-HRP. Blots are representative of 3 independent experiments.

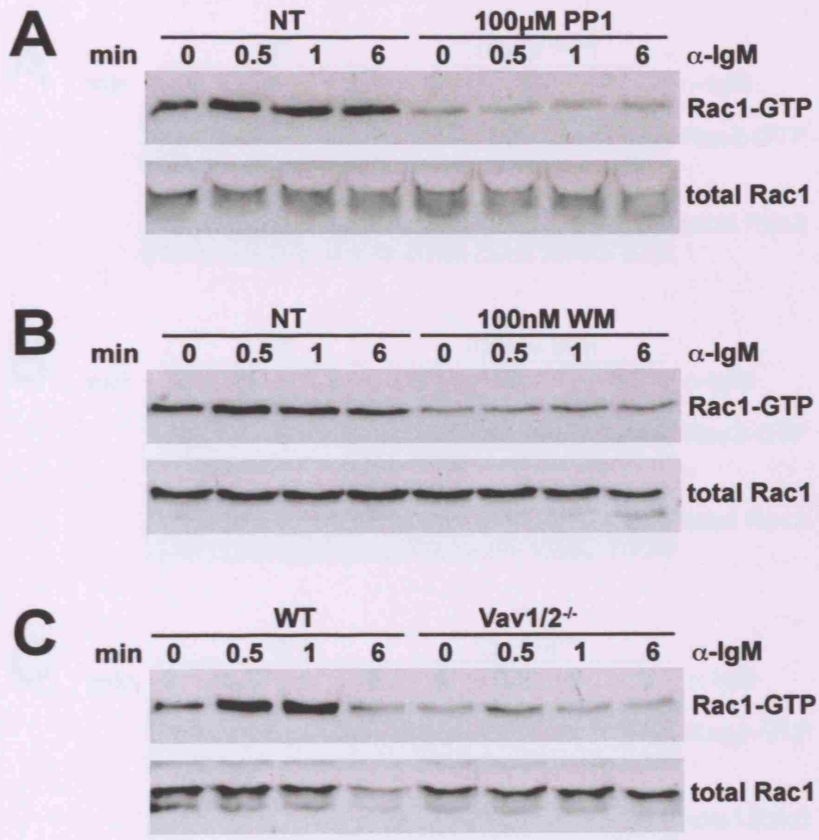

Figure 4.2 Regulation of Rac1 activation
Analysis of Rac1-GTP from lysates of B cells,which were stimulated by BCR cross-linking with anti-IgM $(Fab')_2$ for the indicated times, using GST-CRIB. B cells were treated with **(A)** 100µM PP1 and **(B)** 100nM WM prior to being stimulated. **(C)** Analsysis of Rac1-GTP from Vav1/2$^{-/-}$ B cells compared to WT B cells. Samples for the detection of total Rac1 were taken from the same lysates prior to beeing incubated with GST-CRIB. Blots were probed with mouse anti-Rac1 IgG2b and goat anti-mouse IgG-HRP. Blots are representative of 3 independent experiments.

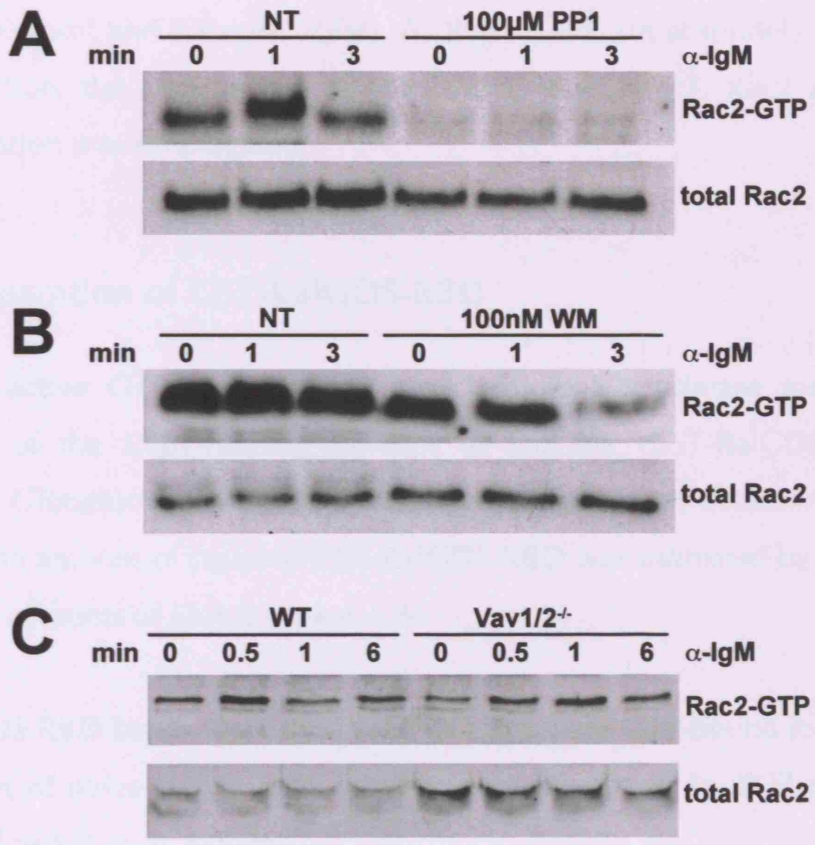

Figure 4.3 Regulation of Rac2 activation
Analysis of Rac2-GTP from lysates of B cells,which were stimulated by BCR cross-linking with anti-IgM $(Fab')_2$ for the indicated times, using GST-CRIB. B cells were treated with **(A)** 100µM PP1 and **(B)** 100nM WM prior to being stimulated. **(C)** Analsysis of Rac2-GTP from Vav1/2$^{-/-}$ B cells compared to WT B cells. Samples for the detection of total Rac2 were taken from the same lysates prior to beeing incubated with GST-CRIB. Blots were probed with rabbit anti-Rac2 IgG and goat anti-rabbit IgG-HRP. Blots are representative of 3 independent experiments.

4.2 Analysis of Rap1 Activation

The small GTPase Rap1 was recently identified as a potent activator of LFA-1 in T cells through its effector molecule RAPL (Katagiri et al., 2003). RAPL is thought to bind to the intracellular domain of LFA-1 to directly transmit signals from antigen receptors (Kinashi and Katagiri, 2004). As Rap1/RAPL are absolutely required for LFA-1 function, the contribution of SFK, Vav1, Vav2, Rac1, Rac2 and PI3K to Rap1 activation was investigated.

4.2.1 Preparation of GST-RalGDS-RBD

To detect active GTP-bound Rap1, a glutathione-S-transferase fusion protein comprised of the Rap1-binding domain of RalGDS (GST-RalGDS-RBD) was coupled to Glutathione beads. The coupling efficiency was determined by SDS-page and the amount of coupled GST-RalGDS-RBD was estimated by comparison to different amounts of BSA (Figure 4.4 A).

GST-RalGDS-RBD beads were then used to precipitate GTP-bound forms of Rap1 from lysates of naïve WT B cells, which where stimulated by BCR cross-linking beforehand or left un-stimulated.
Rap1 activation could be detected rapidly after BCR crosslinking. The level of GTP-bound Rap1 peaked at about 1 minute after BCR cross-linking and declined thereafter (Figure 4.4 B), similar to Rac1 and Rac2 activation (see section 4.1.1 above).

Thus, GST-RalGDS-RBD beads can be used in further experiments for the detection of active Rap1 in lysates of naïve B cells upon stimulation by BCR crosslinking.

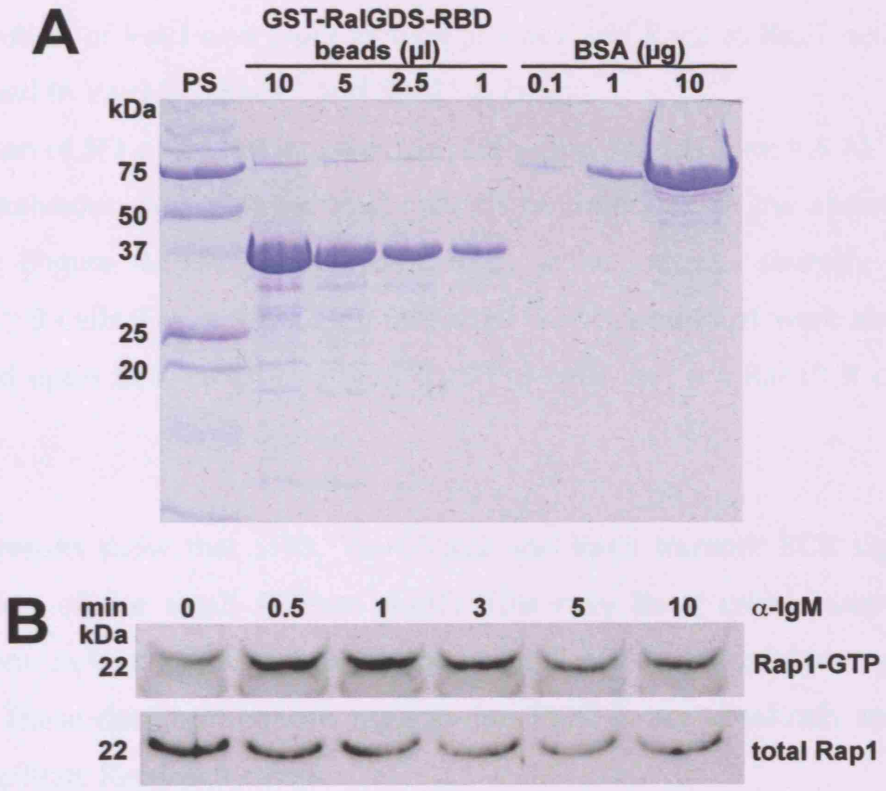

Figure 4.4 Biochemical analysis of Rap1 activation
(A) SDS page analysis of a GST-RalGDS-RBD preparation, compared to BSA. Analysis of **(B)** Rap1-GTP from lysates of B cells, which were stimulated by BCR cross-linking with anti-IgM $(Fab')_2$ for the indicated times, using GST-RalGDS-RBD. Samples for the detection of total Rap1 were taken from the same lysates prior to beeing incubated with GST-RalGDS-RBD. Blots were probed with rabbit anti-Rap1 IgG and goat anti-rabbit IgG-HRP. Blots are representative of 3 experiments.

4.2.2 Regulation of Rap1 Activation Downstream of the BCR

To determine how Rap1 activation is regulated downstream of BCR engagement, naïve WT B cells were treated with the SFK inhibitor PP1 and the PI3K inhibitor WM before BCR crosslinking using the anti-IgM $(Fab')_2$. Furthermore the contribution of Vav1 and Vav2 as well as Rac1 and Rac2 to Rap1 activation was examined in Vav1/2$^{-/-}$, Rac1$^{-/-}$ and Rac2$^{-/-}$ B cells.
Inhibition of SFKs resulted in a loss of GTP-bound Rap1 (Figure 4.5 A). In contrast, Rap1 activation was delayed and only slightly reduced in the absence of PI3K activity (Figure 4.5 B). Furthermore, Rap1 activation was severely affected in Vav1/2$^{-/-}$ B cells (Figure 4.5 C). The levels of GTP-bound Rap1 were also markedly reduced upon BCR cross-linking of Rac2$^{-/-}$ B cells, but not Rac1$^{-/-}$ B cells (Figure 4.5 D).

These results show that SFKs, Vav1/Vav2 and Rac2 transmit BCR signals to the activation of the small GTPase Rap1. This may be a critical step for LFA-1 activation as well as pSMAC formation at the B cell IS and might be regulated by RAPL. These data furthermore suggest that PI3K is not absolutely required, but may facilitate Rap1 activation.

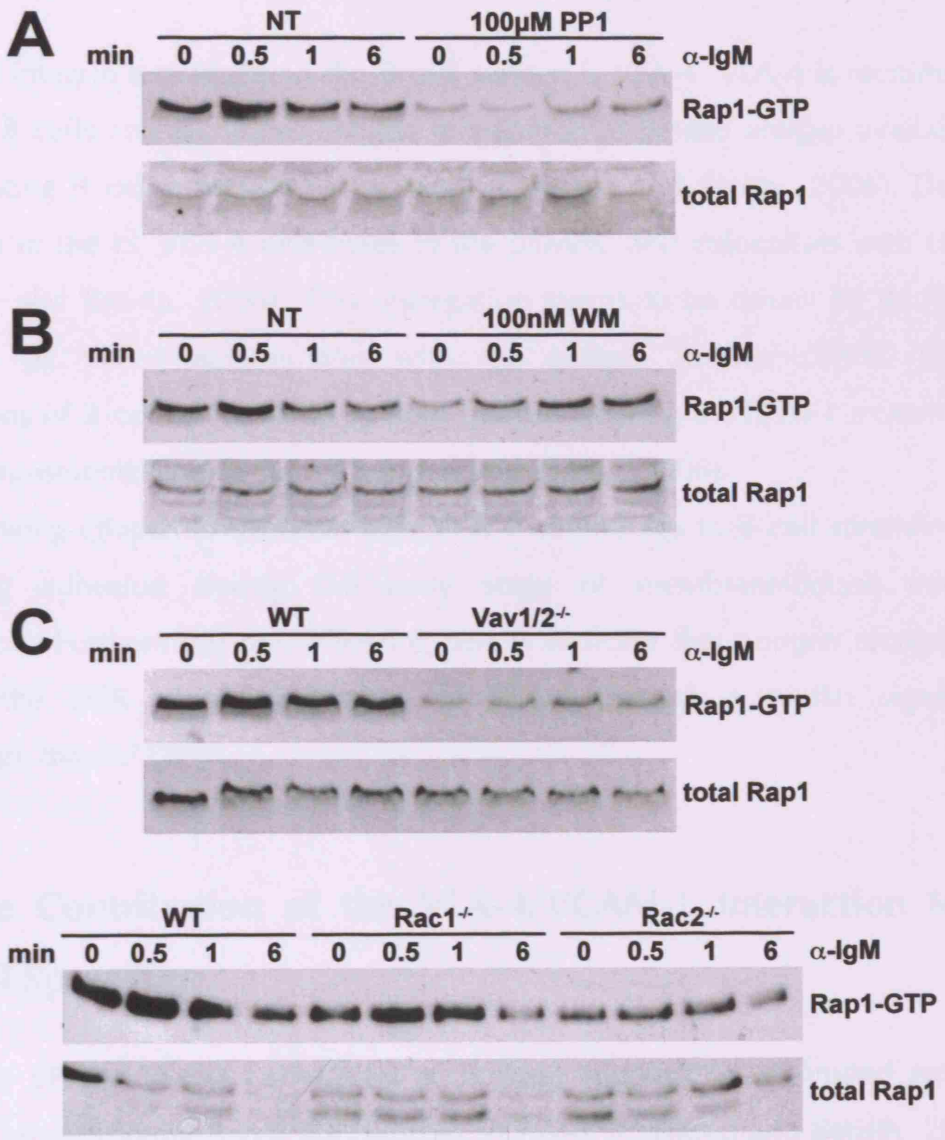

Figure 4.5 Regulation of Rap1 activation depends on SFKs, Vav1/2 and Rac2 and partially on PI3K

Analysis of Rap1-GTP from lysates of B cells,which were stimulated by BCR cross-linking with anti-IgM $(Fab')_2$ for the indicated times, using GST-RalGDS-RBD. B cells were treated with **(A)** 100µM PP1 and **(B)** 100nM WM prior to being stimulated. **(C)** Analsysis of Rap1-GTP from Vav1/2$^{-/-}$ B cells and **(D)** from Rac1$^{-/-}$ and Rac2$^{-/-}$ B cells compared to WT B cells. Samples for the detection of total Rap1 were taken from the same lysates prior to beeing incubated with GST-RalGDS-RBD. Blots were probed with rabbit anti-Rap1 IgG and goat anti-rabbit IgG-HRP. Blots are representative of 3 independent experiments.

5 The Contribution of BCR Signalling to VLA-4 Activation and Accumulation at the Immunological Synapse

A second integrin expressed on the B cell surface is VLA-4. VLA-4 is recruited to the IS in B cells and facilitates antigen recognition at limited antigen availability by mediating B cell adhesion to VCAM-1 (Carrasco and Batista, 2006). During formation of the IS, VLA-4 distributes to the pSMAC and colocalises with LFA-1 (Carrasco and Batista, 2006). This segregation seems to be driven by its ligand VCAM-1, as VLA-4 accumulates with the antigen in the cSMAC during interactions of B cells with APCs or lipid bilayers bearing a VCAM-1 mutant that lacks its transmembrane domain (Carrasco and Batista, 2006).

The following chapter shows that also VLA-4 contributes to B cell spreading by increasing adhesion during the early stage of membrane-bound antigen recognition. Furthermore the following results indicate that antigen recognition through the BCR triggers activation of VLA-4 through a similar signalling mechanism than of LFA-1.

5.1 The Contribution of the VLA-4/VCAM-1 Interaction to B cell Spreading

Similar to LFA-1, VLA-4 contributes to antigen aggregation at limited antigen densities by promoting B cell adhesion to VCAM-1 (Carrasco and Batista, 2006). To establish, whether VLA-4/VCAM-1 promotes antigen aggregation by supporting B cell spreading, naïve MD4 B cells were settled onto lipid bilayers containing a low amount of HEL in the presence or absence of VCAM-1. Confocal microscopy of the first 10 minutes of the B cell interaction with these HEL-bearing lipid bilayers revealed a significant increase in B cell spreading in the presence of VCAM-1 (Figure 5.1 A, B). The increased spreading also resulted in higher antigen accumulation compared to the absence of VCAM-1 (Figure 5.1 C).

Similar to bilayers containing ICAM-1 (see section 3.1 above), IRM analysis of B cell/bilayer attachment at the same timpoints shows large tight contacts in the presence of VCAM-1 and only scattered contacts its absence (Figure 5.1 A, D).

Thus, the BCR triggers VLA-4 activation and adhesion to VCAM-1 during the early stage of membrane bound antigen recognition. Subsequently, this B cell adhesion assists B cell spreading and antigen accumulation at low antigen densities.

5.2 The Role of BCR-Mediated Signalling to B cell Adhesion and VLA-4 Accumulation at the IS

B cell adhesion to VCAM-1 and recruitment of VLA-4 to the IS depends on BCR-mediated signalling (5.1 above and (Carrasco and Batista, 2006)). To examine whether regulation of VLA-4 activation follows the same signalling mechanism described in the previous chapter for LFA-1, the contribution of SFKs, Vav and Rac proteins and PI3K to B cell adhesion to VCAM-1 and VLA-4/VCAM-1 recruitment to the IS was examined.

5.2.1 The Role of SFKs for B Cell Adhesion to VCAM-1 and VLA-4 Recruitment to the IS

To analyse, whether SFKs contribute to VLA-4 activation, naïve WT B cells were pre-treated with various doses of the SFK inhibitors PP1 and PP2. Un-treated and treated B cells were further stimulated by BCR cross-linking with an anti-mouse IgM $(Fab')_2$ or left un-stimulated. B cells were settled onto lipid bilayers containing VCAM-1 only and their adhesion capacity was quantified by IRM.
Adhesion to VCAM-1 was induced by BCR cross-linking in 90% of the untreated B cells, however was completely abolished at a dose of 100μM PP1 or 100μM PP2 (Figure 5.2 A, B). Thus, these results show the importance of SFKs for VLA-4 activation and ligand binding.

To investigate whether SFKs are cruical for the accumulation of VLA-4 at the IS, MD4 B cells were treated with 100μM PP1 and settled onto lipid bilayers containing high amounts of HEL in the presence of VCAM-1. Untreated B cells recruited VLA-4 to the cSMAC of the IS as described previously (Carrasco and Batista, 2006). PP1 treatment however, severely reduced the capacity of B cells to recruit VLA-4 and this correlated with a significant reduction of the B cell contact area with the bilayer as assessed by IRM (Figure 5.3 A, B, C).

These results are in agreement with previous observations demonstrating SFK-transduced signalling as a requirement for VLA-4 activation and B cell adhesion to VCAM-1 (Spaargaren et al., 2003) and additionally show that SFKs are responsible for mediating VLA-4 recruitment to the IS.

5.2.2 The Role of Vav Proteins for B Cell Adhesion to VCAM-1 and VLA-4 Recruitment to the IS

As shown in a previous chapter (see section 3.2.4 above) B cell adhesion to ICAM-1 required the GEFs Vav1 and Vav2. To determine whether also VLA-4 activation depends on Vav proteins, the capacity of C57BL/6 WT, $Vav1^{-/-}$, $Vav2^{-/-}$, $Vav1/2^{-/-}$ and $Vav3^{-/-}$ B cells to adhere to bilayers containing only VCAM-1 molecules was evaluated.

IRM analysis did not reveal any significant differences in the adhesion frequency of $Vav1^{-/-}$, $Vav2^{-/-}$ and $Vav3^{-/-}$ B cells upon BCR crosslinking with the anti-IgM $(Fab')_2$ fragment. However, adhesion of $Vav1/2^{-/-}$ B cells was reduced by 40%, indicating a redundant role of Vav1 and Vav2 for VLA-4 activation (Figure 5.4 A).

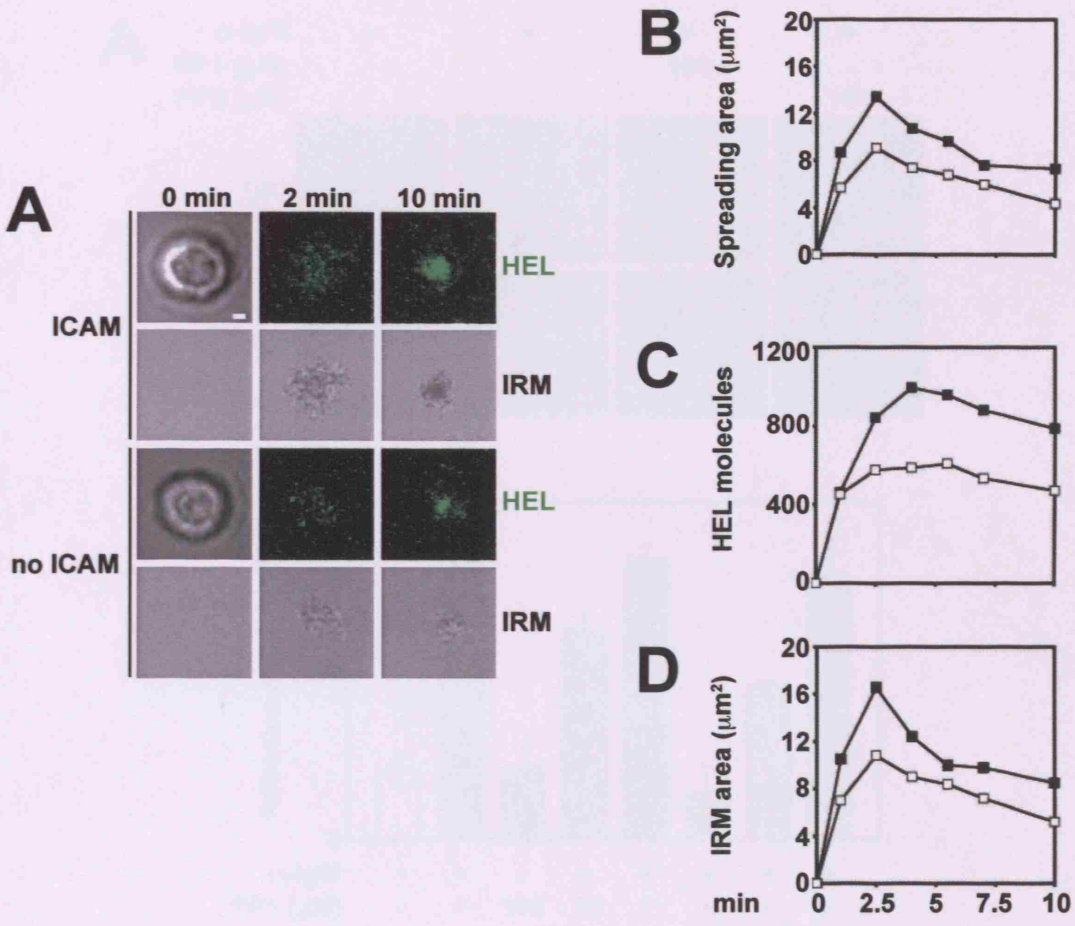

Figure 5.1 VLA-4/VCAM-1 promotes B cell spreading and antigen aggregation at low antigen amounts

(A) MD4 B cells were settled onto lipid bilayers containing a low amount of HEL in the presence and absence of VCAM-1 and the kinetic of interaction was followed by confocal microscopy for 10min. DIC, HEL fluorescence and IRM images of representative B cells at the indicated time points are shown. Scale bar: 1μm. Quantification of **(B)** the area of HEL (spreading), **(C)** the number of accumulated HEL molecules and **(D)** the IRM area. Symbols: ■ + VCAM-1, □ no VCAM-1. Values are a mean of 10-20 cells each. Data are representative of 2 independent experiments.

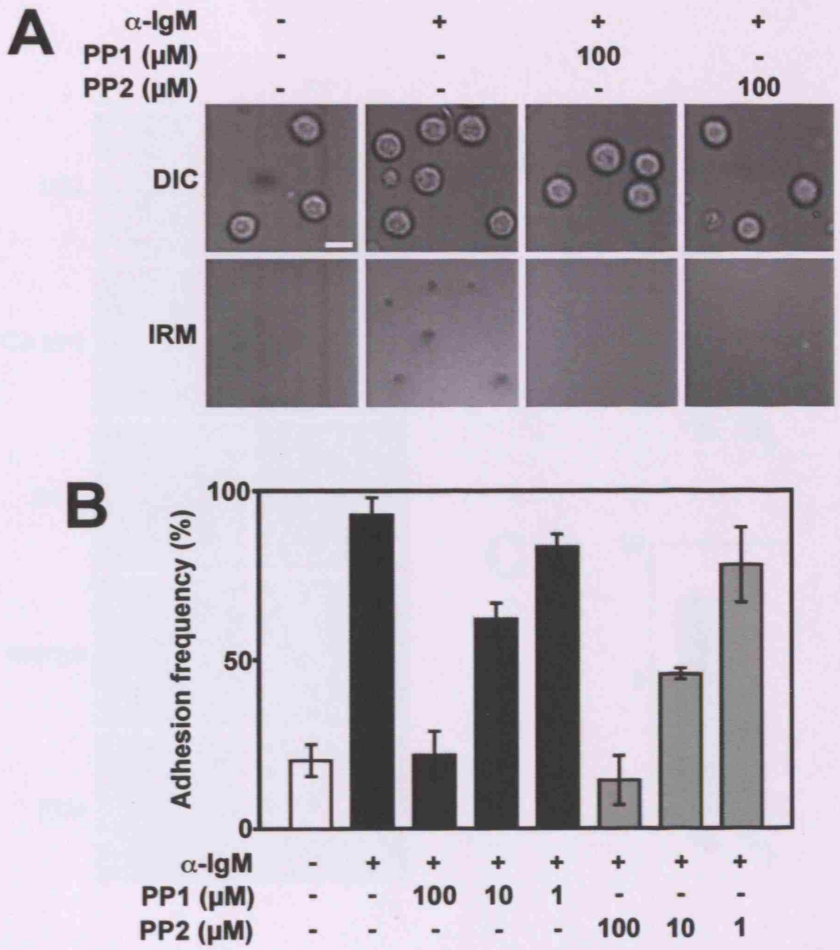

Figure 5.2 Inhibition of SFKs blocks B cell adhesion to VCAM-1
Not stimulated or α-IgM stimulated WT B cells were settled onto lipid bilayers containing VCAM-1 and adhesion capacity was assessed by IRM. B cells were pre-treated with different doses of PP1 or PP2. **(A)** DIC and IRM images of a representative field of B cells treated as indicated are shown. Scale bar: 5μm. **(B)** Quantification of the B cell adhesion frequency by counting B cell-bilayer contacts in 4 different IRM images containing 20-30 cells each. The mean percentage (±se) is shown. Data are representative of 3 independent experiments.

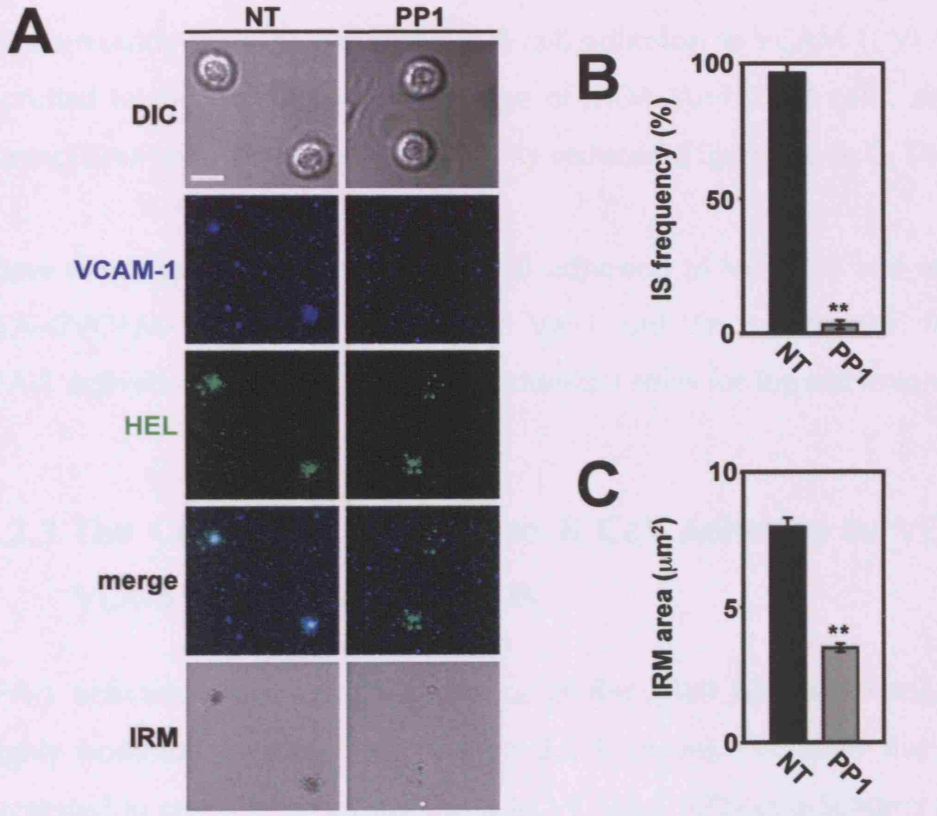

Figure 5.3 Inhibition of SFKs blocks IS formation on bilayers containing VCAM-1
(A) Not treated (NT) and PP1-treated (100μM) MD4 B cells were settled onto lipid bilayers containing a high amount of HEL and VCAM-1 and imaged by confocal microscopy after 20min. DIC, fluorescent, merged and IRM images of representative B cells are shown. Scale bar: 5μm. Quantification of **(B)** the IS frequency and **(C)** the IRM area of 3 different fields containing 20-30 cells each. The mean value (±se) is shown. t-test: ** $p \leq 0.001$ Data are representative of 2 independent experiments.

To examine the role of Vav proteins for VLA-4 recruitment to the IS, MD4 Vav1$^{-/-}$, Vav2$^{-/-}$, Vav1/2$^{-/-}$ and Vav3$^{-/-}$ B cells were settled onto lipid bilayers containing high amounts of HEL in the presence of VCAM-1 molecules. In the absence of either Vav1, Vav2 or Vav3 VCAM-1 was accumulated at the IS as efficiently as in WT B cells (Figure 5.4 B, C). Furthermore, the B cell contact area with the bilayer was similar in MD4 Vav1$^{-/-}$, Vav2$^{-/-}$ and Vav3$^{-/-}$ B cells (Figure 5.4 B, D). Concomitantly with the reduction in B cell adhesion to VCAM-1, VLA-4 was only recruited to the IS in a low percentage of MD4 Vav1/2$^{-/-}$ B cells, and the B cell contact area with the bilayer was slightly reduced (Figure 5.4 B, C, D).

These data demonstrate that also B cell adhesion to VCAM-1 and recruitment of VLA-4/VCAM-1 to the IS depends on Vav1 and Vav2. However, in contrast to LFA-1 activation, both proteins play redundant roles for the activation of VLA-4.

5.2.3 The Contribution of Rac to B Cell Adhesion to VCAM-1 and VLA-4 Recruitment to the IS

LFA-1 activation requires the presence of the small GTPases Rac2, but not the highly homologous Rac1 (see section 3.2.5 above). Although Rac proteins are suggested to regulate T cell adhesion to VCAM-1 (D'Souza-Schorey et al., 1998), it is unclear, whether Rac1 and Rac2 are also required for VLA-4 activation in B cells.

To examine the role of Rac1 and Rac2 for VLA-4 activation, the adhesion capacity of WT, Rac1$^{-/-}$ and Rac2$^{-/-}$ B cells to VCAM-1 containing lipid bilayers was investigated.
BCR crosslinking resulted in 95% adhesion of WT B cells. Adhesion of Rac1$^{-/-}$ B cells to VCAM-1 was similar to WT B cells and did not show any defects. A small decrease in adhesion of Rac2$^{-/-}$ B cells to VCAM-1 could be observed, however this was not significant when compared to WT B cells (Figure 5.5 A).

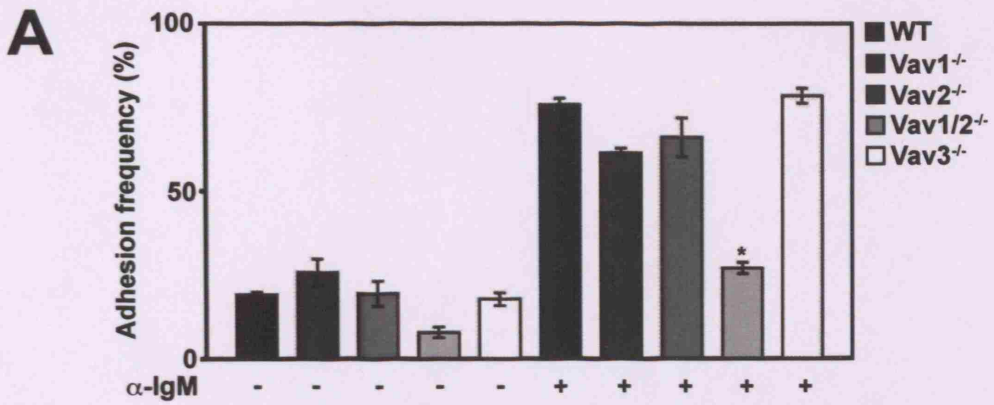
A
Adhesion frequency (%)
100
50
0
WT
Vav1-/-
Vav2-/-
Vav1/2-/-
Vav3-/-
α-IgM
- - - - - + + + + +
*

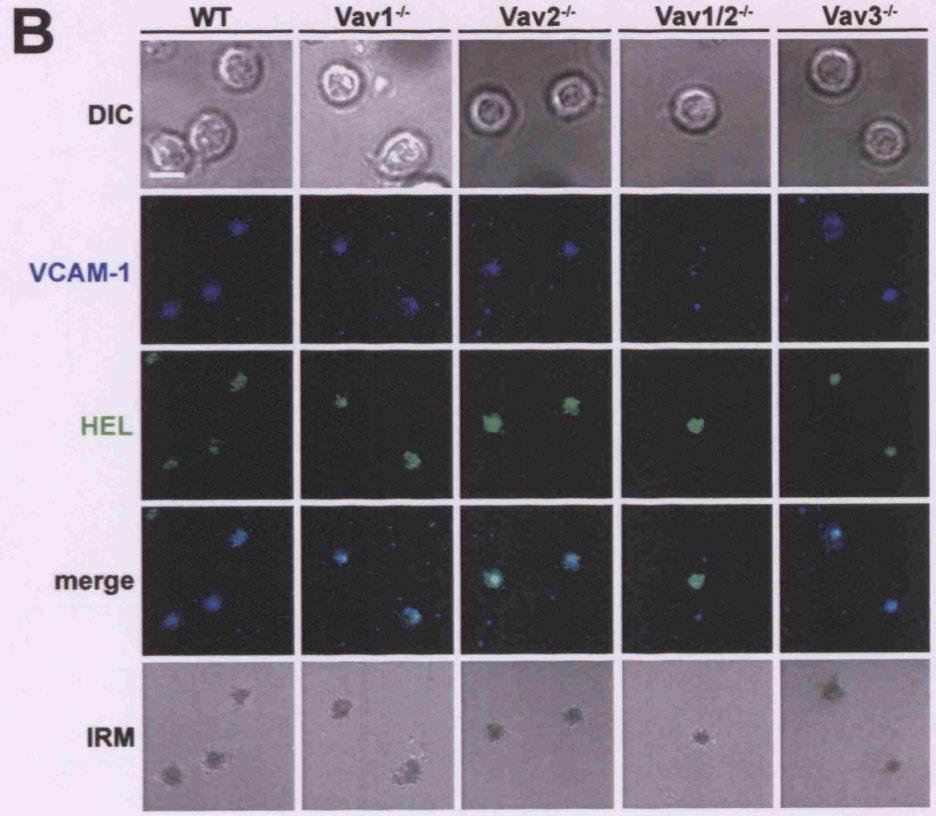
B
WT
Vav1-/-
Vav2-/-
Vav1/2-/-
Vav3-/-
DIC
VCAM-1
HEL
merge
IRM

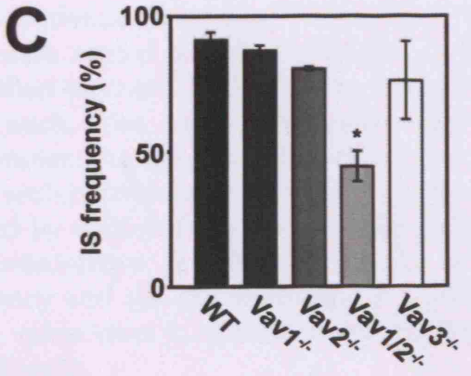
C
IS frequency (%)
100
50
0
*
WT
Vav1-/-
Vav2-/-
Vav1/2-/-
Vav3-/-

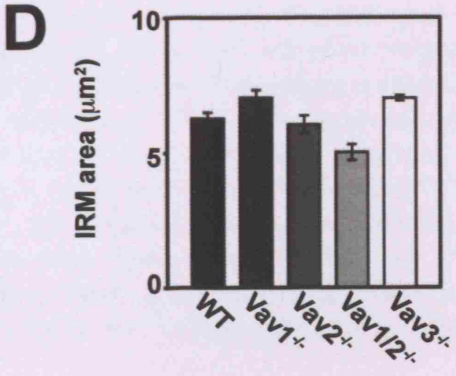
D
IRM area (μm2)
10
5
0
WT
Vav1-/-
Vav2-/-
Vav1/2-/-
Vav3-/-

Figure 5.4 VLA-4 activation and VCAM-1 recruitment to the IS in Vav-deficient B cells

(A) Not stimulated or α-IgM stimulated WT and $Vav1^{-/-}$, $Vav2^{-/-}$, $Vav1/2^{-/-}$ and $Vav3^{-/-}$ B cells were settled onto lipid bilayers containing VCAM-1 and adhesion frequency was quantified by counting B cell-bilayer contacts in 3 different IRM images containing 30-40 cells each. The mean percentage (±se) is shown. Data are representative of 2 independent experiments. **(B)** MD4 WT and $Vav1^{-/-}$, $Vav2^{-/-}$, $Vav1/2^{-/-}$ and $Vav3^{-/-}$ B cells were settled onto lipid bilayers containing a high amount of HEL and VCAM-1 and imaged by confocal microscopy after 20min. DIC, fluorescent, merged and IRM images of representative B cells are shown. Scale bar: 5μm. Quantification of **(C)** the IS frequency and **(D)** the IRM area of 3 different fields containing 10-20 cells each. The mean value (±se) is shown. t-test: *$p \leq 0.01$. Data are representative of 2 independent experiments.

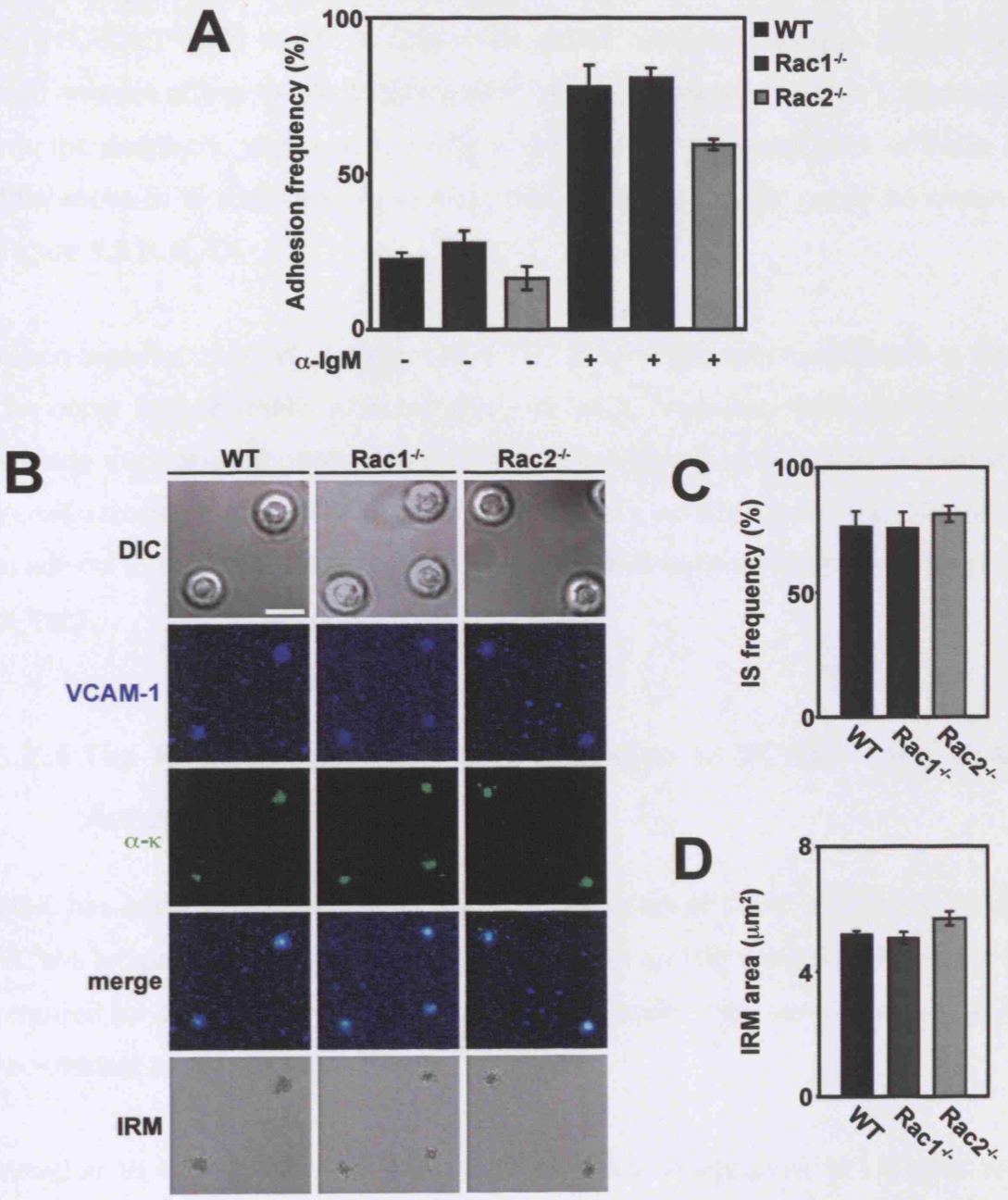

Figure 5.5 VLA-4 activation and VCAM-1 recruitment to the IS in Rac-deficient B cells
(A) Not stimulated or α-IgM stimulated WT, Rac1$^{-/-}$ and Rac2$^{-/-}$ B cells were settled onto lipid bilayers containing VCAM-1 and adhesion capacity was assessed by IRM. Quantification of the B cell adhesion frequency by counting B cell-bilayer contacts in 4 different IRM images containing 30-40 cells each. The mean percentage (±se) is shown. Data are representative of 2 independent experiments. **(B)** WT, Rac1 and Rac2$^{-/-}$ B cells were settled onto lipid bilayers containing a high amount of α-κ and VCAM-1 and imaged by confocal microscopy after 20min. DIC, fluorescent, merged and IRM images of representative B cells are shown. Scale bar: 5μm. Quantification of **(C)** the IS frequency and **(D)** the IRM area of 4 different fields containing 10-25 cells each. The mean value (±se) is shown. Data are representative of 2 independent experiments.

To investigate further, if Rac1 and Rac2 are required for VLA-4 recruitment to the IS, WT, $Rac1^{-/-}$ and $Rac2^{-/-}$ B cells were settled onto lipid bilayers containing a high amount of α-κ in the presence of VCAM-1. In contrast to LFA-1 segregation into the periphery, VLA-4 recruitment to the IS did not require Rac1 or Rac2. No differences in IS formation or contact area with the bilayer could be observed (Figure 5.5 B, C, D).

Taken together, these data suggest that VLA-4 activation and recruitment to the IS can occur independently of either Rac1 or Rac2. However, these results do not exclude the possibility that both GTPases have redundant functions in mediating VLA-4 activation. Indeed, $Rac2^{-/-}$ B cells showed a small reduction in their ability to adhere to VCAM-1, which might be even further reduced by the additional loss of Rac1.

5.2.4 The Role of PI3K for B Cell Adhesion to VCAM-1 and VLA-4 Accumulation at the IS

PI3K has been suggested to contribute to adhesion of DT40 chicken B cells to VCAM-1 (Spaargaren et al., 2003). However, the p110δ subunit of PI3K was not required for T cell adhesion to VCAM-1. Furthermore their contribution to VLA-4 recruitment to the IS is unknown.

Whether VLA-4 activation requires PI3K was first investigated. WT B cells were pre-treated with different doses of WM and LY294002 (LY), activated by BCR cross-linking and their adhesion frequency on bilayers bearing VCAM-1 molecules was determined. Pre-treatment with both inhibitors resulted in the abrogation of B cell adhesion to VCAM-1 (Figure 5.6 A), confirming the dependence of VLA-4 activation on PI3K as reported previously (Spaargaren et al., 2003).

On bilayers bearing a high amount of HEL in the presence of VCAM-1, VLA-4 recruitment to the IS was also abrogated and this correlated with reduction of the B cell contact area with the bilayer (Figure 5.6 B, C, D).

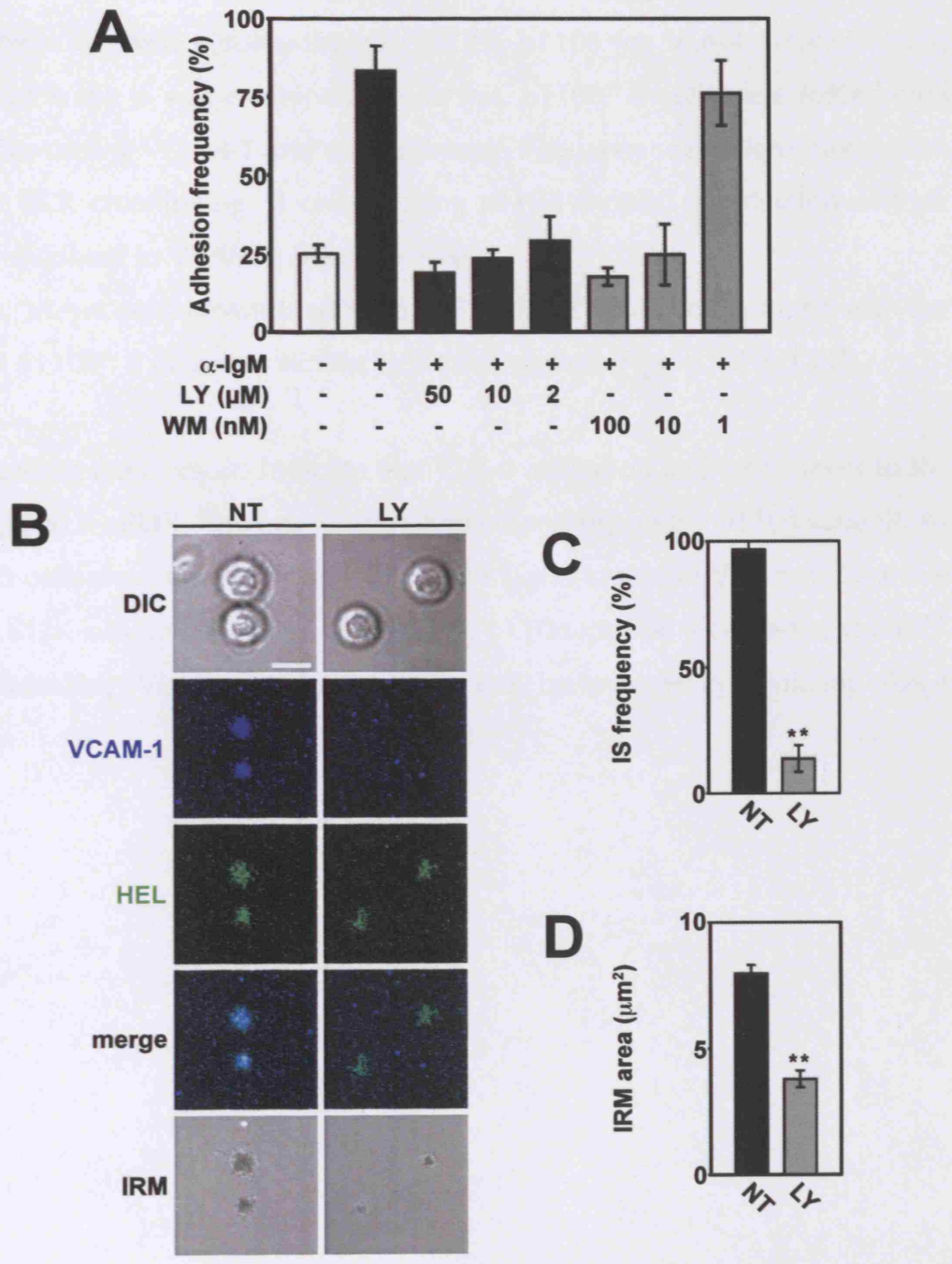

Figure 5.6 Inhibition of PI3K blocks B cell adhesion and VCAM-1 recruitment to the IS
(A) Not stimulated or α-IgM stimulated WT B cells were settled onto lipid bilayers containing VCAM-1 and adhesion capacity was assessed by IRM. B cells were pre-treated with different doses of WM or LY. Quantification of the B cell adhesion frequency by counting B cell-bilayer contacts in 4 different IRM images containing 20-30 cells each. The mean percentage (±se) is shown. Data are representative of 3 independent experiments. **(B)** Not treated (NT) and LY-treated (50μM) MD4 B cells were settled onto lipid bilayers containing a high amount of HEL and VCAM-1 and imaged by confocal microscopy after 20min. DIC, fluorescent, merged and IRM images of representative B cells are shown. Scale bar: 5μm. Quantification of **(C)** the IS frequency and **(D)** the IRM area of 3 different fields containing 30-40 cells each. The mean value (±se) is shown. t-test: ** $p \leq 0.001$. Data are representative of 2 independent experiments.

On the basis of these results, the role of the p110δ for VLA-4 activation and recruitment to the IS was examined. To do this, p110δ$^{-/-}$ B cells were settled onto bilayers containing VCAM-1 and their adhesion frequency was determined before and after BCR crosslinking. B cells lacking p110δ showed a reduction of their capacity to adhere to VCAM-1 (Figure 5.7 A).
However, VLA-4 recruitment towards the IS and the B cell contact area with the bilayer of p110δ$^{-/-}$ B cells was similar to the WT control (Figure 5.7 B, C, D).

Taken together these results indicate that VLA-4 activation and recruitment to the IS is regulated by PI3K, however do not depend entirely on the p110δ subunit. As p110δ$^{-/-}$ B cells were able to adhere to VCAM-1 and to recruit VLA-4 to IS, a role for other PI3K subunits is likely. In this line, p110α can be recruited to the BCR upon crosslinking (Vigorito et al., 2004) and may be involved in regulating VLA-4 activation.

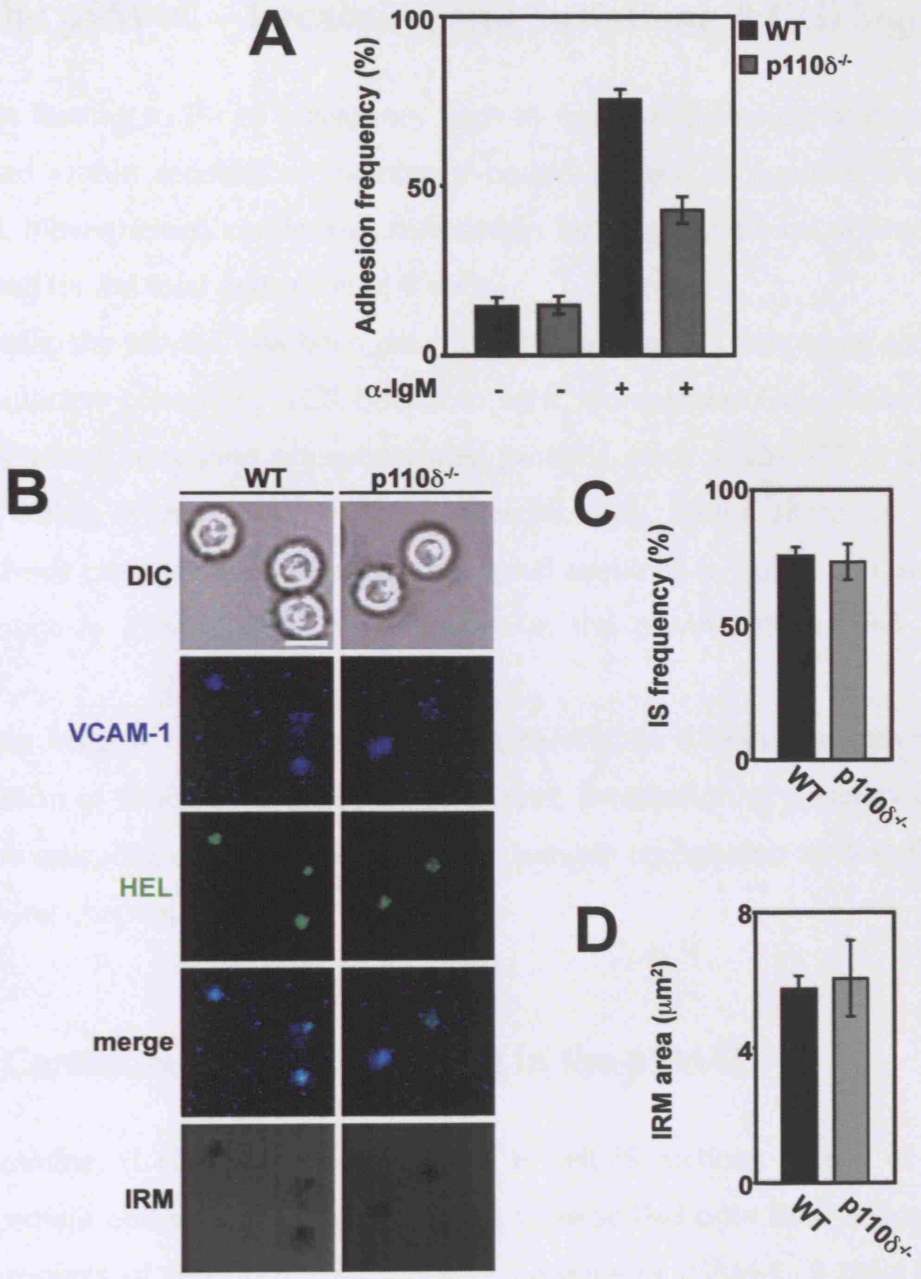

Figure 5.7 B cell adhesion to VCAM-1 and its recruitment to the IS is independent of p110δ

(A) Not stimulated or α-IgM stimulated WT and p110δ$^{-/-}$ B cells were settled onto lipid bilayers containing VCAM-1 and adhesion capacity was assessed by IRM. Quantification of the B cell adhesion frequency by counting B cell-bilayer contacts in 3 different IRM images containing 30-40 cells each. The mean percentage (±se) is shown. Data are representative of 2 independent experiments. **(B)** MD4 WT and p110δ$^{-/-}$ B cells were settled onto lipid bilayers containing a high amount of HEL and VCAM-1 and imaged by confocal microscopy after 20min. DIC, fluorescent, merged and IRM images of representative B cells are shown. Scale bar: 5μm. Quantification of **(C)** the IS frequency and **(D)** the IRM area of 4 different fields containing 10-20 cells each. The mean value (±se) is shown. Data are representative of 2 independent experiments.

6 The pSMAC – Localising and Sustaining B Cell Signalling

Signals leading to B cell activation, such as tyrosine phosphorylation events, are induced within seconds of membrane-bound antigen recognition (Fleire et al., 2006). Nevertheless, continuous stimulation for a longer period of time might be required for the total activation of B cells.

In T cells, the pSMAC has been described as the site for continuous generation of microclusters containing TCR bound to MHC complexes. Only these peripheral microclusters contained phosphorylated proteins, such as ZAP-70 or Lck (Campi et al., 2005), (Varma et al., 2006), (Yokosuka et al., 2005). Therefore the current hypothesis emerges that the sustained signal required for full T cell activation is continuously generated in microclusters in the pSMAC (Saito and Yokosuka, 2006).

To gain insights into the function of the pSMAC in B cells and into the spatial regulation of BCR proximal signalling events, localisation of a variety of proteins was investigated upon membrane bound antigen recognition as described in the following chapter.

6.1 Continuous B Cell Signalling in the pSMAC

To examine, if also the pSMAC at the B cell IS fuctions as site of new BCR engagement and signalling, MD4 B cells were settled onto lipid bilayers bearing low amounts of HEL in the presence or absence of ICAM-1. B cells were fixed after 2 and 20 minutes upon antigen recognition and the phosphotyrosine (pTyr) amount was stained with the anti-pTyr antibodies IG2 and PY2, followed by incubation with an Alexa Fluor 488-conjugated anti-mouse IgG1.

In the presence or absence of ICAM-1, pTyr is initially distributed equally over the whole contact area of the B cell with the bilayer, where it colocalises with the antigen (Figure 6.1 A). At later timepoints pTyr staining could be observed in the pSMAC region and colocalising with the antigen cluster (Figure 6.1 A). Interestingly, stronger pTyr area and fluorescence intensity was observed after 20 minutes in the presence of ICAM-1 compared to its absence (Figure 6.1 B, C).

These data suggest that also in B cells active signalling events occur in the pSMAC. Furthermore, as measured by the pTyr fluorescence intensity, the presence of ICAM-1 promoted B cell signalling events. This is in agreement with the data presented in chapter 3 of this Thesis showing that LFA-1/ICAM-1 binding supports antigen engagement. Furthermore, it is tempting to speculate that continuous BCR/antigen engagement occurs in the pSMAC, as it has been described for T cells.

6.2 Vav Localisation at the IS

pTyr staining could be observed surrounding the antigen. This might imply the local recruitment of signalling molecules and their activation at the pSMAC area. As Vav1 and Vav2 regulate B cell spreading and antigen accumulation, and are also required for LFA-1 activation and pSMAC formation (see section 3.2.4 above), their localisation at the IS was investigated.

To do this, the staining efficiency of commercially available antibodies specific for Vav1, Vav2 and Vav3 was tested by FACS analysis on PFA- or methanol-fixed MD4 B cells. However antibodies against Vav1, Vav2 and Vav3 did not give a positive signal (Figure 6.2 A, B).

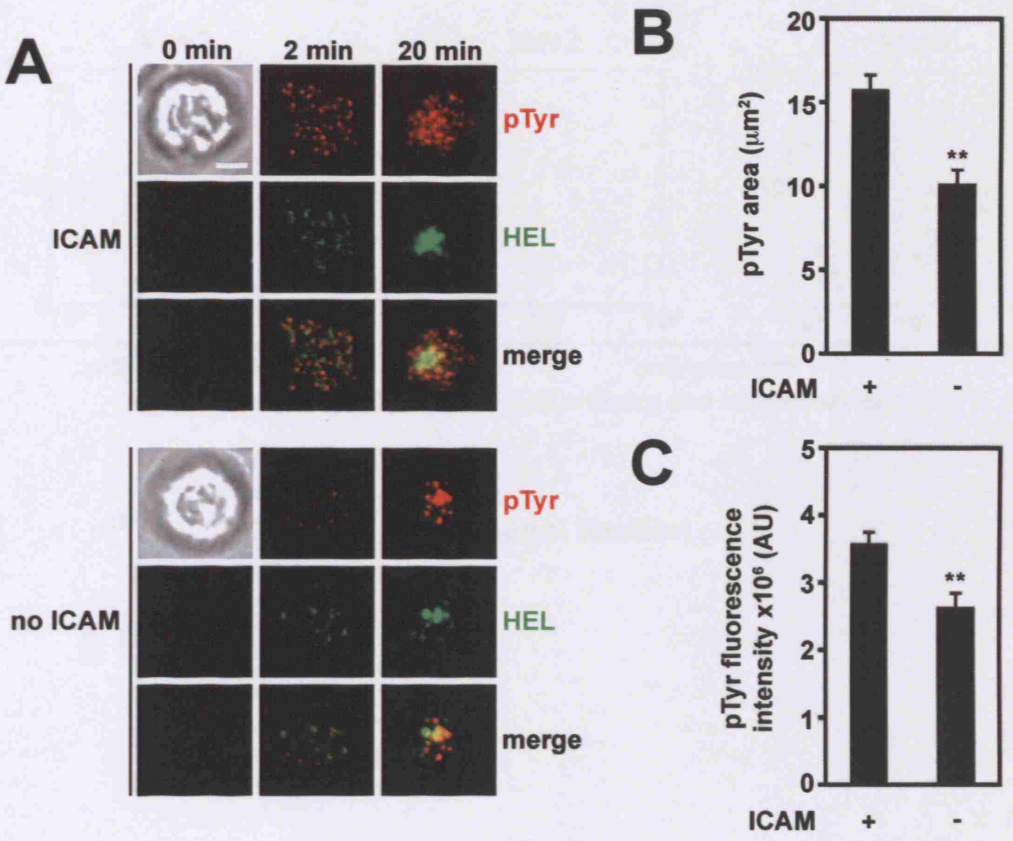

Figure 6.1 B cell signalling events in the pSMAC
(A) MD4 B cells were settled onto lipid bilayers containing a low amount of HEL in the presence and absence of ICAM-1 and fixed with PFA after 2 and 20 minutes of interaction with the bilayers. The phosphotyrosine amount (pTyr) was stained and the cells were analysed by confocal microscopy. **(A)** DIC, fluorescent and merged images of representative B cells at the indicated time points are shown. Scale bar: 2μm. Quantification of **(B)** the area of pTyr and **(C)** the fluorescence intensity of the pTyr amount at 20 min. Values are a mean of 20-30 cells each. t-test: **$p \leq 0.001$. Data are representative of 2 independent experiments.

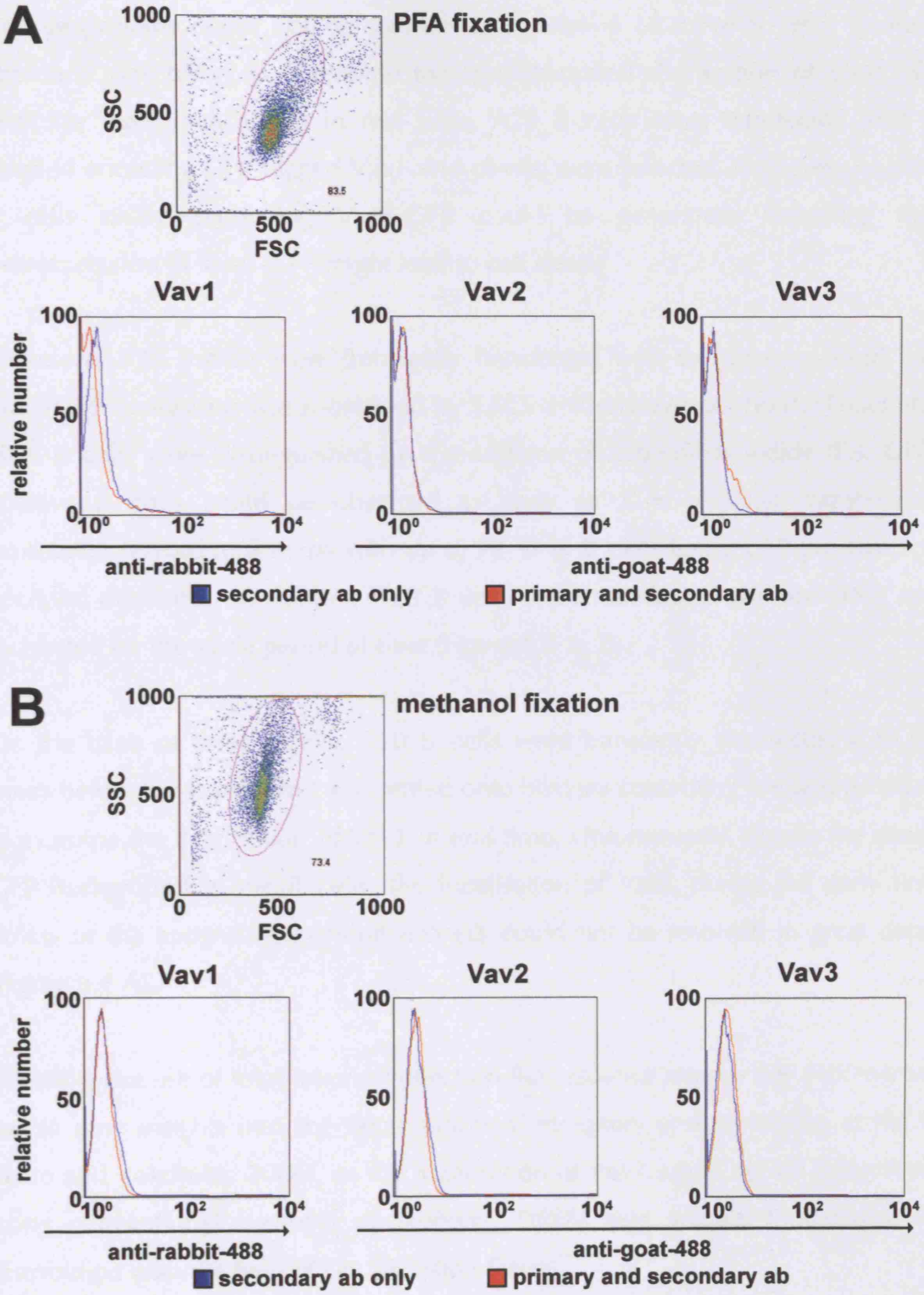

Figure 6.2 FACS staining of Vav1, Vav2 and Vav3
(A) Flow cytometric analysis of the cell population obtained from a MD4 mouse spleen. Cells were fixed with 4% paraformaldehyde, permeabilised and stained with anti-Vav1, anti-Vav2 and anti-Vav3 antibodies (ab) followed by secondary detection (red line). **(B)** MD4 B cells were fixed with methanol and stained with anti-Vav1, anti-Vav2 and anti-Vav3 ab followed by secondary detection (red line). B cells falling into the gates were analysed. As control, a part of the B cells was stained with the secondary ab only (blue line).

As Vav proteins could not be stained upon fixation of naïve B cells, another approach was taken to determine the spatiotemporal distribution of Vav1. To examine Vav1 localisation in real time, A20 B cells were transfected with a plasmid encoding GFP-tagged Vav1 and clones were selected. However, no A20 B cells stably expressing Vav1-GFP could be generated, indicating that overexpression of Vav1-GFP might lead to cell dead.

Therefore, A20 B cells were transiently transfected with the same plasmid and Vav1-GFP expression was monitored by FACS analysis over 24 hours. Dead and alive B cells were distinguished by the addition of propidium iodide (PI). GFP-positive B cells could be observed as early as 2 hours after transfection. Expression peaked at 9 hours with up to 77 % of B cells being GFP-positive and declined thereafter. As control, A20 B cells were transfected without DNA and incubated for the same period of time (Figure 6.3 A, B).

On the basis of these results, A20 B cells were transiently transfected 8 to 10 hours before the experiment and settled onto bilayers containing α-κ and ICAM-1, to examine the distribution of Vav1 in real time. Unfortunately, due to the strong GFP background in the B cells, the localisation of Vav1 during the early time points of the antigen recognition process could not be resolved in great detail (Figure 6.4 A).

Recently, the use of total internal reflection fluorescence microscopy (TIRFM) has led to new insights into the organisation of receptors and molecules at the IS (Saito and Yokosuka, 2006). As the localisation of Vav1 could not be determined using conventional confocal microscopy, TIRFM was applied to examine its distribution with the help of Dr. Sebastian Fleire.
As shown on the two B cells in Figure 6.5 A, Vav1-GFP co-localised with antigen microclusters upon membrane-bound antigen recognition and was additionally found to distribute to the pSMAC, after 30 minutes incubation of B cells with the bilayers. Interestingly, both B cells show a different distribution of the antigen. While the B cell on the left is still spreading and gathering antigen, the cell on the right has fully accumulated the antigen into a cSMAC (Figure 6.5 A, left and right

column, respectively). Considering its crucial role for B cell spreading (see 3.2.4 above) Vav1 over-expression could enhance or even prolong the spreading response, which might explain the different status of antigen accumulation of the two B cells. To support this hypothesis, a larger amount of B cells should be examined in future experiments.

Thus, upon membrane-antigen recognition, Vav1 is recruited to peripheral BCR/antigen microclusters, where it contributes to signalling events and may regulate B cell spreading. Moreover, these results are in agreement with a previous report showing Vav1 localisation with TCR/pMHC microclusters in T cells (Miletic et al., 2006).

6.3 Rac Localisation at the IS

Rac1 and Rac2 have been shown to overtake different functions in neutrophils and this was dependent on their distinct localization (Filippi et al., 2004). In B cells Rac2 contributes to pSMAC formation, while this process is independent of Rac1. One could speculate that this difference in pSMAC formation is due to a different localisation of Rac1 and Rac2 upon antigen recognition, which was examined by expression of Rac1- and Rac2-GFP in A20-1158 B cells, which express a BCR specific for HEL.

To do this, plasmids coding for Rac1-GFP or Rac2-GFP were cotransfected with a second plasmid encoding for HygromycinB resistance into A20-1158 B cells and clones were selected as described in section 2.3.3.3 above.

Several A20-1158 clones positive for Rac1-GFP or Rac2-GFP were generated using this strategy, as determined by FACS analysis (Figure 6.6 A, B, C).

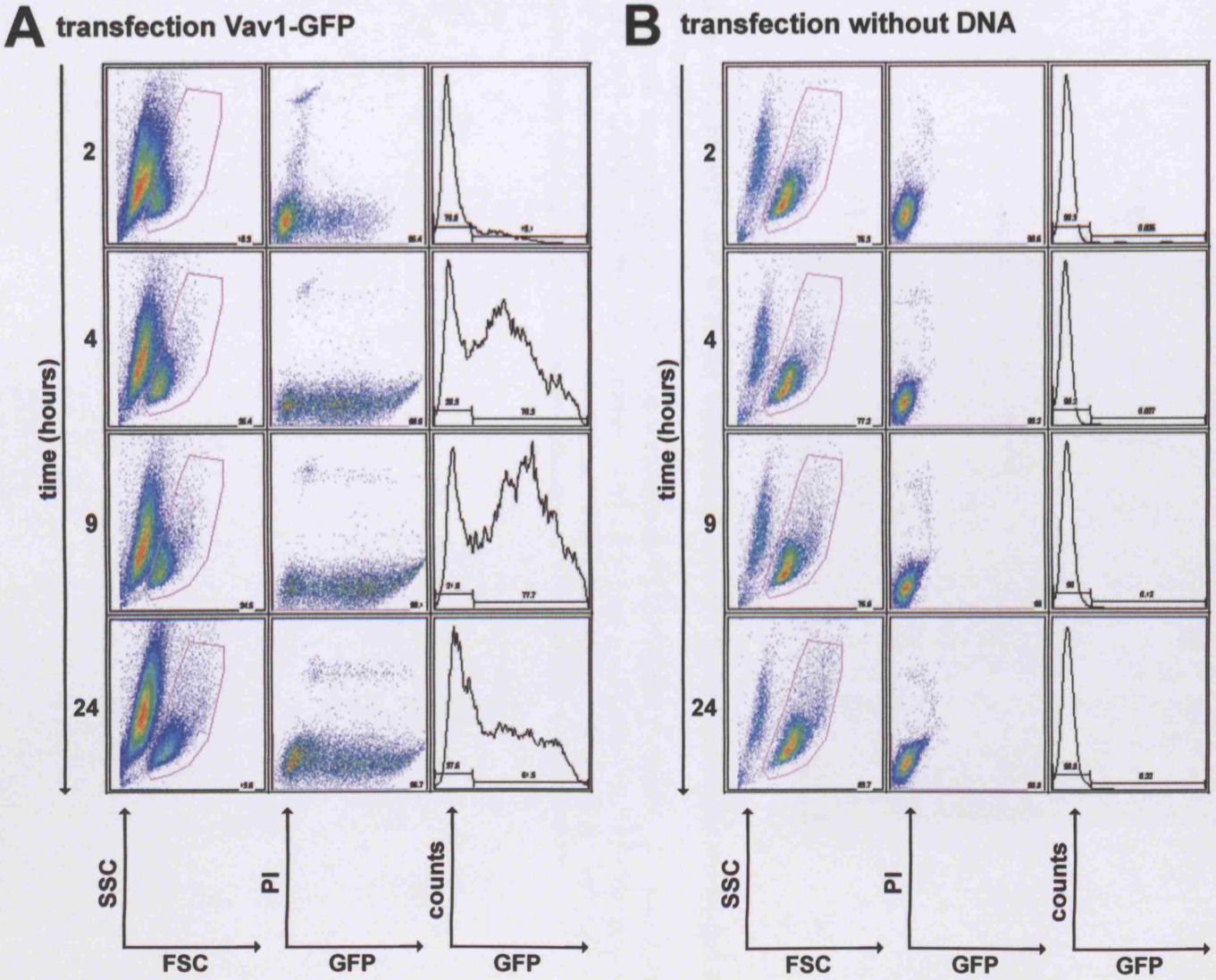

Figure 6.3 FACS analysis of transient transfection time course of A20 B cells with Vav1-GFP

A20 B cells were transfected with **(A)** Vav1-GFP or **(B)** as control without DNA. After transfection A20 B cells were incubated with propidium iodide to distinguish alive and dead cells at the indicated times. B cells falling into the PI-negative gate were analysed for expression of Vav1-GFP. Expression of Vav1-GFP peaked at 9 hours after transfection with 77% of cells beeing GFP-positive.

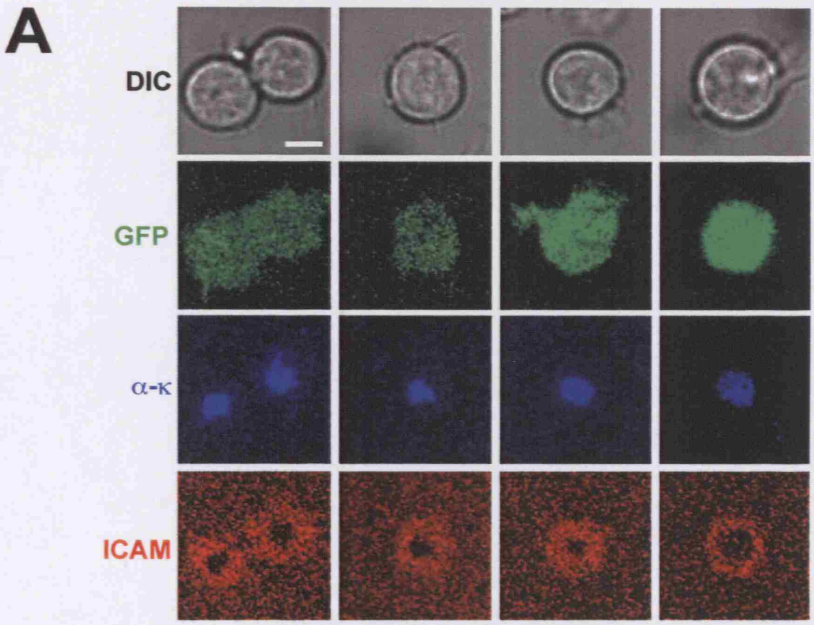

Figure 6.4 Confocal analysis of the distribution of Vav1-GFP upon membrane-bound antigen recognition
A20 B cells expressing Vav1-GFP were settled onto lipid bilayers containing α-κ and ICAM-1 and Vav1-GFP distribution was imaged after 30 minutes using confocal microscopy. **(A)** DIC and fluorescent images of four representative A20 B cells expressing Vav1-GFP are shown. Scale bar: 5μm. Data are representative of 3 independent experiments.

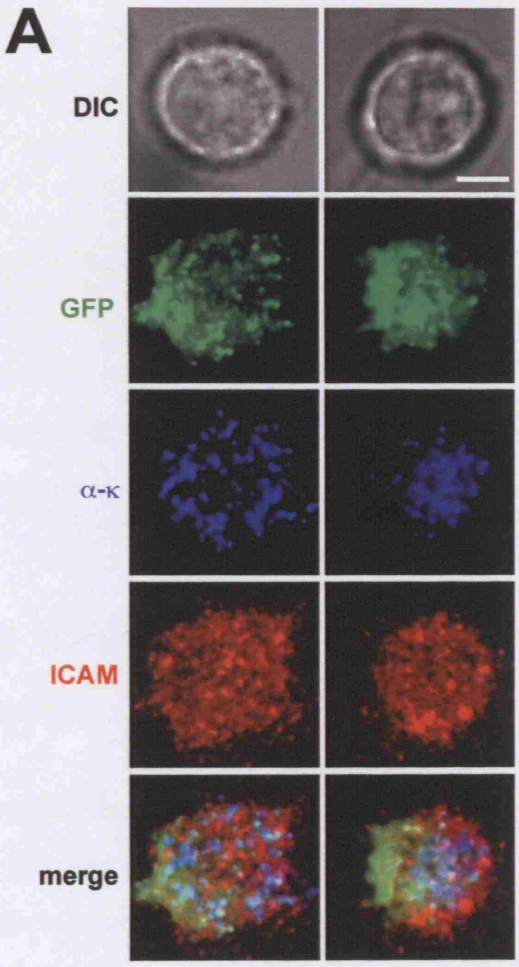

Figure 6.5 TIRFM analysis of the distribution of Vav1-GFP upon IS formation
A20 B cells expressing Vav1-GFP were settled onto lipid bilayers containing α-κ and ICAM-1 and Vav1 distribution was imaged after 30 minutes using TIRFM **(A)** DIC, fluorescent and merged images of two representative A20 B cells expressing Vav1-GFP are shown. Scale bar: 5μm. Data are representative of 2 independent experiments. Images were aquired by Dr. Sebastian Fleire.

Rac1-GFP and Rac2-GFP-expressing B cells were settled onto bilayers containing HEL and ICAM-1 and interactions with the bilayer were followed by confocal microscopy. Although B cells expressing Rac1-GFP and Rac2-GFP aggregated antigen, no pSMAC formation could be observed. Furthermore the contact area with the bilayer was reduced in comparison to B cells transfected without plasmids, making it impossible to determine the distribution of Rac1 and Rac2 at the IS (Figure 6.7 A).

These data suggest that strong overexpression of these small GTPases may interfere with BCR signalling cascades triggering LFA-1 activation or cytoskeletal rearrangements in the A20-1158 B cells. Thus, another strategy, such as retroviral transfection of naïve B cells combined with TIRFM might help to address these outstanding questions.

6.4 Rac2V12 Induced Adhesion in the Signalling Deficient B Cell Line H2

The approaches described in the previous section did not offer information about the spatial organisation of Rac1 or Rac2 at the IS. However, it was interesting to determine whether pSMAC formation requires coordinated localised signalling events triggered by antigen recognition through the BCR.

To address this question, a plasmid coding for constitutively activated Rac2 (Rac2V12)-GFP was cotransfected with a plasmid encoding HygromycinB resistance into the H2 B cell line and clones were selected. H2 B cells express a HEL-specifc BCR, which cannot trigger intracellular signalling upon antigen recognition (see section 2.3.3.1 above).

The transfection yielded the GFP-positive clones H2-V12$^{1\text{-}15}$ and H2-V12$^{2\text{-}6}$ as judged by FACS analysis. As control for further experiments, a HygromycinB-resistant H2 clone was also generated (H2-Hygro$^{1\text{-}4}$) (Figure 6.8 A, B, C).

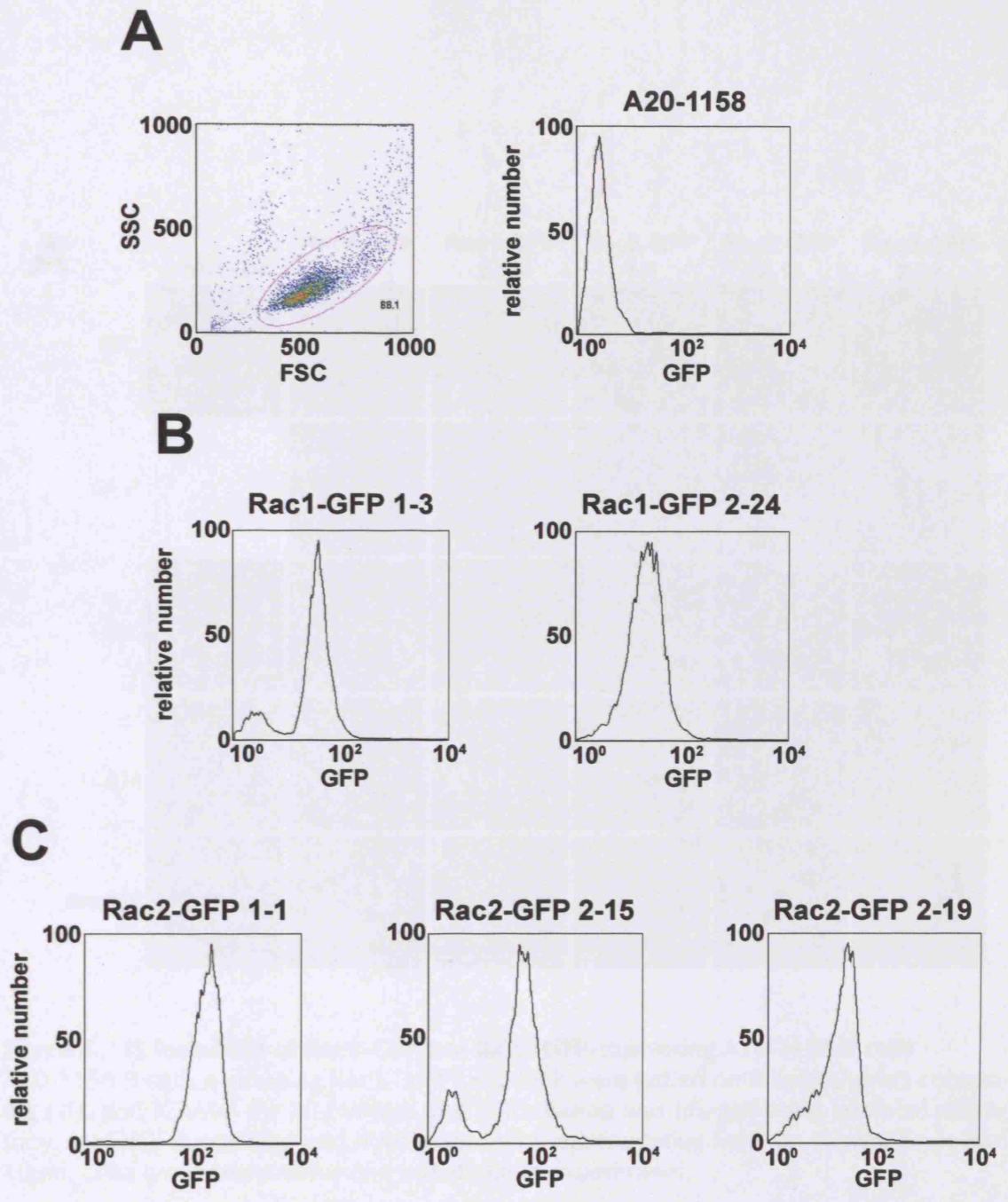

Figure 6.6 FACS analysis of A20-1158 B cell clones stably expressing Rac1-GFP and Rac2-GFP

(A) Flow cytometric analysis of a not transfected A20-1158 B cell population. B cells falling into the gate were analysed for GFP-expression. **(B)** GFP expression profile of two A20-1158 clones stably expressing Rac1-GFP. **(C)** GFP expression profile of three A20-1158 clones stably expressing Rac2-GFP.

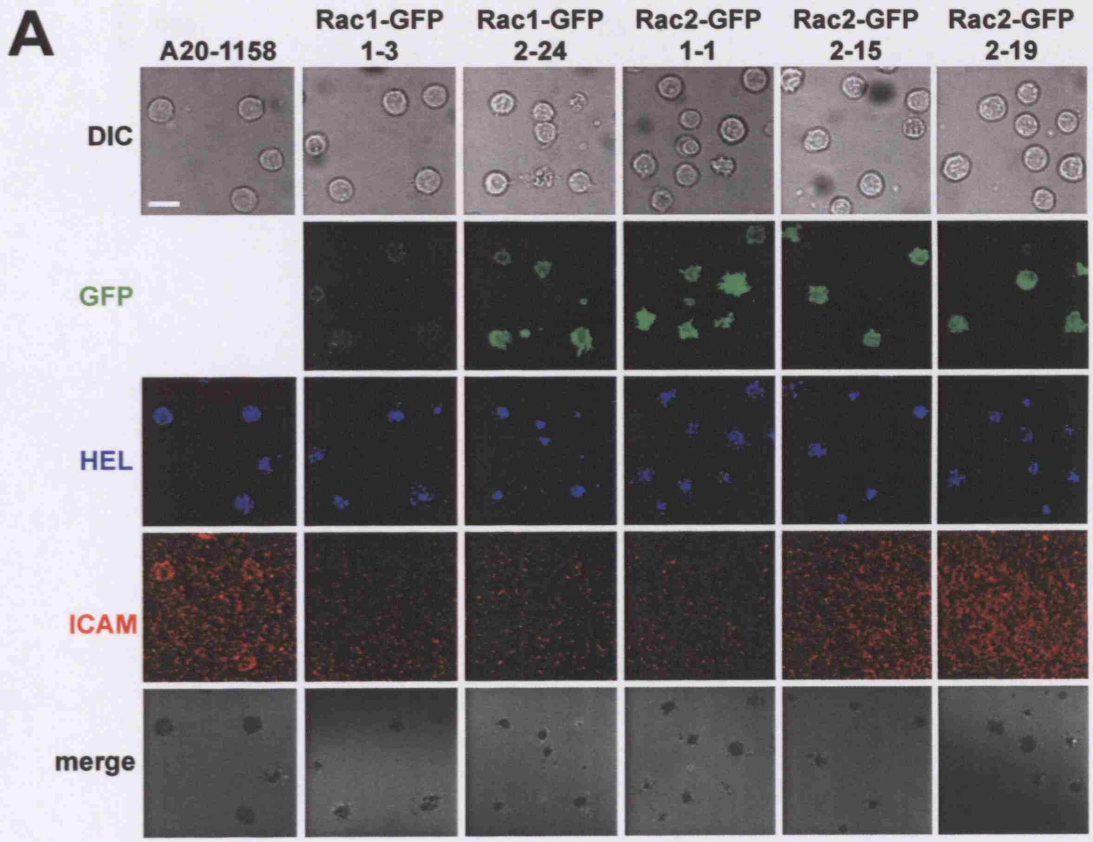

Figure 6.7 IS formation of Rac1-GFP and Rac2-GFP-expressing A20-1158 B cells
A20-1158 B cells expressing Rac1- and Rac2-GFP were settled onto lipid bilayers containing HEL and ICAM-1 for 20 minutes and IS formation was imaged using confocal microscoy. **(A)** DIC, fluorescent and IRM images of a representative field are shown. Scale bar: 10μm. Data are representative of 4 independent experiments.

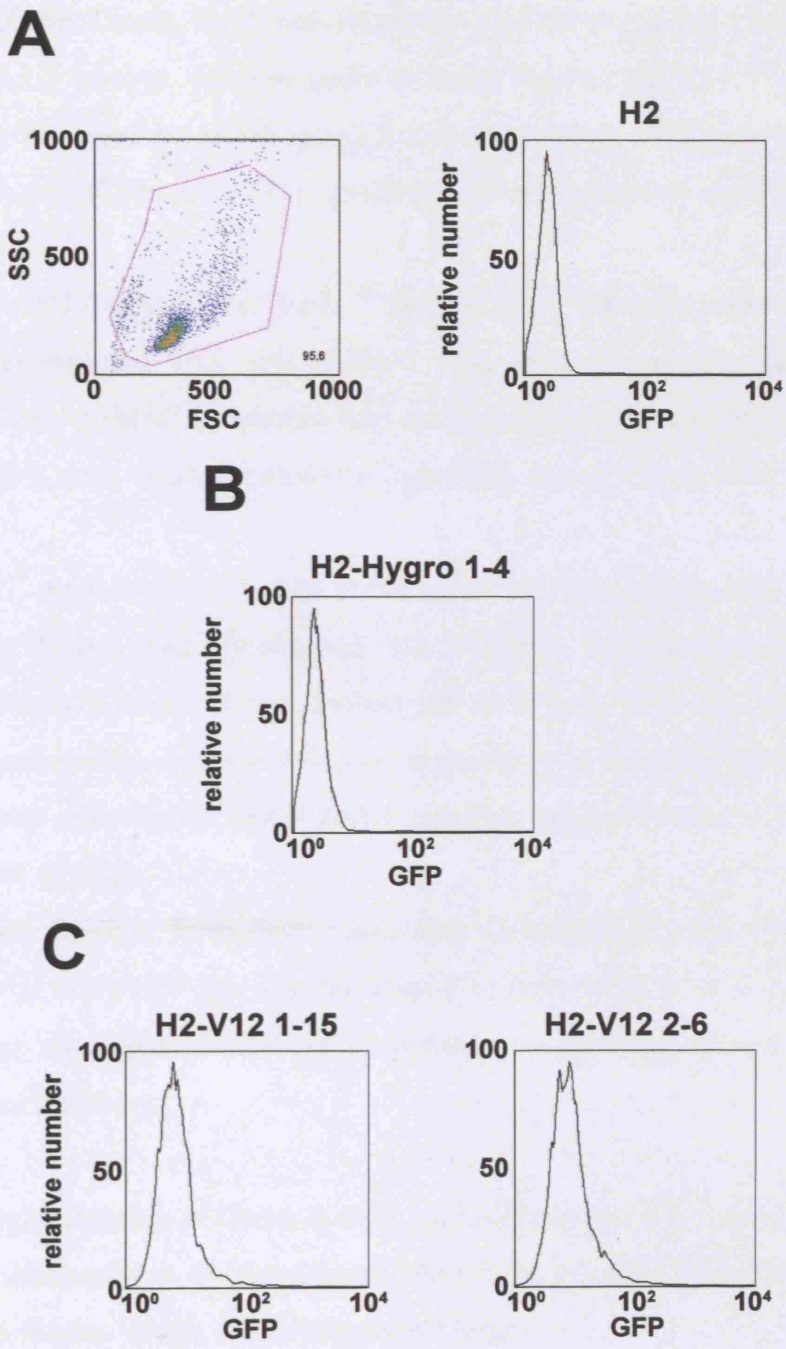

Figure 6.8 FACS analysis of H2 B cell clones stably expressing GFP-Rac2V12
(A) Flow cytometric analysis of a not transfected H2 B cell population. B cells falling into the gate were analysed for GFP-expression. **(B)** GFP expression profile of a HygromycinB resistant H2 B cell clone. **(C)** GFP expression profile of two H2 B cell clones stably expressing Rac2V12.

As shown recently, H2 B cells are able to passively accumulate a small amount of HEL without eliciting an intracellular signal (Fleire et al., 2006). In a previous chapter of this Thesis, Rac2 was shown crucial for triggering LFA-1 activation (see section 3.2.5 above). On the basis of these results, H2-V12$^{1-15}$ and H2-V12$^{2-6}$ B cells can be used to investigate, if overexpression of Rac2V12 triggers LFA-1 activation and ICAM-1 binding, leading to B cell adhesion and pSMAC formation.

To do this H2-Hygro$^{1-4}$, H2-V12$^{1-15}$ and H2-V12$^{2-6}$ B cells were settled onto lipid bilayers containing HEL and ICAM-1 and after 20 minutes incubation B cell adhesion and pSMAC formation was compared to not transfected H2 B cells, and A20-1158 B cells as an example for signalling competent B cells.

H2-V12$^{1-15}$ and H2-V12$^{2-6}$ cells showed an increased IRM area as compared to H2-Hygro$^{1-4}$ and not transfected H2 B cells, which was accompanied by aggregation of ICAM-1 at the contact site in 40% to 50% of the cells. (Figure 6.9 A, B). These results indicate that over-expression of Rac2V12 indeed induces LFA-1 activation and subsequent ICAM-1 binding independently of B cell stimulation by specific antigen.
In contrast, pSMAC formation could only be observed in a small percentage of H2-V12$^{1-15}$, H2-V12$^{2-6}$ B cells compared to A20-1158 B cells (Figure 6.9 A, B), suggesting the requirement of coordinated signalling events triggered upon antigen recognition.

Interestingly, fixation of those B cells and subsequent staining of F-actin revealed large lamellopodia in the presence of Rac2V12, as it has been described for other cell types (Ridley et al., 1992) (Figure 6.10 A).

In conclusion, these results indicate that over-expression of Rac2V12 induces LFA-1 activation and subsequent ICAM independent of any other signal triggered upon antigen recognition by the BCR. This in turn might be attributable to the activation of downstream effectors by the constitutively active Rac2 leading to changes in LFA-1 affinity and cytoskeletal rearrangements.

On the one hand these results are in agreement with previous data showing that Rac2 is crucial for LFA-1 activation (see section 3.2.5 above). However, on the other hand, these results indicate that pSMAC formation requires coordinated local signalling events induced by the BCR upon antigen recognition.

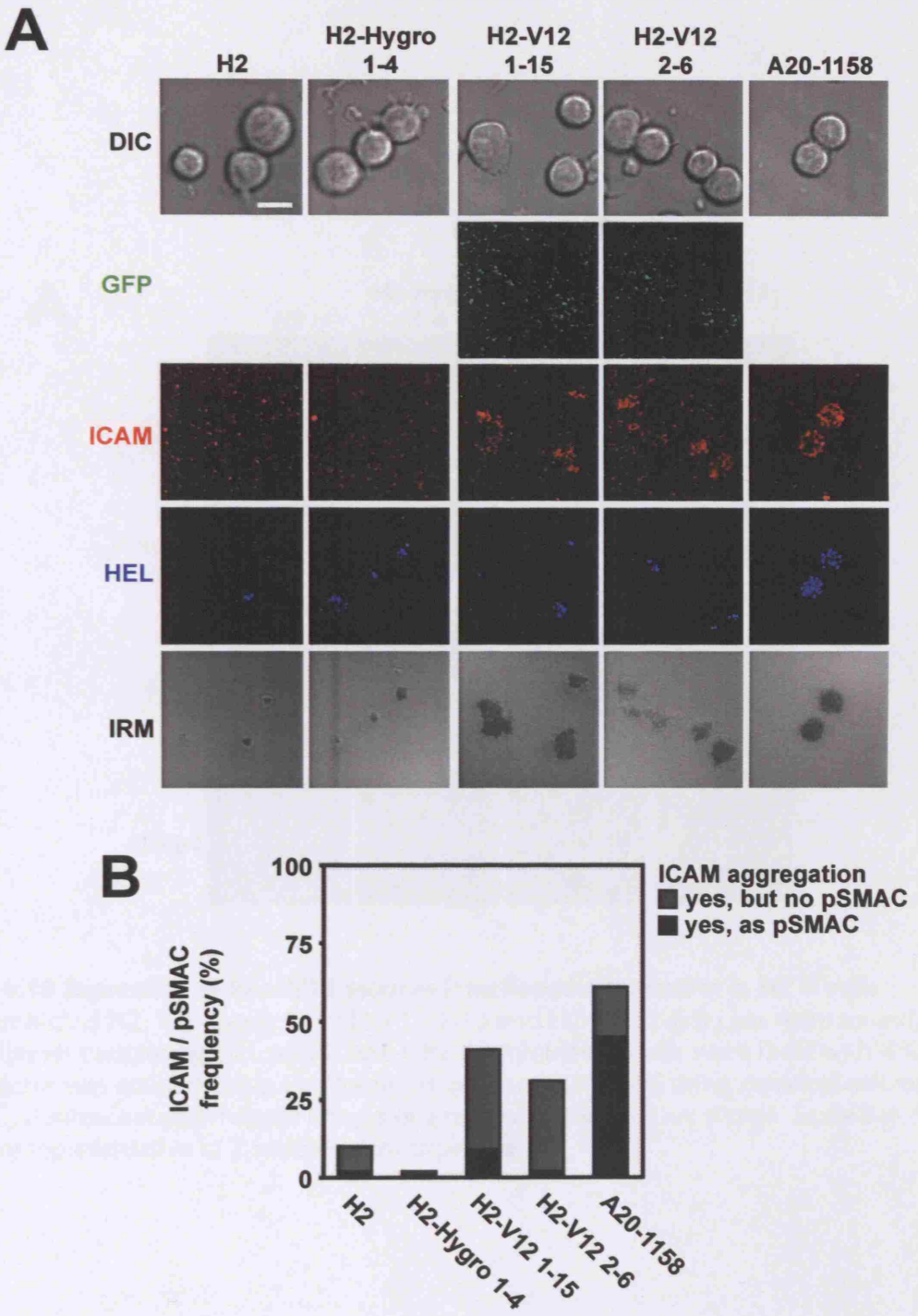

Figure 6.9 Expression of Rac2V12 induces H2 B cell adhesion to ICAM-1
Not transfected H2, H2-Hygro 1-4, H2-V12 1-15 and H2-V12 2-6 B cells were settled onto lipid bilayers containing HEL and ICAM-1 for 20 minutes and IS formation was imaged using confocal microscoy. As a reference of IS formation, A20-1158 B cells were also incubated on these bilayers. **(A)** DIC, fluorescent and IRM images of a representative field are shown. Scale bar: 10μm. **(B)** The percentage of B cells accumulating ICAM or forming a pSMAC is shown. Quantification was done on 20-40 B cells. Data are representative of 3 independent experiments.

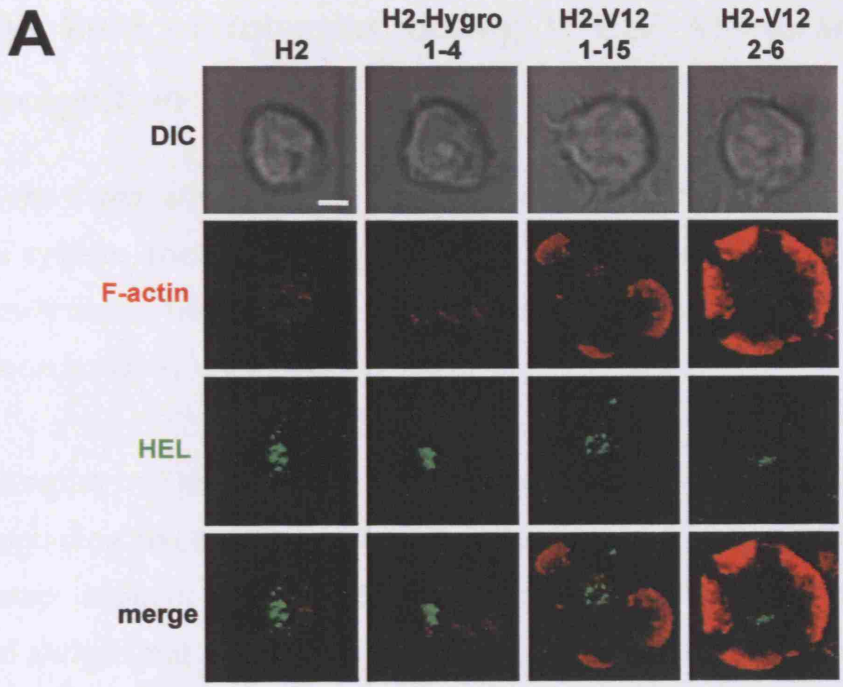

Figure 6.10 Expression of Rac2V12 induces lamellopodia formation in H2 B cells
Not transfected H2, H2-Hygro 1-4, H2-V12 1-15 and H2-V12 2-6 B cells were settled onto lipid bilayers containing HEL and ICAM-1 for 20 minutes. B cells were fixed with 4% PFA and F-actin was stained using Phalloidin. B cells were imaged using confocal microscoy. **(A)** DIC, fluorescent and merged images of a representative cell are shown. Scale bar: 5µm. Data are representative of 2 independent experiments.

7 Discussion

This final chapter summarises the main findings and discusses the major issues arising from the work presented in this Thesis.

7.1 The Role of Integrins during B Cell Membrane Antigen Recognition

Integrin-mediated adhesive cell-to-cell interactions play a central role in the immune system. They regulate lymphocyte development, migration and cell-to-cell interactions, however the role of integrins during membrane antigen recognition is poorly understood.

A recent report by Fleire et al. shows that membrane antigen recognition triggers a B cell spreading and contraction response that enables B cells to efficiently collect and extract antigen. The magnitude of spreading determined the amount of gathered antigen and thereby the extent of B cell activation (Fleire et al., 2006).
In this line two reports by Carrasco et al. show that engagement of the integrins LFA-1 and VLA-4 and the formation of the pSMAC at the IS are required for efficient B cell activation in situation of limited antigen availability. Both reports argue that LFA-1- and VLA-4-mediated adhesion increase the chances of antigen engagement by the BCR and therefore B cell activation (Carrasco et al., 2004), (Carrasco and Batista, 2006). Taken together, these evidences indicate that integrins may contribute to B cell spreading and so facilitate antigen aggregation. However, the molecular mechanism underlying these observations has not been shown.

The results presented in section 3.1 and 5.1 show for the first time that, during the early stage of membrane antigen recognition, binding of the integrins LFA-1 and VLA-4 to their ligands ICAM-1 and VCAM-1 results in tight adhesion of the B cells, which supports spreading when the amount of antigen is low. The increase in B cell spreading results in a higher amount of antigen accumulation, which

could account for the more efficient B cell activation observed by Carrasco et al. (Carrasco et al., 2004), (Carrasco and Batista, 2006).

These observations are of particular interest for the immune response, when B cell fate is decided by means of cell-to-cell interactions in the germinal centres of secondary lymphoid organs. In these anatomical locations, the BCR can undergo somatic hypermutation and class-switch recombination resulting in the production of high affinity BCRs. B cells bearing BCRs with high affinity are positively selected to become memory or plasma B cells as they can efficiently compete for antigen-specific survival signals and T cell help (Tarlinton, 1998). Germinal centre B cells are found in close association with FDCs (MacLennan, 1994), (Camacho et al., 1998), which are known to retain small amounts of intact antigen in form of immune complexes tethered to their cell surface by Fc or complement receptors (Haberman and Shlomchik, 2003), (Kosco-Vilbois, 2003). B cells most likely recognize these immune complexes on FDCs, which have been shown to support B cell activation and differentiation into memory and plasma B cells (Szakal et al., 1988), (Wu et al., 1996), and to promote B cell survival (Koopman et al., 1994).

In this line, Fleire et al. reported that the density of the antigen on the target membrane and the affinity of the BCR for the antigen are critical parameters determining the extent of B cell spreading and antigen aggregation (Fleire et al., 2006). A high density of antigen or a high affinity antigen/BCR interaction triggered B cell spreading, which allows uptake of large amounts of antigen, therefore increases the chances of efficient interaction with helper T cells. B cell interaction with FDCs is mediated by LFA-1 and VLA-4 (Freedman et al., 1990), (Koopman et al., 1991), (Kushnir et al., 1998). As LFA-1 and VLA-4 facilitate B cell spreading when the amount of antigen is low, it is possible that these two integrins contribute actively to membrane antigen recognition, B cell activation and B cell selection during the germinal centre reaction *in vivo*.

7.2 The Regulation of Integrin Activation upon Antigen Recognition

To date, the signalling mechanism regulating integrin activation in B cells are poorly understood. Several signalling molecules have been shown to mediate LFA-1 activation downstream of the BCR, such as the cytosolic adaptor SKAP-HOM (Togni et al., 2005) and the Rap GTPases (McLeod et al., 2004), (Duchniewicz et al., 2006). Futhermore, an elegant report by Spaargaren et al. shows that the BCR triggers inside-out activation of the integrin VLA-4 through the tyrosine kinases Lyn and Syk, PI3K, PLCγ2, IP_3 receptor-mediated Ca^{2+}-release and PKC (Spaargaren et al., 2003).

In concordance with this report, the results presented in section 3.2.1 of this Thesis demonstrate that, downstream of the BCR, SFKs mediate inside-out activation of LFA-1 and VLA-4 resulting in B cell adhesion to ICAM-1 and VCAM-1, respectively. In contrast to Spaagaren et al., loss of the SFK Lyn did not affect B cell adhesion to ICAM-1, indicating a signalling mechanism independent of this kinase leading to LFA-1 activation. This could be explained by the fact that several SFKs are expressed in murine B cells, which could compensate for the loss of Lyn (Law et al., 1992). However, taken together these results strongly indicate that integrin activation relies on SFKs.

The presented data show that loss of SKAP-HOM did not affect B cell adhesion to ICAM-1 (see section 3.2.3). Togni et al. however, show a significant reduction of B cell adhesion to ICAM-1 (Togni et al., 2005). These differences could partly be due to the different experimental conditions used: While for the here presented experiments B cells were settled onto lipid bilayers containing ICAM-1, Togni et al. assessed B cell adhesion on plastic dishes bearing immobilized ICAM-1. Whether this is indeed the reason for the contradictory results should be clarified.

LFA-1 activation requires Vav1 and Vav2, as B cell adhesion capacity to ICAM-1 was significantly reduced in Vav1$^{-/-}$ or Vav2$^{-/-}$ B cells (see section 3.2.4). This is in agreement with previous reports showing the requirement of Vav1 for LFA-1-mediated conjugate formation of T cells with APCs (Ardouin et al., 2003), (Krawczyk et al., 2000). Loss of either Vav1 or Vav2 did not result in any significant changes in adhesion to VCAM-1, indicating a redundant role for both proteins for VLA-4 activation. Indeed, Vav1/2$^{-/-}$ B cells adhered less efficiently to VCAM-1 and showed an even further reduced adhesion frequency to ICAM-1. Although Vav3$^{-/-}$ B cells did not show any defects in adhesion to either ICAM-1 or VCAM-1, its role for integrin activation cannot be excluded. Indeed, a small percentage of Vav1/2$^{-/-}$ B cells were still able to adhere to ICAM-1 and VCAM-1 and this might be due to the presence of Vav3. Analysis of the adhesion capacity of Vav1/2/3$^{-/-}$ B cells would clarify this issue. But this is rather complicated, as deletion of all three Vav proteins results in a loss of mature B cells due to a block of B cell development at the transitional B cell stage (Fujikawa et al., 2003). In conclusion, our results define a crucial role of the family of Vav proteins for B cell adhesion and extend the current knowledge of integrin regulation in B cells.

Although there is evidence that implicates Rac proteins in the regulation of VLA-4 in T cells (D'Souza-Schorey et al., 1998), their exact role for integrin activation in B cells is unclear. The results presented in section 3.2.5 now suggest that a BCR-mediated signalling pathway involving SFKs, Vav1, Vav2 and PI3K regulates LFA-1 activation through Rac2, while it seems independent of Rac1. Interestingly, VLA-4 activation is not affected by the loss of either Rac1 or Rac2 (see section 5.2.3). Although redundancy between Rac1 and Rac2 cannot be excluded, these results clearly implicate Rac proteins in integrin activation downstream of the BCR.

PI3K has been suggested to enhance Vav GEF activity, probably by its recruitment to the plasma membrane (Palmby et al., 2002). In this line, phospholipid products of PI3K have been implicated in supporting Rac activation (Reif et al., 1996), (Han et al., 1998). The fact that Rac1 and Rac2 activation is diminished upon inhibition of PI3K supports these ideas (see section 4.1.2). B cell adhesion to ICAM-1 and

VCAM-1 was strongly dependent on PI3K activity and, therefore, suggests PI3K as a key player in mediating integrin activation in B cells. This is in agreement with a previous report showing defective adhesion of B cells to VCAM-1 upon treatment with Wortmannin or LY294002 (Spaargaren et al., 2003).
LFA-1- and VLA-4-mediated T cell adhesion is independent of the p110δ catalytic subunit of PI3K (Okkenhaug et al., 2002). Interstingly, B cell adhesion to ICAM-1 is significantly reduced in the absence of p110δ. A small percentage of $p110\delta^{-/-}$ B cells were still able to adhere to ICAM-1, while adhesion to VCAM-1 was not affected. On the basis of these results, one can conclude that, in contrast to T cells, LFA-1 activation in B cells requires p110δ. The residual LFA-1 activation in $p110\delta^{-/-}$ B cells and their capacity to activate VLA-4 might be due to the presence of the p110α subunit that is activated upon BCR crosslinking (Vigorito et al., 2004).

One of the latest events triggered upon crosslinking of the TCR is the association of RAPL with LFA-1, which is mediated by the GTPase Rap1 and required for LFA-1 activation (Katagiri et al., 2003).
As shown by biochemical analysis (see section 4.2.2), Rap1 activation in B cells requires SFKs, Vav1 and Vav2 and Rac2 and was delayed in the absence of PI3K activity. Thus, PI3K may facilitate Rap1 activation by enhancing Vav GEF activity or Rac activation (Palmby et al., 2002), (Reif et al., 1996), (Han et al., 1998).

In conclusion, these data show that SFKs, Vav1, Vav2, Rac2 and PI3K regulate integrin activation and subsequent B cell adhesion to ICAM-1 and VCAM-1. Furthermore, these results suggest that this signalling mechanism mediates integrin activation via the small GTPase Rap1 and presumably its effector molecule RAPL.
Moreover, by regulating the activation of LFA-1 and VLA-4 during the early stages of membrane-bound antigen recognition, this signalling pathway supports B cell spreading and antigen aggregation. This signalling cascade is critical when the amount of available antigen is low, as integrin activation facilitates B cell triggering.

7.3 The Regulation of B Cell Spreading and Antigen Aggregation

Spreading was first described in T cells while interacting with glass-coverslips coated with anti-TCR antibodies (Parsey and Lewis, 1993), (Bunnell et al., 2001) and on APCs bearing specific antigen on their cell surface (Negulescu et al., 1996). This spreading response depends on TCR-generated intracellular signalling cascades involving the adaptor protein LAT, calcium flux and cytoskeletal rearrangements (Negulescu et al., 1996), (Bunnell et al., 2001), (Nolz et al., 2006).

The report by Fleire et al. now shows that this response is a common mechanism of lymphocytes, as also B cells spread upon antigen recognition (Fleire et al., 2006). In their study the authors show that B cell spreading is clearly dependent on activation of SFKs and polymerization of F-actin. However, nothing is known about the actual signalling molecules involved in the regulation of B cell spreading (Fleire et al., 2006).

Downstream of lymphocyte antigen receptors, Vav proteins are rapidely activated by SFKs (Deckert et al., 1996), (Schuebel et al., 1998), (Movilla and Bustelo, 1999). The results presented in section 3.2.4 clearly identify Vav1 as master regulator of B cell spreading. Already at high amounts of antigen, $Vav1^{-/-}$ B cells show an almost complete loss of their ability to spread. Also Vav2 seems to regulate this process, as $Vav2^{-/-}$ B cells show a reduction in the spreading area at low antigen availability. Interestingly, a recent report shows that a Vav1-Rac1-mediated dephosphorylation of ERM proteins resulted in T cell relaxation and promoted their conjugate formation with APCs (Faure et al., 2004). One could speculate that, by a similar mechanism, Vav1 actively regulates B cell spreading and IS formation. However, this needs to be investigated in depth in the future.

As the amount of accumulated antigen is determined by the magnitude of B cell spreading (Fleire et al., 2006), one would expect that Vav deficient B cells show defects in antigen accumulation. This hypothesis is confirmed in section 3.2.4, where the amount of antigen accumulated by Vav deficient B cells is smaller compared to WT B cells at low antigen availability. Additionally the kinetic of antigen aggregation is much slower. This has implications for humoral immune responses, as efficient antigen recognition is required for proper B cell activation and fulfilment of effector functions.

The critical contribution of Vav proteins to BCR signalling *in vivo* has been shown in $Vav2^{-/-}$ and $Vav1/2^{-/-}$ B cells, which have defects in response against type II thymus-independent antigens (TI-2) (Doody et al., 2001), (Tedford et al., 2001). A defect in germinal centre formation and isotype switching has been reported in mice lacking Vav1 or Vav2 as well (Doody et al., 2001), (Bachmann et al., 1999). Finally, a recent report shows that Vav proteins are responsible for the regulation of plasma B cell development and the production of antibodies (Stephenson et al., 2006).

Interestingly, although spreading was completely abolished in $Vav1/2^{-/-}$ B cells, antigen aggregation still occurred at high amounts of antigen availability and was comparable to WT B cells. This is in contrast to H2 B cell line expressing a BCR variant in which the tyrosine residues of the ITAM motifs have been mutated. At high antigen density, these H2 B cells do not spread and show much less antigen aggregation compared to signalling competent B cells (Fleire et al., 2006). This difference could be explained in the following way: As Vav-deficient B cells express a signalling competent BCR, antigen recognition can still trigger early BCR signalling events or Vav-independent signalling cascades. This is also supported by results showing that phosphotyrosine staining in Vav deficient B cells is comparable to WT B cells upon antigen recognition (see section 6.1). Interestingly, in a recent report Hao and August describe that BCR crosslinking induces rapid actin depolymerisation, which could be mimicked by incubation of DT40 B cells with the actin depolymerising agent Latrunculin B (LatB). LatB treatment promoted BCR translocation into lipid rafts and passive lipid raft clustering (Hao and August, 2005). It is tempting to speculate that also in Vav

deficient B cells antigen recognition induces early actin depolymerisation, BCR translocation into lipid rafts and their passive clustering. This mechanism could account for the antigen accumulation observed in Vav deficient B cells, however this hypothesis needs further investigation.

Rac proteins are initiators of actin polymerisation through activation of the Arp2/3 complex via Wave proteins triggered downstream of Vav (Movilla and Bustelo, 1999), (Crespo et al., 1997), (Abe et al., 2000). Interestingly, suppression of Wave2 in Jurkat T cells inhibited their spreading on anti-CD3 coated coverslips (Nolz et al., 2006). Therefore, considering the crucial role of Vav to B cell spreading, Rac proteins were expected to regulate this process upon antigen recognition.

Intriguingly, the results shown in section 3.2.5 do not support this hypothesis, as $Rac1^{-/-}$ and $Rac2^{-/-}$ B cells spread comparably to WT B cells at high or low amounts of antigen. One possible explanation could be that $Rac1^{-/-}$ and $Rac2^{-/-}$ B cells can overcome defects in spreading due to the strong stimulus given by the α-κ antibody that was tethered to the bilayer.
On the other hand, Rac1 and Rac2 could have compensatory functions and only deletion of both GTPases would reveal their role for the spreading response. Mice with deletion of Rac1 and Rac2 have been reported (Walmsley et al., 2003). However, mature B cells are missing in these mice because of a block of B cell development at the transitional B cell stage. This makes it difficult to examine the role of both GTPases. The generation of mice, in which deletion of Rac1 and Rac2 could be induced in the mature B cell compartment, would be one possibility to further investigate this issue.

Furthermore, as Vav proteins also exert their GEF function on the small GTPases Cdc42 and Rho (Abe et al., 2000), (Han et al., 1997), (Schuebel et al., 1998), a role for these molecules for B cell spreading cannot be excluded. Cdc42 triggers actin polymerization via the WASP-Arp2/3 pathway, while Rho contributes by activation of formins (Jaffe and Hall, 2005). In this line, a recent report by Borroto et al. suggests that Rho is the key regulator of T cell spreading. In this study,

expression of a dominant negative RhoA mutant abolished spreading on anti-CD3-coated glass slides, while dominant negative or constitutively active mutants of Cdc42 and Rac did not affect T cell spreading (Borroto et al., 2000). Although this indicates that Rho regulates T cell spreading, it is not clear whether the same pathway also applies to B cells. Which of the small Rho GTPases actually mediate B cell spreading remains a key issue in the understanding of the regulation of membrane antigen recognition.

Through its ability to recruit Vav to the plasma membrane, the PI3K product PIP_3 has been suggested to contribute to Vav activity (Palmby et al., 2002). Furthermore, *in vitro* studies implicate phospholipid products of PI3K in the regulation of Rac activation (Reif et al., 1996), (Han et al., 1998).
The results presented in section 3.2.6 show that inhibition of PI3K using Wortmannin did not affect B cell spreading, even when the amount of antigen is low. These results are in agreement with another report showing no effect of WM or LY294002 on T cell spreading (Borroto et al., 2000). Therefore a major role of PI3K for B cell spreading can be excluded.

7.4 The Regulation of pSMAC Formation in B Cells

The signalling mechanisms by which membrane antigen recognition controls the formation of a pSMAC at the IS are largely unknown. The work presented in this Thesis is the first evidence proposing how pSMAC formation is regulated in B cells. As discussed above, a signalling mechanism involving SFKs, Vav1, Vav2, PI3K and Rac2 regulates integrin activation in B cells. This is a prerequisite for pSMAC formation, as defects in B cell adhesion concomitantly resulted in a loss of the pSMAC at the IS.

As shown in section 3.3.1.1, induction of the high affinity conformation of LFA-1 by Mn^{2+} results in B cell adhesion to ICAM-1. This is in agreement with studies showing that Mn^{2+} induces the LFA-1 high affinity conformation in T cells, which results in ICAM-1 binding (Dransfield et al., 1992).

Mn^{2+}-induced B cell adhesion to ICAM-1 is independent of the BCR-mediated inside-out regulation of LFA-1 and restored adhesion defects observed upon treatment with PP1 and WM and in $Vav1^{-/-}$ and $Vav2^{-/-}$ B cells. Mn^{2+} addition did not restore adhesion of $Rac2^{-/-}$ B cells to ICAM-1. Interestingly, a recent report shows that also treatment of Rap1-deficient T cells with Mn^{2+} did not lead to adhesion (de Bruyn et al., 2002), thus emphasising the relationship between Rac2 and Rap1 shown by biochemical analysis in the present study.
It may well be that Rac2 and Rap1 are activated form the outside-in, downstream of LFA-1 engagement, and that this is required for ligand binding. Indeed, Rac1 is activated upon Mn^{2+} treatment of T cells (Sanchez-Martin et al., 2004). However this does not seem to be the case for Rap1 (de Bruyn et al., 2002). Thus, the mechanism underlying these observations is not clear and should be further addressed.

Although the high affinity conformation of LFA-1 was efficient in mediating adhesion to ICAM-1, it was not sufficient to restore pSMAC formation in B cells treated with WM or $Vav1^{-/-}$, $Vav2^{-/-}$, $Vav1/2^{-/-}$ and $Rac2^{-/-}$ B cells. These data indicate that pSMAC formation may additionally require LFA-1 avidity changes and B cell polarisation, processes that are mediated by cytoskeletal rearrangements. In agreement with this hypothesis, B cells treated with PP1, WM or $Vav1^{-/-}$, $Vav2^{-/-}$, $Vav1/2^{-/-}$ and $Rac2^{-/-}$ B cells exhibited a defect in F-actin polarisation upon membane antigen recognition. However these experiments do not address directly whether cytoskeletal rearrangements regulate pSMAC formation. This needs to be addressed in the future, for example, by using biochemical inhibitors of cytoskeletal dynamics.

A previous report suggests that the adaptor ADAP is critical for LFA-1 segregation into the periphery of the T cell IS, while it was not required for LFA-1 activation (Wang et al., 2004). This is interesting, as it raises the question to whether specific localisation of proteins at the IS determines the segregation of integrins into the pSMAC. Indeed, Rac1 and Rac2 have been shown to localise differently in neutrophils and this results in different functions (Filippi et al., 2004).

The experiments described in chapter 6 represent different strategies to address the localisation of Vav and Rac proteins in the B cell IS. However, due to the low quality of antibodies, immunfluorescence staining did not provide any conclusive results regarding the localisation of Vav or Rac proteins.
A different approach to determine Vav1 localisation was the transient transfection of A20 B cells with Vav1-GFP. However, due to the strong GFP fluorescence of transfected A20 B cells, the exact localisation of Vav1 at the IS could not be addressed in great detail by confocal microscopy.
Nevertheless, the application of TIRFM showed that Vav1 colocalises with antigen clusters, reminiscent of its crucial role for the transduction of BCR signals. This finding is in agreement with a recent report showing colocalisation of Vav1 with TCR/pMHC microclusters in T cells (Miletic et al., 2006).

To examine the localisation of Rac1 and Rac2 upon membrane antigen recognition, A20-1158 B cells stably expressing Rac1-GFP and Rac2-GFP were generated. Unfortunately, it was impossible to determine the exact localisation of Rac1 and Rac2, probably due to the strong overexpression of these small GTPases.
Therefore, determining the specific localisation of Rac proteins at the IS and whether their localisation affects pSMAC formation are key issues that need to be examined in future.

7.5 A Model of Integrin Regulation during B Cell Membrane Antigen Recognition and Immunological Synapse Formation

The data presented in this Thesis allows proposing the following model of integrin regulation during membrane antigen recognition and IS formation, which is illustrated in Figure 7.1 and Figure 7.2.

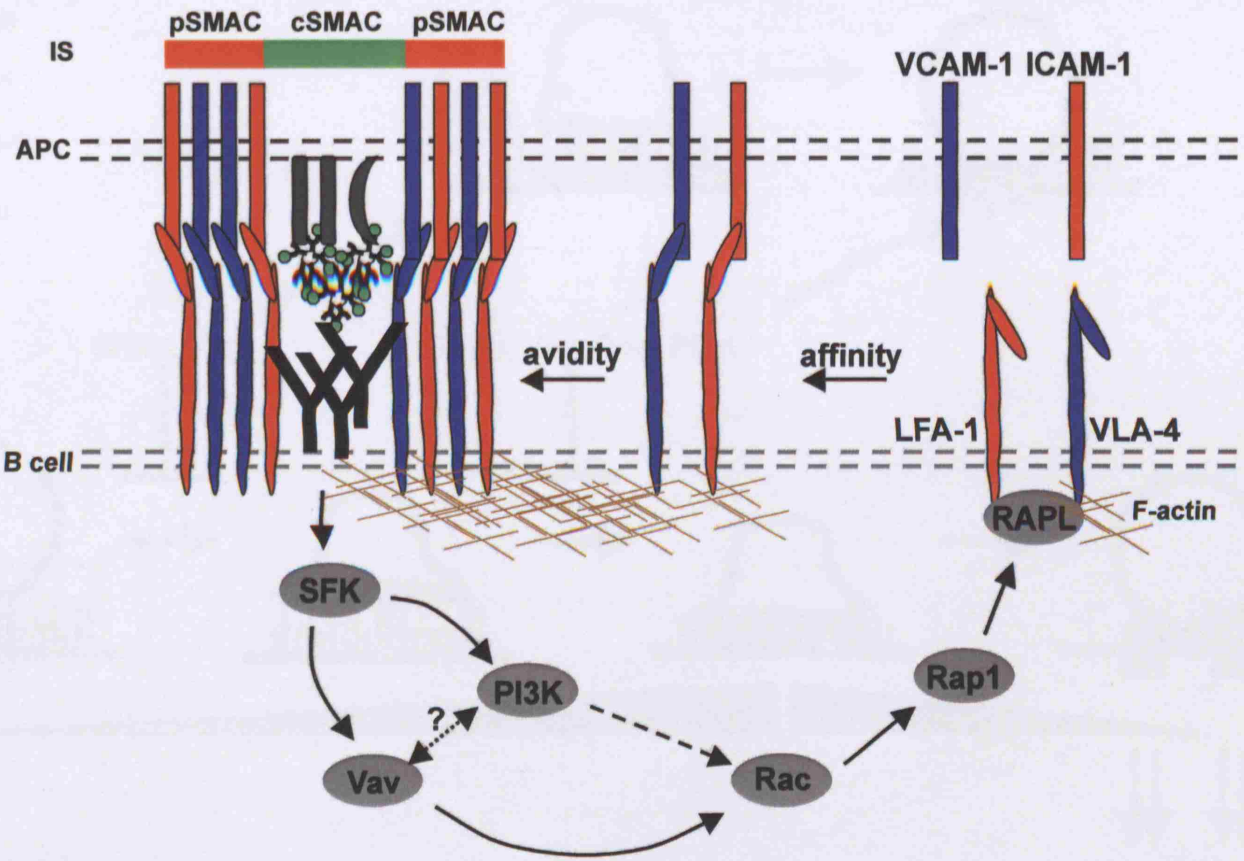

Figure 7.1 A signalling pathway involving SFKs, Vav, Rac and PI3K triggers integrin activation in B cells
This figure shows a model of a signalling pathway leading to integrin activation in B cells, which is described in this Thesis. Antigen recognition by the BCR initiates an inside-out signalling pathway involving Src-family tyrosine kinases (SFKs), Vav, Rac, and partially PI3K. This cascade triggers changes in integrin affinity, which promote ligand binding. Furthermore it induces cytoskeletal rearrangements and contributes to changes in integrin avidity, cell polarisation and pSMAC formation. This pathway may promote activation of Rap1 and may therefore regulate integrin activation through RAPL.

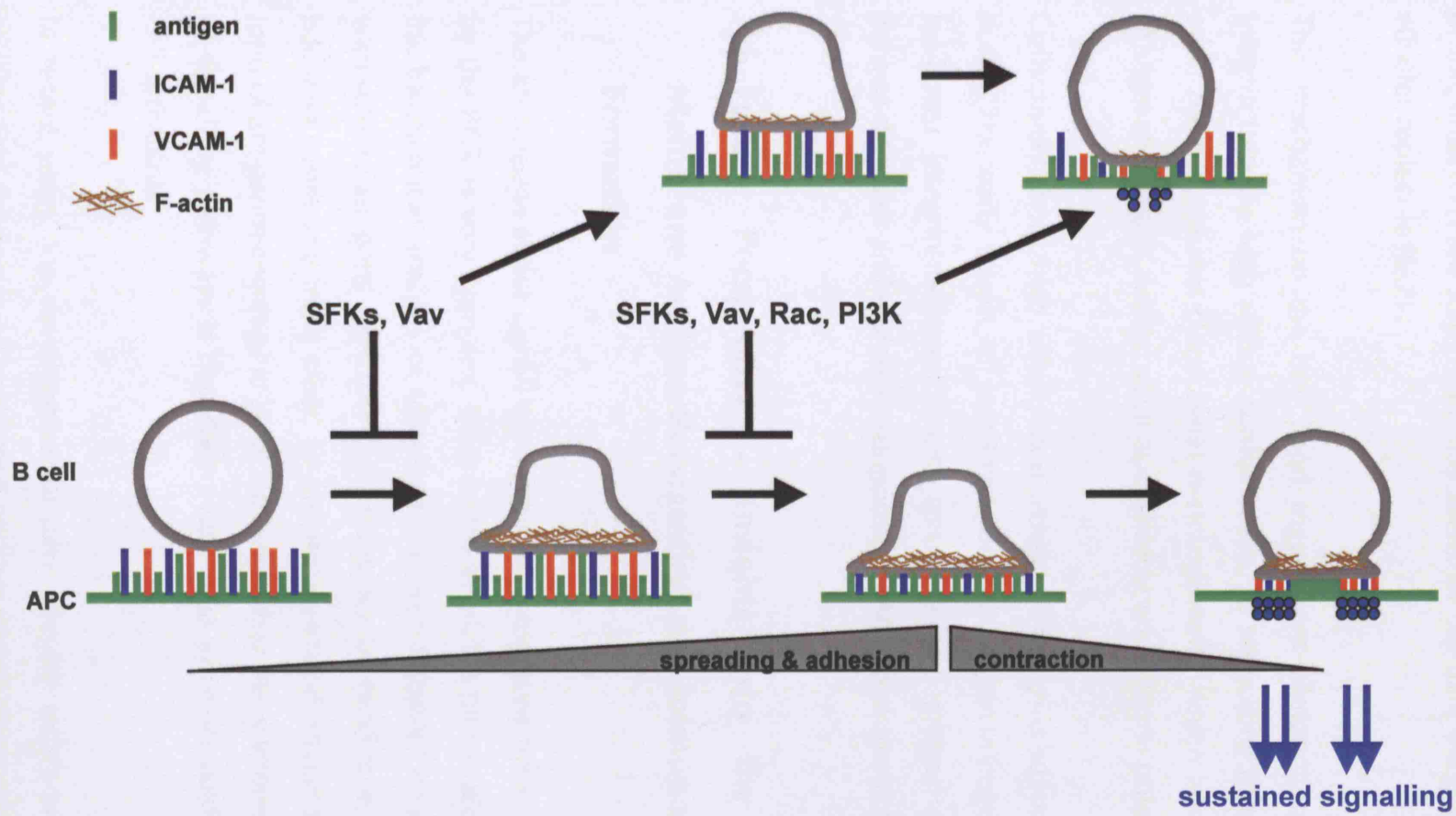

Figure 7.2 Integrin activation during membrane-bound antigen recognition triggers B cell adhesion and supports B cell spreading, antigen aggregation and immunological synapse formation

This figure shows a model of processes that contribute to membrane-bound antigen recognition: specific antigen triggers B cell spreading and B cell adhesion on the membrane of the antigen presenting cell (APC). By contracting, the B cell collects antigen into the cSMAC. pSMAC formation facilitates sustained signalling at the immunological synapse. Src-family tyrosine kinases (SFK), Vav and cytoskeletal rearrangements are required for B cell spreading. SFKs, Vav and Rac and and PI3K regulate integrin activation and therefore contribute to B cell spreading antigen aggregation and pSMAC formation.

Membrane-bound antigen recognition by the BCR initiates an intracellular signalling pathway involving SFKs, Vav and Rac proteins and PI3K, which is crucial for integrin activation. This signalling cascade contributes to the activation of the small GTPase Rap1 and may therefore regulate integrin activation via the effector molecule RAPL.

This mechanism on the one hand triggers the conformational change of the integrin into the high affinity conformation, so supporting ligand binding. On the other hand it induces cytoskeletal rearrangements, which are known to regulate changes in integrin avidity, such as clustering and integrin polarisation.

Collectively, both high affinity and avidity of integrins support B cell adhesion during the early stages of membrane-bound antigen recognition. This in turn facilitates integrin-mediated B cell spreading and antigen aggregation at low antigen densities and moreover supports pSMAC formation at the IS.

7.6 Future Perspective - Insights into the Processes of Membrane Antigen Recognition and Immunological Synapse Formation

The knowledge about signalling mechanisms triggered upon antigen recognition by the BCR is very complex. Most of the available information is retrieved from the biochemical analysis of signalling cascades triggered upon BCR crosslinking with soluble antigens. However the importance of membrane antigen recognition becomes more and more clear, as membrane-bound antigens may be the major form of antigen recognised *in vivo*. Understanding the spatiotemporal organisation of signalling pathways is therefore a key issue in understanding regulation of B cell activation.

In recent years, the development of new imaging techniques has led to new insights into the basics of membrane antigen recognition and IS formation. It has been shown by several groups, that the TCR forms microcluster upon antigen

recognition on artificial APCs, which move towards the centre of the contact zone and form the cSMAC (Campi et al., 2005), (Yokosuka et al., 2005). These reports also shed light on how signalling may occur at the IS. A recent study suggests that signalling continues in peripheral micro-clusters, highlighting the role of the pSMAC for sustained calcium flux and proper T cell activation (Varma et al., 2006). Micro-cluster formation and their movement were dependent on the actin cytoskeleton (Varma et al., 2006), however the exact mechanisms are not understood. First insights into micro-cluster dynamics come from studies that show their association with Zap-70 and SLP-76 (Yokosuka et al., 2005) and a recent report shows recruitment of Vav (Miletic et al., 2006).

The data presented in this Thesis suggests that also the pSMAC in B cells may serve as site for sustained BCR signalling, as phosphotyrosine localised in the periphery surrounding the cSMAC. Furthermore, in agreement with studies in T cells, Vav seems to be recruited to antigen clusters. However, the role of these clusters, and which are the signalling mechanisms that underlie their formation in B cells is a fundamental question to be addressed in the near future.

A lot of work has been done that contributes to our current understanding of the regulation of IS formation. However, it is still unclear how, where and when antigen recognition and IS formation happens *in vivo*.
Using two-photon microscopy, Qi et al. recently showed that upon lymph node entry through high endothelial venules naïve B cells scan local DCs for their specific antigen. Interestingly, the interaction B cells with DC primed with specific antigen lasted three times longer than their contacts with DC bearing non-specific antigen (Qi et al., 2006).
The behaviour of follicular B cells in the lymph node was analysed in another study, which shows that 1 to 3 hours after administration of soluble antigen into recipient mice, follicular B cells bound to antigen showed decreased velocities, attributed to enhanced adhesion to neighbouring cells. Upon antigen binding B cells moved towards the T cell zone in a chemokine-dependent manner and formed conjugates with helper T cells (Okada et al., 2005).

In a recent report, Allen et al. directly visualise B cell behaviour in germinal centres of the lymph node. In this particular study the authors show, that six days after antigen administration germinal centre B cells are highly motile and migrate bi-directional between dark and light zones, consistent with multiple rounds of mutation and B cell selection in these anatomical locations. Furthermore, B cells seemed to move along FDCs and rarely stopped for prolonged times, possibly due to the limited antigen availability at this late stage of the immune response (Allen et al., 2007).
Although, for the first time, these studies examine directly how B cells encounter their specific antigen *in vivo*, still much has to be learned about this process in future.

Recent studies suggest that the affinity of the BCR for the specific antigen plays a crucial role in determining the fate of a B cell. For example, B cells expressing a high affinity BCR are destined to become short-lived plasma cells, which produce the first wave of protective antibodies during the course of an immune response. In contrast, moderate and low BCR affinity support affinity maturation in the germinal centre and the formation of long-lived plasma cells and memory B cells (O'Connor et al., 2006), (Phan et al., 2006), (Paus et al., 2006).
However, the effect of the BCR affinity during the early stages of antigen recognition has not been addressed *in vivo* and it would be interesting to examine B cell behaviour in this context in lymphoid organs in future experiments, for example by administration of mutant HEL molecules of different affinities.

Another exiting aspect of B cell biology is the contribution of other receptors, such as complement receptors or TLRs, to B cell activation and differentiation upon antigen encounter. On the one hand, the complement receptor CD21 has been reported to support T-dependent antibody responses (Fischer et al., 1996). On the other hand, TLRs have been suggested to contribute to the induction of humoral immune responses (Pasare and Medzhitov, 2005), (Ruprecht and Lanzavecchia, 2006).

Interestingly, coupling of two or three C3d fragments to HEL increased its immunogenicity 1000 to 10000 times, respectively, when injected into mice (Dempsey et al., 1996). These results indicate that the complement recpetor complex (CD19/CD21/CD81) might actively contribute to B cell fate decisions during an immune response, possibly by lowering the threshold for B cell activation. To address this hypothesis, future experiments could involve the coupling of C3d fragments to HEL mutants of different affinities to test their impact on B cell differentiation into plasma cells and antibody production *in vivo*.
Also TLRs have been suggested to cooperate with the BCR upon antigen recognition, as only immune complexes containing a TLR7 or TLR9 ligand as well as antigen induced proliferation of autoreactive B cells (Lau et al., 2005), (Leadbetter et al., 2002). As both, TLR7 and TLR9, reside in the endosomal compartment, these results suggest that BCR-mediated uptake of immune complexes followed by TLR engagement in the endosome is essential for full B cell activation and differentiation. To strengthen these indications, the impact of TLR signalling on B cell differentiation in the context of BCR affinity could be examined in future experiments. This could be addressed by coupling TLR ligands to HEL molecules of different affinities. In this line, the effect of BCR-TLR cooperation during the initial stages of antigen recognition, B cell motility in lymphoid tissues or B cell interaction with other immune cells, could also be investigated using two-photon microscopy.

In recent years, much work has been done to broaden our understanding of the parameters governing B cell activation and differentiation. However, fundamental issues, such as which cells are presenting antigen to B cells, their exact location and the molecular mechanisms driving BCR triggering and antigen uptake, still need to be elucidated further. New imaging techniques, such as multi-photon microscopy, are currently being developed and applied to follow these processes *in vivo* and assist to expand our current knowledge of B cell antigen recognition, B cell activation and differentiation.

8 References

Abe, K., Rossman, K. L., Liu, B., Ritola, K. D., Chiang, D., Campbell, S. L., Burridge, K., and Der, C. J. (2000). Vav2 is an activator of Cdc42, Rac1, and RhoA. J Biol Chem *275*, 10141-10149.

Allen, C. D., Okada, T., Tang, H. L., and Cyster, J. G. (2007). Imaging of germinal center selection events during affinity maturation. Science *315*, 528-531.

Ardouin, L., Bracke, M., Mathiot, A., Pagakis, S. N., Norton, T., Hogg, N., and Tybulewicz, V. L. (2003). Vav1 transduces TCR signals required for LFA-1 function and cell polarization at the immunological synapse. Eur J Immunol *33*, 790-797.

Aydar, Y., Sukumar, S., Szakal, A. K., and Tew, J. G. (2005). The influence of immune complex-bearing follicular dendritic cells on the IgM response, Ig class switching, and production of high affinity IgG. J Immunol *174*, 5358-5366.

Bach, T. L., Kerr, W., Wang, Y., Bauman, E. M., Kine, P., Whiteman, E. L., Morgan, R. S., Williamson, E. K., Ostap, E. M., Burkhardt, J. K., *et al.* (2006). PI3K regulates pleckstrin-2 in T-cell cytoskeletal re-organization. Blood.

Bachmann, M. F., Nitschke, L., Krawczyk, C., Tedford, K., Ohashi, P. S., Fischer, K. D., and Penninger, J. M. (1999). The guanine-nucleotide exchange factor Vav is a crucial regulator of B cell receptor activation and B cell responses to nonrepetitive antigens. J Immunol *163*, 137-142.

Balazs, M., Martin, F., Zhou, T., and Kearney, J. (2002). Blood dendritic cells interact with splenic marginal zone B cells to initiate T-independent immune responses. Immunity *17*, 341-352.

Batista, F. D., Iber, D., and Neuberger, M. S. (2001). B cells acquire antigen from target cells after synapse formation. Nature *411*, 489-494.

Batista, F. D., and Neuberger, M. S. (1998). Affinity dependence of the B cell response to antigen: a threshold, a ceiling, and the importance of off-rate. Immunity *8*, 751-759.

Bazzoni, G., and Hemler, M. E. (1998). Are changes in integrin affinity and conformation overemphasized? Trends Biochem Sci *23*, 30-34.

Benschop, R. J., Aviszus, K., Zhang, X., Manser, T., Cambier, J. C., and Wysocki, L. J. (2001). Activation and anergy in bone marrow B cells of a novel immunoglobulin transgenic mouse that is both hapten specific and autoreactive. Immunity *14*, 33-43.

Benschop, R. J., and Cambier, J. C. (1999). B cell development: signal transduction by antigen receptors and their surrogates. Curr Opin Immunol *11*, 143-151.

Bergtold, A., Desai, D. D., Gavhane, A., and Clynes, R. (2005). Cell surface recycling of internalized antigen permits dendritic cell priming of B cells. Immunity *23*, 503-514.

Berney, C., Herren, S., Power, C. A., Gordon, S., Martinez-Pomares, L., and Kosco-Vilbois, M. H. (1999). A member of the dendritic cell family that enters B cell follicles and stimulates primary antibody responses identified by a mannose receptor fusion protein. J Exp Med *190*, 851-860.

Borroto, A., Gil, D., Delgado, P., Vicente-Manzanares, M., Alcover, A., Sanchez-Madrid, F., and Alarcon, B. (2000). Rho regulates T cell receptor ITAM-induced lymphocyte spreading in an integrin-independent manner. Eur J Immunol *30*, 3403-3410.

Brian, A. A., and McConnell, H. M. (1984). Allogeneic stimulation of cytotoxic T cells by supported planar membranes. Proc Natl Acad Sci U S A *81*, 6159-6163.

Bunnell, S. C., Kapoor, V., Trible, R. P., Zhang, W., and Samelson, L. E. (2001). Dynamic actin polymerization drives T cell receptor-induced spreading: a role for the signal transduction adaptor LAT. Immunity *14*, 315-329.

Burack, W. R., Lee, K. H., Holdorf, A. D., Dustin, M. L., and Shaw, A. S. (2002). Cutting edge: quantitative imaging of raft accumulation in the immunological synapse. J Immunol *169*, 2837-2841.

Burkhardt, A. L., Brunswick, M., Bolen, J. B., and Mond, J. J. (1991). Anti-immunoglobulin stimulation of B lymphocytes activates src-related protein-tyrosine kinases. Proc Natl Acad Sci U S A *88*, 7410-7414.

Cairo, C. W., Mirchev, R., and Golan, D. E. (2006). Cytoskeletal regulation couples LFA-1 conformational changes to receptor lateral mobility and clustering. Immunity *25*, 297-308.

Camacho, S. A., Kosco-Vilbois, M. H., and Berek, C. (1998). The dynamic structure of the germinal center. Immunol Today *19*, 511-514.

Cambier, J. C. (1995). New nomenclature for the Reth motif (or ARH1/TAM/ARAM/YXXL). Immunol Today *16*, 110.

Campbell, J. J., Hedrick, J., Zlotnik, A., Siani, M. A., Thompson, D. A., and Butcher, E. C. (1998). Chemokines and the arrest of lymphocytes rolling under flow conditions. Science *279*, 381-384.

Campi, G., Varma, R., and Dustin, M. L. (2005). Actin and agonist MHC-peptide complex-dependent T cell receptor microclusters as scaffolds for signaling. J Exp Med *202*, 1031-1036.

Carman, C. V., and Springer, T. A. (2003). Integrin avidity regulation: are changes in affinity and conformation underemphasized? Curr Opin Cell Biol *15*, 547-556.

Carrasco, Y. R., and Batista, F. D. (2006). B-cell activation by membrane-bound antigens is facilitated by the interaction of VLA-4 with VCAM-1. Embo J *25*, 889-899.

Carrasco, Y. R., Fleire, S. J., Cameron, T., Dustin, M. L., and Batista, F. D. (2004). LFA-1/ICAM-1 interaction lowers the threshold of B cell activation by facilitating B cell adhesion and synapse formation. Immunity *20*, 589-599.

Carroll, M. (1999). Role of complement receptors CD21/CD35 in B lymphocyte activation and survival. Curr Top Microbiol Immunol *246*, 63-68; discussion 69.

Carter, R. H., and Barrington, R. A. (2004). Signaling by the CD19/CD21 complex on B cells. Curr Dir Autoimmun *7*, 4-32.

Carter, R. H., and Fearon, D. T. (1989). Polymeric C3dg primes human B lymphocytes for proliferation induced by anti-IgM. J Immunol *143*, 1755-1760.

Carter, R. H., Park, D. J., Rhee, S. G., and Fearon, D. T. (1991). Tyrosine phosphorylation of phospholipase C induced by membrane immunoglobulin in B lymphocytes. Proc Natl Acad Sci U S A *88*, 2745-2749.

Chakraborty, A. K. (2002). How and why does the immunological synapse form? Physical chemistry meets cell biology. Sci STKE *2002*, PE10.

Chan, V. W., Lowell, C. A., and DeFranco, A. L. (1998). Defective negative regulation of antigen receptor signaling in Lyn-deficient B lymphocytes. Curr Biol *8*, 545-553.

Chan, V. W., Meng, F., Soriano, P., DeFranco, A. L., and Lowell, C. A. (1997). Characterization of the B lymphocyte populations in Lyn-deficient mice and the role of Lyn in signal initiation and down-regulation. Immunity *7*, 69-81.

Chantry, D., Vojtek, A., Kashishian, A., Holtzman, D. A., Wood, C., Gray, P. W., Cooper, J. A., and Hoekstra, M. F. (1997). p110delta, a novel phosphatidylinositol 3-kinase catalytic subunit that associates with p85 and is expressed predominantly in leukocytes. J Biol Chem *272*, 19236-19241.

Cheng, P. C., Dykstra, M. L., Mitchell, R. N., and Pierce, S. K. (1999). A role for lipid rafts in B cell antigen receptor signaling and antigen targeting. J Exp Med *190*, 1549-1560.

Cherukuri, A., Cheng, P. C., Sohn, H. W., and Pierce, S. K. (2001). The CD19/CD21 complex functions to prolong B cell antigen receptor signaling from lipid rafts. Immunity *14*, 169-179.

Chung, J. B., Silverman, M., and Monroe, J. G. (2003). Transitional B cells: step by step towards immune competence. Trends Immunol *24*, 343-349.

Clayton, E., Bardi, G., Bell, S. E., Chantry, D., Downes, C. P., Gray, A., Humphries, L. A., Rawlings, D., Reynolds, H., Vigorito, E., and Turner, M. (2002). A crucial role for the p110delta subunit of phosphatidylinositol 3-kinase in B cell development and activation. J Exp Med *196*, 753-763.

Colino, J., Shen, Y., and Snapper, C. M. (2002). Dendritic cells pulsed with intact Streptococcus pneumoniae elicit both protein- and polysaccharide-specific immunoglobulin isotype responses in vivo through distinct mechanisms. J Exp Med *195*, 1-13.

Corcoran, A. E. (2005). Immunoglobulin locus silencing and allelic exclusion. Semin Immunol *17*, 141-154.

Costello, P. S., Gallagher, M., and Cantrell, D. A. (2002). Sustained and dynamic inositol lipid metabolism inside and outside the immunological synapse. Nat Immunol *3*, 1082-1089.

Crespo, P., Schuebel, K. E., Ostrom, A. A., Gutkind, J. S., and Bustelo, X. R. (1997). Phosphotyrosine-dependent activation of Rac-1 GDP/GTP exchange by the vav proto-oncogene product. Nature *385*, 169-172.

D'Souza-Schorey, C., Boettner, B., and Van Aelst, L. (1998). Rac regulates integrin-mediated spreading and increased adhesion of T lymphocytes. Mol Cell Biol *18*, 3936-3946.

de Bruyn, K. M., Rangarajan, S., Reedquist, K. A., Figdor, C. G., and Bos, J. L. (2002). The small GTPase Rap1 is required for Mn(2+)- and antibody-induced LFA-1- and VLA-4-mediated cell adhesion. J Biol Chem *277*, 29468-29476.

Deckert, M., Tartare-Deckert, S., Couture, C., Mustelin, T., and Altman, A. (1996). Functional and physical interactions of Syk family kinases with the Vav proto-oncogene product. Immunity *5*, 591-604.

Dempsey, P. W., Allison, M. E., Akkaraju, S., Goodnow, C. C., and Fearon, D. T. (1996). C3d of complement as a molecular adjuvant: bridging innate and acquired immunity. Science *271*, 348-350.

Doody, G. M., Bell, S. E., Vigorito, E., Clayton, E., McAdam, S., Tooze, R., Fernandez, C., Lee, I. J., and Turner, M. (2001). Signal transduction through Vav-2 participates in humoral immune responses and B cell maturation. Nat Immunol *2*, 542-547.

Dransfield, I., Cabanas, C., Craig, A., and Hogg, N. (1992). Divalent cation regulation of the function of the leukocyte integrin LFA-1. J Cell Biol *116*, 219-226.

Duchniewicz, M., Zemojtel, T., Kolanczyk, M., Grossmann, S., Scheele, J. S., and Zwartkruis, F. J. (2006). Rap1A-deficient T and B cells show impaired integrin-mediated cell adhesion. Mol Cell Biol *26*, 643-653.

Dustin, M. L., Ferguson, L. M., Chan, P. Y., Springer, T. A., and Golan, D. E. (1996). Visualization of CD2 interaction with LFA-3 and determination of the two-dimensional dissociation constant for adhesion receptors in a contact area. J Cell Biol *132*, 465-474.

Dustin, M. L., Golan, D. E., Zhu, D. M., Miller, J. M., Meier, W., Davies, E. A., and van der Merwe, P. A. (1997). Low affinity interaction of human or rat T cell adhesion molecule CD2 with its ligand aligns adhering membranes to achieve high physiological affinity. J Biol Chem *272*, 30889-30898.

Dustin, M. L., Olszowy, M. W., Holdorf, A. D., Li, J., Bromley, S., Desai, N., Widder, P., Rosenberger, F., van der Merwe, P. A., Allen, P. M., and Shaw, A. S. (1998). A novel adaptor protein orchestrates receptor patterning and cytoskeletal polarity in T-cell contacts. Cell *94*, 667-677.

Dustin, M. L., and Springer, T. A. (1989). T-cell receptor cross-linking transiently stimulates adhesiveness through LFA-1. Nature *341*, 619-624.

Faure, S., Salazar-Fontana, L. I., Semichon, M., Tybulewicz, V. L., Bismuth, G., Trautmann, A., Germain, R. N., and Delon, J. (2004). ERM proteins regulate cytoskeleton relaxation promoting T cell-APC conjugation. Nat Immunol *5*, 272-279.

Fearon, D. T., and Carroll, M. C. (2000). Regulation of B lymphocyte responses to foreign and self-antigens by the CD19/CD21 complex. Annu Rev Immunol *18*, 393-422.

Filippi, M. D., Harris, C. E., Meller, J., Gu, Y., Zheng, Y., and Williams, D. A. (2004). Localization of Rac2 via the C terminus and aspartic acid 150 specifies superoxide generation, actin polarity and chemotaxis in neutrophils. Nat Immunol *5*, 744-751.

Fischer, M. B., Ma, M., Goerg, S., Zhou, X., Xia, J., Finco, O., Han, S., Kelsoe, G., Howard, R. G., Rothstein, T. L., *et al.* (1996). Regulation of the B cell response to T-dependent antigens by classical pathway complement. J Immunol *157*, 549-556.

Fleire, S. J., Goldman, J. P., Carrasco, Y. R., Weber, M., Bray, D., and Batista, F. D. (2006). B cell ligand discrimination through a spreading and contraction response. Science *312*, 738-741.

Freedman, A. S., Munro, J. M., Rice, G. E., Bevilacqua, M. P., Morimoto, C., McIntyre, B. W., Rhynhart, K., Pober, J. S., and Nadler, L. M. (1990). Adhesion of human B cells to germinal centers in vitro involves VLA-4 and INCAM-110. Science *249*, 1030-1033.

Fu, C., Turck, C. W., Kurosaki, T., and Chan, A. C. (1998). BLNK: a central linker protein in B cell activation. Immunity *9*, 93-103.

Fujikawa, K., Miletic, A. V., Alt, F. W., Faccio, R., Brown, T., Hoog, J., Fredericks, J., Nishi, S., Mildiner, S., Moores, S. L., *et al.* (2003). Vav1/2/3-null mice define an essential role for Vav family proteins in lymphocyte development and activation but a differential requirement in MAPK signaling in T and B cells. J Exp Med *198*, 1595-1608.

Gauld, S. B., Merrell, K. T., and Cambier, J. C. (2006). Silencing of autoreactive B cells by anergy: a fresh perspective. Curr Opin Immunol *18*, 292-297.

Gay, D., Saunders, T., Camper, S., and Weigert, M. (1993). Receptor editing: an approach by autoreactive B cells to escape tolerance. J Exp Med *177*, 999-1008.

Glick, B. (1991). Historical perspective: the bursa of Fabricius and its influence on B-cell development, past and present. Vet Immunol Immunopathol *30*, 3-12.

Goodnow, C. C., Crosbie, J., Adelstein, S., Lavoie, T. B., Smith-Gill, S. J., Brink, R. A., Pritchard-Briscoe, H., Wotherspoon, J. S., Loblay, R. H., Raphael, K., and et al. (1988). Altered immunoglobulin expression and functional silencing of self-reactive B lymphocytes in transgenic mice. Nature *334*, 676-682.

Grakoui, A., Bromley, S. K., Sumen, C., Davis, M. M., Shaw, A. S., Allen, P. M., and Dustin, M. L. (1999). The immunological synapse: a molecular machine controlling T cell activation. Science *285*, 221-227.

Griffiths, E. K., Krawczyk, C., Kong, Y. Y., Raab, M., Hyduk, S. J., Bouchard, D., Chan, V. S., Kozieradzki, I., Oliveira-Dos-Santos, A. J., Wakeham, A., *et al.* (2001). Positive regulation of T cell activation and integrin adhesion by the adapter Fyb/Slap. Science *293*, 2260-2263.

Groves, J. T., and Dustin, M. L. (2003). Supported planar bilayers in studies on immune cell adhesion and communication. J Immunol Methods *278*, 19-32.

Gupta, N., and DeFranco, A. L. (2003). Visualizing lipid raft dynamics and early signaling events during antigen receptor-mediated B-lymphocyte activation. Mol Biol Cell *14*, 432-444.

Haberman, A. M., and Shlomchik, M. J. (2003). Reassessing the function of immune-complex retention by follicular dendritic cells. Nat Rev Immunol *3*, 757-764.

Han, J., Das, B., Wei, W., Van Aelst, L., Mosteller, R. D., Khosravi-Far, R., Westwick, J. K., Der, C. J., and Broek, D. (1997). Lck regulates Vav activation of members of the Rho family of GTPases. Mol Cell Biol *17*, 1346-1353.

Han, J., Luby-Phelps, K., Das, B., Shu, X., Xia, Y., Mosteller, R. D., Krishna, U. M., Falck, J. R., White, M. A., and Broek, D. (1998). Role of substrates and products of PI 3-kinase in regulating activation of Rac-related guanosine triphosphatases by Vav. Science *279*, 558-560.

Hao, S., and August, A. (2005). Actin depolymerization transduces the strength of B-cell receptor stimulation. Mol Biol Cell *16*, 2275-2284.

Hardy, R. R., and Hayakawa, K. (2001). B cell development pathways. Annu Rev Immunol *19*, 595-621.

Harriague, J., and Bismuth, G. (2002). Imaging antigen-induced PI3K activation in T cells. Nat Immunol *3*, 1090-1096.

Hartley, S. B., Crosbie, J., Brink, R., Kantor, A. B., Basten, A., and Goodnow, C. C. (1991). Elimination from peripheral lymphoid tissues of self-reactive B lymphocytes recognizing membrane-bound antigens. Nature *353*, 765-769.

Hashimoto, S., Iwamatsu, A., Ishiai, M., Okawa, K., Yamadori, T., Matsushita, M., Baba, Y., Kishimoto, T., Kurosaki, T., and Tsukada, S. (1999). Identification of the SH2 domain binding protein of Bruton's tyrosine kinase as BLNK--functional significance of Btk-SH2 domain in B-cell antigen receptor-coupled calcium signaling. Blood *94*, 2357-2364.

Hemler, M. E. (1990). VLA proteins in the integrin family: structures, functions, and their role on leukocytes. Annu Rev Immunol *8*, 365-400.

Hempel, W. M., Schatzman, R. C., and DeFranco, A. L. (1992). Tyrosine phosphorylation of phospholipase C-gamma 2 upon cross-linking of membrane Ig on murine B lymphocytes. J Immunol *148*, 3021-3027.

Hermiston, M. L., Xu, Z., and Weiss, A. (2003). CD45: a critical regulator of signaling thresholds in immune cells. Annu Rev Immunol *21*, 107-137.

Hibbs, M. L., Tarlinton, D. M., Armes, J., Grail, D., Hodgson, G., Maglitto, R., Stacker, S. A., and Dunn, A. R. (1995). Multiple defects in the immune system of Lyn-deficient mice, culminating in autoimmune disease. Cell *83*, 301-311.

Hombach, J., Tsubata, T., Leclercq, L., Stappert, H., and Reth, M. (1990). Molecular components of the B-cell antigen receptor complex of the IgM class. Nature *343*, 760-762.

Inabe, K., Ishiai, M., Scharenberg, A. M., Freshney, N., Downward, J., and Kurosaki, T. (2002). Vav3 modulates B cell receptor responses by regulating phosphoinositide 3-kinase activation. J Exp Med *195*, 189-200.

Jaffe, A. B., and Hall, A. (2005). Rho GTPases: biochemistry and biology. Annu Rev Cell Dev Biol *21*, 247-269.

Janeway, C. A., Jr., Travers, P., Walport, M., and Shlomchik, M. J. (2005). Immunobiology, 6 edn, Garland Science Publishing).

Jin, T., and Li, J. (2002). Dynamitin controls Beta 2 integrin avidity by modulating cytoskeletal constraint on integrin molecules. J Biol Chem *277*, 32963-32969.

Jo, E. K., Wang, H., and Rudd, C. E. (2005). An essential role for SKAP-55 in LFA-1 clustering on T cells that cannot be substituted by SKAP-55R. J Exp Med *201*, 1733-1739.

Johmura, S., Oh-hora, M., Inabe, K., Nishikawa, Y., Hayashi, K., Vigorito, E., Kitamura, D., Turner, M., Shingu, K., Hikida, M., and Kurosaki, T. (2003). Regulation of Vav localization in membrane rafts by adaptor molecules Grb2 and BLNK. Immunity *18*, 777-787.

Jou, S. T., Carpino, N., Takahashi, Y., Piekorz, R., Chao, J. R., Carpino, N., Wang, D., and Ihle, J. N. (2002). Essential, nonredundant role for the phosphoinositide 3-kinase p110delta in signaling by the B-cell receptor complex. Mol Cell Biol *22*, 8580-8591.

Katagiri, K., Maeda, A., Shimonaka, M., and Kinashi, T. (2003). RAPL, a Rap1-binding molecule that mediates Rap1-induced adhesion through spatial regulation of LFA-1. Nat Immunol *4*, 741-748.

Katzav, S., Martin-Zanca, D., and Barbacid, M. (1989). vav, a novel human oncogene derived from a locus ubiquitously expressed in hematopoietic cells. Embo J *8*, 2283-2290.

Kim, K. J., Kanellopoulos-Langevin, C., Merwin, R. M., Sachs, D. H., and Asofsky, R. (1979). Establishment and characterization of BALB/c lymphoma lines with B cell properties. J Immunol *122*, 549-554.

Kim, M., Carman, C. V., and Springer, T. A. (2003). Bidirectional transmembrane signaling by cytoplasmic domain separation in integrins. Science *301*, 1720-1725.

Kim, M., Carman, C. V., Yang, W., Salas, A., and Springer, T. A. (2004). The primacy of affinity over clustering in regulation of adhesiveness of the integrin {alpha}L{beta}2. J Cell Biol *167*, 1241-1253.

Kinashi, T., and Katagiri, K. (2004). Regulation of lymphocyte adhesion and migration by the small GTPase Rap1 and its effector molecule, RAPL. Immunol Lett *93*, 1-5.

Kliche, S., Breitling, D., Togni, M., Pusch, R., Heuer, K., Wang, X., Freund, C., Kasirer-Friede, A., Menasche, G., Koretzky, G. A., and Schraven, B. (2006). The ADAP/SKAP55 signaling module regulates T-cell receptor-mediated integrin activation through plasma membrane targeting of Rap1. Mol Cell Biol *26*, 7130-7144.

Koopman, G., Keehnen, R. M., Lindhout, E., Newman, W., Shimizu, Y., van Seventer, G. A., de Groot, C., and Pals, S. T. (1994). Adhesion through the LFA-1 (CD11a/CD18)-ICAM-1 (CD54) and the VLA-4 (CD49d)-VCAM-1 (CD106) pathways prevents apoptosis of germinal center B cells. J Immunol *152*, 3760-3767.

Koopman, G., Parmentier, H. K., Schuurman, H. J., Newman, W., Meijer, C. J., and Pals, S. T. (1991). Adhesion of human B cells to follicular dendritic cells involves both the lymphocyte function-associated antigen 1/intercellular adhesion molecule 1 and very late antigen 4/vascular cell adhesion molecule 1 pathways. J Exp Med *173*, 1297-1304.

Kosco-Vilbois, M. H. (2003). Are follicular dendritic cells really good for nothing? Nat Rev Immunol *3*, 764-769.

Kouskoff, V., Famiglietti, S., Lacaud, G., Lang, P., Rider, J. E., Kay, B. K., Cambier, J. C., and Nemazee, D. (1998). Antigens varying in affinity for the B cell receptor induce differential B lymphocyte responses. J Exp Med *188*, 1453-1464.

Krawczyk, C., Bachmaier, K., Sasaki, T., Jones, R. G., Snapper, S. B., Bouchard, D., Kozieradzki, I., Ohashi, P. S., Alt, F. W., and Penninger, J. M. (2000). Cbl-b is a negative regulator of receptor clustering and raft aggregation in T cells. Immunity *13*, 463-473.

Kucik, D. F., Dustin, M. L., Miller, J. M., and Brown, E. J. (1996). Adhesion-activating phorbol ester increases the mobility of leukocyte integrin LFA-1 in cultured lymphocytes. J Clin Invest *97*, 2139-2144.

Kurosaki, T., and Tsukada, S. (2000). BLNK: connecting Syk and Btk to calcium signals. Immunity *12*, 1-5.

Kushnir, N., Liu, L., and MacPherson, G. G. (1998). Dendritic cells and resting B cells form clusters in vitro and in vivo: T cell independence, partial LFA-1 dependence, and regulation by cross-linking surface molecules. J Immunol *160*, 1774-1781.

Landis, R. C., Bennett, R. I., and Hogg, N. (1993). A novel LFA-1 activation epitope maps to the I domain. J Cell Biol *120*, 1519-1527.

Lang, J., Jackson, M., Teyton, L., Brunmark, A., Kane, K., and Nemazee, D. (1996). B cells are exquisitely sensitive to central tolerance and receptor editing induced by ultralow affinity, membrane-bound antigen. J Exp Med *184*, 1685-1697.

Lau, C. M., Broughton, C., Tabor, A. S., Akira, S., Flavell, R. A., Mamula, M. J., Christensen, S. R., Shlomchik, M. J., Viglianti, G. A., Rifkin, I. R., and Marshak-Rothstein, A. (2005). RNA-associated autoantigens activate B cells by combined B cell antigen receptor/Toll-like receptor 7 engagement. J Exp Med *202*, 1171-1177.

Law, D. A., Gold, M. R., and DeFranco, A. L. (1992). Examination of B lymphoid cell lines for membrane immunoglobulin-stimulated tyrosine phosphorylation and src-family tyrosine kinase mRNA expression. Mol Immunol *29*, 917-926.

Leadbetter, E. A., Rifkin, I. R., Hohlbaum, A. M., Beaudette, B. C., Shlomchik, M. J., and Marshak-Rothstein, A. (2002). Chromatin-IgG complexes activate B cells by dual engagement of IgM and Toll-like receptors. Nature *416*, 603-607.

Liu, S., Calderwood, D. A., and Ginsberg, M. H. (2000). Integrin cytoplasmic domain-binding proteins. J Cell Sci *113 (Pt 20)*, 3563-3571.

Loder, F., Mutschler, B., Ray, R. J., Paige, C. J., Sideras, P., Torres, R., Lamers, M. C., and Carsetti, R. (1999). B cell development in the spleen takes place in discrete steps and is determined by the quality of B cell receptor-derived signals. J Exp Med *190*, 75-89.

Lowell, C. A., and Soriano, P. (1996). Knockouts of Src-family kinases: stiff bones, wimpy T cells, and bad memories. Genes Dev *10*, 1845-1857.

Lu, C., Takagi, J., and Springer, T. A. (2001). Association of the membrane proximal regions of the alpha and beta subunit cytoplasmic domains constrains an integrin in the inactive state. J Biol Chem *276*, 14642-14648.

MacLennan, I. C. (1994). Germinal centers. Annu Rev Immunol *12*, 117-139.

McLeod, S. J., Shum, A. J., Lee, R. L., Takei, F., and Gold, M. R. (2004). The Rap GTPases regulate integrin-mediated adhesion, cell spreading, actin polymerization, and Pyk2 tyrosine phosphorylation in B lymphocytes. J Biol Chem *279*, 12009-12019.

Medzhitov, R., and Janeway, C. A., Jr. (1997). Innate immunity: impact on the adaptive immune response. Curr Opin Immunol *9*, 4-9.

Merrell, K. T., Benschop, R. J., Gauld, S. B., Aviszus, K., Decote-Ricardo, D., Wysocki, L. J., and Cambier, J. C. (2006). Identification of Anergic B Cells within a Wild-Type Repertoire. Immunity *25*, 953-962.

Miletic, A. V., Sakata-Sogawa, K., Hiroshima, M., Hamann, M. J., Gomez, T. S., Ota, N., Kloeppel, T., Kanagawa, O., Tokunaga, M., Billadeau, D. D., and Swat, W. (2006). Vav1 Acidic Region Tyrosine 174 Is Required for the Formation of T Cell Receptor-induced Microclusters and Is Essential in T Cell Development and Activation. J Biol Chem *281*, 38257-38265.

Monks, C. R., Freiberg, B. A., Kupfer, H., Sciaky, N., and Kupfer, A. (1998). Three-dimensional segregation of supramolecular activation clusters in T cells. Nature *395*, 82-86.

Movilla, N., and Bustelo, X. R. (1999). Biological and regulatory properties of Vav-3, a new member of the Vav family of oncoproteins. Mol Cell Biol *19*, 7870-7885.

Negulescu, P. A., Krasieva, T. B., Khan, A., Kerschbaum, H. H., and Cahalan, M. D. (1996). Polarity of T cell shape, motility, and sensitivity to antigen. Immunity *4*, 421-430.

Nemazee, D., Gavin, A., Hoebe, K., and Beutler, B. (2006). Immunology: Toll-like receptors and antibody responses. Nature *441*, E4; discussion E4.

Nemazee, D. A., and Burki, K. (1989). Clonal deletion of B lymphocytes in a transgenic mouse bearing anti-MHC class I antibody genes. Nature *337*, 562-566.

Niiro, H., and Clark, E. A. (2002). Regulation of B-cell fate by antigen-receptor signals. Nat Rev Immunol *2*, 945-956.

Nishizumi, H., Horikawa, K., Mlinaric-Rascan, I., and Yamamoto, T. (1998). A double-edged kinase Lyn: a positive and negative regulator for antigen receptor-mediated signals. J Exp Med *187*, 1343-1348.

Nishizumi, H., Taniuchi, I., Yamanashi, Y., Kitamura, D., Ilic, D., Mori, S., Watanabe, T., and Yamamoto, T. (1995). Impaired proliferation of peripheral B cells and indication of autoimmune disease in lyn-deficient mice. Immunity *3*, 549-560.

Nolz, J. C., Gomez, T. S., Zhu, P., Li, S., Medeiros, R. B., Shimizu, Y., Burkhardt, J. K., Freedman, B. D., and Billadeau, D. D. (2006). The WAVE2 complex regulates actin cytoskeletal reorganization and CRAC-mediated calcium entry during T cell activation. Curr Biol *16*, 24-34.

Nossal, G. J., and Pike, B. L. (1980). Clonal anergy: persistence in tolerant mice of antigen-binding B lymphocytes incapable of responding to antigen or mitogen. Proc Natl Acad Sci U S A *77*, 1602-1606.

O'Connor, B. P., Vogel, L. A., Zhang, W., Loo, W., Shnider, D., Lind, E. F., Ratliff, M., Noelle, R. J., and Erickson, L. D. (2006). Imprinting the fate of antigen-reactive B cells through the affinity of the B cell receptor. J Immunol *177*, 7723-7732.

Odegard, V. H., and Schatz, D. G. (2006). Targeting of somatic hypermutation. Nat Rev Immunol *6*, 573-583.

Okada, T., Miller, M. J., Parker, I., Krummel, M. F., Neighbors, M., Hartley, S. B., O'Garra, A., Cahalan, M. D., and Cyster, J. G. (2005). Antigen-engaged B cells undergo chemotaxis toward the T zone and form motile conjugates with helper T cells. PLoS Biol *3*, e150.

Okkenhaug, K., Bilancio, A., Farjot, G., Priddle, H., Sancho, S., Peskett, E., Pearce, W., Meek, S. E., Salpekar, A., Waterfield, M. D., *et al.* (2002). Impaired B and T cell antigen receptor signaling in p110delta PI 3-kinase mutant mice. Science *297*, 1031-1034.

Okkenhaug, K., and Vanhaesebroeck, B. (2003). PI3K in lymphocyte development, differentiation and activation. Nat Rev Immunol *3*, 317-330.

Osmond, D. G., Rolink, A., and Melchers, F. (1998). Murine B lymphopoiesis: towards a unified model. Immunol Today *19*, 65-68.

Palmby, T. R., Abe, K., and Der, C. J. (2002). Critical role of the pleckstrin homology and cysteine-rich domains in Vav signaling and transforming activity. J Biol Chem *277*, 39350-39359.

Parsey, M. V., and Lewis, G. K. (1993). Actin polymerization and pseudopod reorganization accompany anti-CD3-induced growth arrest in Jurkat T cells. J Immunol *151*, 1881-1893.

Pasare, C., and Medzhitov, R. (2005). Control of B-cell responses by Toll-like receptors. Nature *438*, 364-368.

Paus, D., Phan, T. G., Chan, T. D., Gardam, S., Basten, A., and Brink, R. (2006). Antigen recognition strength regulates the choice between extrafollicular plasma cell and germinal center B cell differentiation. J Exp Med *203*, 1081-1091.

Peters, I. M., van Kooyk, Y., van Vliet, S. J., de Grooth, B. G., Figdor, C. G., and Greve, J. (1999). 3D single-particle tracking and optical trap measurements on adhesion proteins. Cytometry *36*, 189-194.

Peterson, E. J., Woods, M. L., Dmowski, S. A., Derimanov, G., Jordan, M. S., Wu, J. N., Myung, P. S., Liu, Q. H., Pribila, J. T., Freedman, B. D., *et al.* (2001). Coupling of the TCR to integrin activation by Slap-130/Fyb. Science *293*, 2263-2265.

Petrie, R. J., Schnetkamp, P. P., Patel, K. D., Awasthi-Kalia, M., and Deans, J. P. (2000). Transient translocation of the B cell receptor and Src homology 2 domain-containing inositol phosphatase to lipid rafts: evidence toward a role in calcium regulation. J Immunol *165*, 1220-1227.

Phan, T. G., Paus, D., Chan, T. D., Turner, M. L., Nutt, S. L., Basten, A., and Brink, R. (2006). High affinity germinal center B cells are actively selected into the plasma cell compartment. J Exp Med *203*, 2419-2424.

Poe, J. C., Hasegawa, M., and Tedder, T. F. (2001). CD19, CD21, and CD22: multifaceted response regulators of B lymphocyte signal transduction. Int Rev Immunol *20*, 739-762.

Potter, T. A., Grebe, K., Freiberg, B., and Kupfer, A. (2001). Formation of supramolecular activation clusters on fresh ex vivo CD8+ T cells after engagement of the T cell antigen receptor and CD8 by antigen-presenting cells. Proc Natl Acad Sci U S A *98*, 12624-12629.

Qi, H., Egen, J. G., Huang, A. Y., and Germain, R. N. (2006). Extrafollicular activation of lymph node B cells by antigen-bearing dendritic cells. Science *312*, 1672-1676.

Qi, S. Y., Groves, J. T., and Chakraborty, A. K. (2001). Synaptic pattern formation during cellular recognition. Proc Natl Acad Sci U S A *98*, 6548-6553.

Rawlings, D. J., Saffran, D. C., Tsukada, S., Largaespada, D. A., Grimaldi, J. C., Cohen, L., Mohr, R. N., Bazan, J. F., Howard, M., Copeland, N. G., and et al. (1993). Mutation of unique region of Bruton's tyrosine kinase in immunodeficient XID mice. Science *261*, 358-361.

Reif, K., Nobes, C. D., Thomas, G., Hall, A., and Cantrell, D. A. (1996). Phosphatidylinositol 3-kinase signals activate a selective subset of Rac/Rho-dependent effector pathways. Curr Biol *6*, 1445-1455.

Reth, M. (1989). Antigen receptor tail clue. Nature *338*, 383-384.

Reynolds, L. F., Smyth, L. A., Norton, T., Freshney, N., Downward, J., Kioussis, D., and Tybulewicz, V. L. (2002). Vav1 transduces T cell receptor signals to the activation of phospholipase C-gamma1 via phosphoinositide 3-kinase-dependent and -independent pathways. J Exp Med *195*, 1103-1114.

Rickert, R. C. (2005). Regulation of B lymphocyte activation by complement C3 and the B cell coreceptor complex. Curr Opin Immunol *17*, 237-243.

Rickert, R. C., Roes, J., and Rajewsky, K. (1997). B lymphocyte-specific, Cre-mediated mutagenesis in mice. Nucleic Acids Res *25*, 1317-1318.

Ridley, A. J., Paterson, H. F., Johnston, C. L., Diekmann, D., and Hall, A. (1992). The small GTP-binding protein rac regulates growth factor-induced membrane ruffling. Cell *70*, 401-410.

Roberts, A. W., Kim, C., Zhen, L., Lowe, J. B., Kapur, R., Petryniak, B., Spaetti, A., Pollock, J. D., Borneo, J. B., Bradford, G. B., *et al.* (1999). Deficiency of the hematopoietic cell-specific Rho family GTPase Rac2 is characterized by abnormalities in neutrophil function and host defense. Immunity *10*, 183-196.

Rodriguez, R., Matsuda, M., Perisic, O., Bravo, J., Paul, A., Jones, N. P., Light, Y., Swann, K., Williams, R. L., and Katan, M. (2001). Tyrosine residues in phospholipase Cgamma 2 essential for the enzyme function in B-cell signaling. J Biol Chem *276*, 47982-47992.

Rowley, R. B., Burkhardt, A. L., Chao, H. G., Matsueda, G. R., and Bolen, J. B. (1995). Syk protein-tyrosine kinase is regulated by tyrosine-phosphorylated Ig alpha/Ig beta immunoreceptor tyrosine activation motif binding and autophosphorylation. J Biol Chem *270*, 11590-11594.

Ruprecht, C. R., and Lanzavecchia, A. (2006). Toll-like receptor stimulation as a third signal required for activation of human naive B cells. Eur J Immunol *36*, 810-816.

Saito, T., and Yokosuka, T. (2006). Immunological synapse and microclusters: the site for recognition and activation of T cells. Curr Opin Immunol *18*, 305-313.

Sanchez-Martin, L., Sanchez-Sanchez, N., Gutierrez-Lopez, M. D., Rojo, A. I., Vicente-Manzanares, M., Perez-Alvarez, M. J., Sanchez-Mateos, P., Bustelo, X. R., Cuadrado, A., Sanchez-Madrid, F., *et al.* (2004). Signaling through the leukocyte integrin LFA-1 in T cells induces a transient activation of Rac-1 that is regulated by Vav and PI3K/Akt-1. J Biol Chem *279*, 16194-16205.

Schamel, W. W., and Reth, M. (2000). Monomeric and oligomeric complexes of the B cell antigen receptor. Immunity *13*, 5-14.

Scharenberg, A. M., El-Hillal, O., Fruman, D. A., Beitz, L. O., Li, Z., Lin, S., Gout, I., Cantley, L. C., Rawlings, D. J., and Kinet, J. P. (1998). Phosphatidylinositol-3,4,5-trisphosphate (PtdIns-3,4,5-P3)/Tec kinase-dependent calcium signaling pathway: a target for SHIP-mediated inhibitory signals. Embo J *17*, 1961-1972.

Schuebel, K. E., Bustelo, X. R., Nielsen, D. A., Song, B. J., Barbacid, M., Goldman, D., and Lee, I. J. (1996). Isolation and characterization of murine vav2, a member of the vav family of proto-oncogenes. Oncogene *13*, 363-371.

Schuebel, K. E., Movilla, N., Rosa, J. L., and Bustelo, X. R. (1998). Phosphorylation-dependent and constitutive activation of Rho proteins by wild-type and oncogenic Vav-2. Embo J *17*, 6608-6621.

Shimaoka, M., and Springer, T. A. (2003). Therapeutic antagonists and conformational regulation of integrin function. Nat Rev Drug Discov *2*, 703-716.
Simons, K., and Ikonen, E. (1997). Functional rafts in cell membranes. Nature *387*, 569-572.

Smith, K. G., Tarlinton, D. M., Doody, G. M., Hibbs, M. L., and Fearon, D. T. (1998). Inhibition of the B cell by CD22: a requirement for Lyn. J Exp Med *187*, 807-811.

Spaargaren, M., Beuling, E. A., Rurup, M. L., Meijer, H. P., Klok, M. D., Middendorp, S., Hendriks, R. W., and Pals, S. T. (2003). The B cell antigen receptor controls integrin activity through Btk and PLCgamma2. J Exp Med *198*, 1539-1550.

Springer, T. A. (1990). Adhesion receptors of the immune system. Nature *346*, 425-434.

Stephenson, L. M., Miletic, A. V., Kloeppel, T., Kusin, S., and Swat, W. (2006). Vav proteins regulate the plasma cell program and secretory Ig production. J Immunol *177*, 8620-8625.

Stewart, M. P., Cabanas, C., and Hogg, N. (1996). T cell adhesion to intercellular adhesion molecule-1 (ICAM-1) is controlled by cell spreading and the activation of integrin LFA-1. J Immunol *156*, 1810-1817.

Stinchcombe, J. C., Bossi, G., Booth, S., and Griffiths, G. M. (2001). The immunological synapse of CTL contains a secretory domain and membrane bridges. Immunity *15*, 751-761.

Szakal, A. K., Kosco, M. H., and Tew, J. G. (1988). A novel in vivo follicular dendritic cell-dependent iccosome-mediated mechanism for delivery of antigen to antigen-processing cells. J Immunol *140*, 341-353.

Takagi, J., Petre, B. M., Walz, T., and Springer, T. A. (2002). Global conformational rearrangements in integrin extracellular domains in outside-in and inside-out signaling. Cell *110*, 599-511.

Takata, M., Sabe, H., Hata, A., Inazu, T., Homma, Y., Nukada, T., Yamamura, H., and Kurosaki, T. (1994). Tyrosine kinases Lyn and Syk regulate B cell receptor-coupled Ca2+ mobilization through distinct pathways. Embo J *13*, 1341-1349.

Tarlinton, D. (1998). Germinal centers: form and function. Curr Opin Immunol *10*, 245-251.

Tarlinton, D. M., and Smith, K. G. (2000). Dissecting affinity maturation: a model explaining selection of antibody-forming cells and memory B cells in the germinal centre. Immunol Today *21*, 436-441.

Tedford, K., Nitschke, L., Girkontaite, I., Charlesworth, A., Chan, G., Sakk, V., Barbacid, M., and Fischer, K. D. (2001). Compensation between Vav-1 and Vav-2 in B cell development and antigen receptor signaling. Nat Immunol *2*, 548-555.

Texido, G., Su, I. H., Mecklenbrauker, I., Saijo, K., Malek, S. N., Desiderio, S., Rajewsky, K., and Tarakhovsky, A. (2000). The B-cell-specific Src-family kinase Blk is dispensable for B-cell development and activation. Mol Cell Biol *20*, 1227-1233.

Togni, M., Swanson, K. D., Reimann, S., Kliche, S., Pearce, A. C., Simeoni, L., Reinhold, D., Wienands, J., Neel, B. G., Schraven, B., and Gerber, A. (2005). Regulation of in vitro and in vivo immune functions by the cytosolic adaptor protein SKAP-HOM. Mol Cell Biol *25*, 8052-8063.

Tsukada, S., Saffran, D. C., Rawlings, D. J., Parolini, O., Allen, R. C., Klisak, I., Sparkes, R. S., Kubagawa, H., Mohandas, T., Quan, S., and et al. (1993). Deficient expression of a B cell cytoplasmic tyrosine kinase in human X-linked agammaglobulinemia. Cell *72*, 279-290.

Turner, M., Mee, P. J., Costello, P. S., Williams, O., Price, A. A., Duddy, L. P., Furlong, M. T., Geahlen, R. L., and Tybulewicz, V. L. (1995). Perinatal lethality and blocked B-cell development in mice lacking the tyrosine kinase Syk. Nature *378*, 298-302.

Turner, M., Mee, P. J., Walters, A. E., Quinn, M. E., Mellor, A. L., Zamoyska, R., and Tybulewicz, V. L. (1997). A requirement for the Rho-family GTP exchange factor Vav in positive and negative selection of thymocytes. Immunity *7*, 451-460.

Tuveson, D. A., Carter, R. H., Soltoff, S. P., and Fearon, D. T. (1993). CD19 of B cells as a surrogate kinase insert region to bind phosphatidylinositol 3-kinase. Science *260*, 986-989.

van Kooyk, Y., and Figdor, C. G. (2000). Avidity regulation of integrins: the driving force in leukocyte adhesion. Curr Opin Cell Biol *12*, 542-547.

Vanhaesebroeck, B., Welham, M. J., Kotani, K., Stein, R., Warne, P. H., Zvelebil, M. J., Higashi, K., Volinia, S., Downward, J., and Waterfield, M. D. (1997). P110delta, a novel phosphoinositide 3-kinase in leukocytes. Proc Natl Acad Sci U S A *94*, 4330-4335.

Varma, R., Campi, G., Yokosuka, T., Saito, T., and Dustin, M. L. (2006). T cell receptor-proximal signals are sustained in peripheral microclusters and terminated in the central supramolecular activation cluster. Immunity *25*, 117-127.

Vigorito, E., Bardi, G., Glassford, J., Lam, E. W., Clayton, E., and Turner, M. (2004). Vav-dependent and vav-independent phosphatidylinositol 3-kinase activation in murine B cells determined by the nature of the stimulus. J Immunol *173*, 3209-3214.

Viola, A., Schroeder, S., Sakakibara, Y., and Lanzavecchia, A. (1999). T lymphocyte costimulation mediated by reorganization of membrane microdomains. Science *283*, 680-682.

Vorechovsky, I., Vihinen, M., de Saint Basile, G., Honsova, S., Hammarstrom, L., Muller, S., Nilsson, L., Fischer, A., and Smith, C. I. (1995). DNA-based mutation analysis of Bruton's tyrosine kinase gene in patients with X-linked agammaglobulinaemia. Hum Mol Genet *4*, 51-58.

Walmsley, M. J., Ooi, S. K., Reynolds, L. F., Smith, S. H., Ruf, S., Mathiot, A., Vanes, L., Williams, D. A., Cancro, M. P., and Tybulewicz, V. L. (2003). Critical roles for Rac1 and Rac2 GTPases in B cell development and signaling. Science *302*, 459-462.

Wang, H., McCann, F. E., Gordan, J. D., Wu, X., Raab, M., Malik, T. H., Davis, D. M., and Rudd, C. E. (2004). ADAP-SLP-76 binding differentially regulates supramolecular activation cluster (SMAC) formation relative to T cell-APC conjugation. J Exp Med *200*, 1063-1074.

Wang, H., Moon, E. Y., Azouz, A., Wu, X., Smith, A., Schneider, H., Hogg, N., and Rudd, C. E. (2003). SKAP-55 regulates integrin adhesion and formation of T cell-APC conjugates. Nat Immunol *4*, 366-374.

Wang, Y., Brooks, S. R., Li, X., Anzelon, A. N., Rickert, R. C., and Carter, R. H. (2002). The physiologic role of CD19 cytoplasmic tyrosines. Immunity *17*, 501-514.

Williams, G. T., Peaker, C. J., Patel, K. J., and Neuberger, M. S. (1994). The alpha/beta sheath and its cytoplasmic tyrosines are required for signaling by the B-cell antigen receptor but not for capping or for serine/threonine-kinase recruitment. Proc Natl Acad Sci U S A *91*, 474-478.

Wu, J., Qin, D., Burton, G. F., Szakal, A. K., and Tew, J. G. (1996). Follicular dendritic cell-derived antigen and accessory activity in initiation of memory IgG responses in vitro. J Immunol *157*, 3404-3411.

Wulfing, C., Bauch, A., Crabtree, G. R., and Davis, M. M. (2000). The vav exchange factor is an essential regulator in actin-dependent receptor translocation to the lymphocyte-antigen-presenting cell interface. Proc Natl Acad Sci U S A *97*, 10150-10155.

Wulfing, C., and Davis, M. M. (1998). A receptor/cytoskeletal movement triggered by costimulation during T cell activation. Science *282*, 2266-2269.

Wykes, M., Pombo, A., Jenkins, C., and MacPherson, G. G. (1998). Dendritic cells interact directly with naive B lymphocytes to transfer antigen and initiate class switching in a primary T-dependent response. J Immunol *161*, 1313-1319.

Yamanashi, Y., Fukui, Y., Wongsasant, B., Kinoshita, Y., Ichimori, Y., Toyoshima, K., and Yamamoto, T. (1992). Activation of Src-like protein-tyrosine kinase Lyn and its association with phosphatidylinositol 3-kinase upon B-cell antigen receptor-mediated signaling. Proc Natl Acad Sci U S A *89*, 1118-1122.

Yamanashi, Y., Okada, M., Semba, T., Yamori, T., Umemori, H., Tsunasawa, S., Toyoshima, K., Kitamura, D., Watanabe, T., and Yamamoto, T. (1993). Identification of HS1 protein as a major substrate of protein-tyrosine kinase(s) upon B-cell antigen receptor-mediated signaling. Proc Natl Acad Sci U S A *90*, 3631-3635.

Yokosuka, T., Sakata-Sogawa, K., Kobayashi, W., Hiroshima, M., Hashimoto-Tane, A., Tokunaga, M., Dustin, M. L., and Saito, T. (2005). Newly generated T cell receptor microclusters initiate and sustain T cell activation by recruitment of Zap70 and SLP-76. Nat Immunol *6*, 1253-1262.

Yu, H., Leitenberg, D., Li, B., and Flavell, R. A. (2001). Deficiency of small GTPase Rac2 affects T cell activation. J Exp Med *194*, 915-926.

Zipfel, P. A., Bunnell, S. C., Witherow, D. S., Gu, J. J., Chislock, E. M., Ring, C., and Pendergast, A. M. (2006). Role for the Abi/wave protein complex in T cell receptor-mediated proliferation and cytoskeletal remodeling. Curr Biol *16*, 35-46.